ILLINOIS

UNIVERSITY OF ILLINOIS AT URBANA-CHAMPAIGN

-

PRODUCTION NOTE

University of Illinois at
Urbana-Champaign Library
Large-scale Digitization Project, 2007.

UNIVERSITY OF ILLINOIS ENGINEERING EXPERIMENT STATION

Bulletin Series No. 405

Studies of Slab and Beam Highway Bridges, Part IV

FULL-SCALE TESTS OF CHANNEL SHEAR CONNECTORS AND COMPOSITE T-BEAMS

I. M. Viest

C. P. Siess

J. H. Appleton

N. M. Newmark

UNIVERSITY OF ILLINOIS BULLETIN

A REPORT OF AN INVESTIGATION

Conducted by

THE ENGINEERING EXPERIMENT STATION

UNIVERSITY OF ILLINOIS

In cooperation with

THE DIVISION OF HIGHWAYS

STATE OF ILLINOIS

and

THE BUREAU OF PUBLIC ROADS

U. S. DEPARTMENT OF COMMERCE

Price: One Dollar

UNIVERSITY OF ILLINOIS BULLETIN

Volume 50, Number 29; December, 1952. Published seven times each month by the University of Illinois. Entered as second-class matter December 11, 1912, at the post office at Urbana, Illinois, under the Act of August 24, 1912. Office of Publication, 358 Administration Building, Urbana, Illinois.

UNIVERSITY OF ILLINOIS ENGINEERING EXPERIMENT STATION

Bulletin Series No. 405

Studies of Slab and Beam Highway Bridges, Part IV

FULL-SCALE TESTS OF CHANNEL SHEAR CONNECTORS AND COMPOSITE T-BEAMS

IVAN M. VIEST

Research Assistant Professor of Theoretical and Applied Mechanics

CHESTER P. SIESS

Research Associate Professor of Civil Engineering

JOSEPH H. APPLETON

Research Associate in Civil Engineering

NATHAN M. NEWMARK

Research Professor of Structural Engineering

Published by the University of Illinois, Urbana

4000—0-52

UNIVERSITY
OF ILLINOIS
:: PRESS

CONTENTS

FIGURES

TABLES

I. INTRODUCTION

1. Historical Background of Investigation

One of the most common types of highway bridges in current use is the I-beam bridge, which consists of several steel I-beams supporting a reinforced concrete floor slab cast on top of the beams. The concrete slab may either rest freely on the beams or may be connected to their top flanges. Both types of bridges, called noncomposite and composite respectively, have been the subject of extensive theoretical and experimental investigations at the University of Illinois.* In the scale-model composite bridges, tested at the University of Illinois, the slab was connected to the beams by means of channel shear connectors made of short pieces of steel channel welded to the top flanges of the I-beams and embedded in the slab. As a result of these investigations it was considered desirable to investigate further the behavior of both composite beams and shear connectors themselves.

Numerous field and laboratory tests of composite T-beams and shear connectors have been made in various countries; among these the experimental studies of Roš† in Switzerland and of Meier-Leibnitz‡ in Germany were the most extensive. Nevertheless, numerous questions regarding the behavior of composite T-beams remained unanswered and the behavior of channel shear connectors was not known at all.

Prior to the tests reported in this bulletin numerous small-scale push-out specimens and T-beams were tested at the University of Illinois.¶ Most of these tests were made with flexible channel shear connectors. The push-out specimens were tested under static loading; the majority of the T-beams, under repeated loading. The effects on the behavior of channel connectors of variations in the dimensions of channels and in the strength of concrete were investigated. As a result of these studies the hypothesis was advanced that the behavior of a flexible connector is similar to that of a flexible elastic dowel embedded in an elastic medium. The fatigue tests suggested that a state of multiaxial compression existed in the concrete adjacent to the connectors. In the static tests of T-beams

* See references 18, 36 and 50 in the Selective Bibliography, Appendix C.
† References 6 and 29.
‡ Reference 16.
¶ References 61 and 112.

nearly full composite action was maintained up to the ultimate flexural capacity with the exception of one beam having an extremely weak shear connection. This beam had a considerably lower ultimate capacity than that computed for full interaction between the beam and the slab. A comparison of the results of push-out and T-beam tests indicated that the behavior of the channel connector in a push-out specimen was reasonably similar to that of an identical connector in a T-beam.

Although the tests of the small-scale specimens yielded much valuable information on the behavior of shear connectors and composite T-beams, conclusive answers were not obtained to all questions and in some cases additional questions were raised by the results of these tests. The investigators felt that for the most part the questions still remaining appeared to be answerable only by tests of full-scale shear connectors and full-scale T-beams.

2. Object and Scope of Investigation

The primary objectives of the full-scale tests reported in this bulletin were to investigate the behavior of composite steel and concrete T-beams and the behavior of channel shear connectors used in such beams.

Two types of specimens were tested: composite T-beams and push-out specimens. The full-scale composite T-beams consisted of a simple-supported rolled steel wide-flange beam with a reinforced concrete slab resting on the top flange of the beam. The connection between the slab and the beam consisted of channel shear connectors. These beams were intended to simulate the conditions in a highway bridge. All specimens were tested with concentrated loads applied as short-time static loading. These tests were designed to provide answers regarding five problems:

1. The behavior of composite T-beams under static loading before, at, and after first yielding and at the ultimate load.
2. The behavior of a shear connection made of flexible channel connectors, and the effects of this type of connection and of variations in its characteristics on the behavior of composite T-beams.
3. The behavior of flexible channel shear connectors in composite T-beams.
4. The effect on the behavior of composite T-beams of supporting the I-beams during casting and curing the slab.
5. The effectiveness and reliability as a shear connection of natural bond between the slab and the I-beam.

The tests of four composite T-beams were made in the years 1948–1950. The results of these tests are presented and compared with various theories in Chapter III.

The push-out specimens consisted of two concrete slabs connected to the two flanges of an I-beam by a single full-size channel shear connector on each flange. The push-out specimens were tested so as to subject the connectors to a shearing force, representing the predominant action of a connector in a composite T-beam. These tests were designed to provide answers regarding:

1. The behavior of flexible channel shear connectors.
2. The effects of variations of properties of connectors and slabs on the behavior and the load-carrying capacity of channnel connectors.
3. The location and the magnitude of maximum stress in a channel connector.
4. The magnitude of pressure on the concrete adjacent to the channel connector.
5. The effects of the direction and the manner of load application on the behavior of a channel connector.

Tests of 43 push-out specimens were made in the years 1947–1950. The test results are reported and analyzed in Chapter II.

Various assumptions had to be made for computing the deformations of composite beams stressed beyond the elastic limit. These assumptions, an addendum to the theory for composite beams with incomplete interaction, and a selective bibliography are given in the appendixes. The bibliography contains those references concerned with tests and design of composite steel and concrete T-beams; tests, design, construction, and description of bridges of composite construction; tests, design, and description of shear connectors; and the theory of composite beams.

3. Acknowledgments

The tests reported in this bulletin were made as part of an investigation of slab and beam highway bridges conducted at the Talbot Laboratory by the Engineering Experiment Station of the University of Illinois in cooperation with the Illinois Division of Highways and the Bureau of Public Roads of the U. S. Department of Commerce.

The program of the investigation during the period covered by the tests reported herein was guided by an Advisory Committee having the following personnel.

Representing the Illinois Division of Highways:
G. F. Burch, then Bridge Engineer
W. J. Mackay, then Engineer of Railroad Crossings
L. E. Philbrook, then Assistant Bridge Engineer
Representing the Bureau of Public Roads:
E. F. Kelley, Chief, Physical Research Branch

R. Archibald, Chairman, Bridge Committee, American Association of State Highway Officials

E. L. Erickson, Chief, Bridge Branch

Representing the University of Illinois:

F. E. Richart,* Research Professor of Engineering Materials

N. M. Newmark, Research Professor of Structural Engineering

C. P. Siess, Research Associate Professor of Civil Engineering

General direction of the investigation was provided by N. M. Newmark. All work in connection with this bulletin was under the supervision of C. P. Siess, who also planned the tests. The tests of the first two composite T-beams were carried out by J. H. Appleton and reported by him in a thesis.† Some of the push-out specimens were also tested by Appleton. The remaining tests of both push-out specimens and T-beams were made by I. M. Viest and all tests were reported and interpreted by him in a thesis‡ which was used as a basis for this bulletin. The following additional personnel of the concrete slab investigation took part in the work described in this bulletin: F. X. Blechinger and J. R. Gaston, part-time Research Assistants, and Necati Akcaglilar, graduate student in Civil Engineering.

* Deceased.

† J. H. Appleton, "Tests of Full-Size Composite T-Beams," thesis submitted in partial fulfilment of the requirements for the degree of Master of Science in Civil Engineering in the Graduate College of the University of Illinois, 1949.

‡ I. M. Viest, "Full-Scale Tests of Channel Shear Connectors and Composite T-Beams," thesis submitted in partial fulfilment of the requirements for the degree of Doctor of Philosophy in Engineering in the Graduate College of the University of Illinois, 1951.

II. PUSH-OUT TESTS OF SHEAR CONNECTORS

A. SPECIMENS AND APPARATUS

4. Outline of Test Program

The tests of push-out specimens were made for the purpose of investigating the behavior of a channel shear connector. Forty-three push-out specimens were tested in seven groups as outlined in Table 1. The principal variables were the strength of concrete, the dimensions of channel connectors, the restraint of concrete under the connector, and the direction of load. Each group of specimens was designed primarily to investigate one of the principal variables.

Group I included eleven specimens with concrete strength as the only variable. The average compressive cylinder strength varied from 2070 to 6320 psi. All shear connectors were made from 4-in. 5.4-lb. rolled steel standard channels.

The effects of the dimensions of a channel connector on its behavior were investigated with the 23 specimens of Groups II–V. One group was devoted to each of the following variables: connector web thickness, connector flange thickness, connector height and connector width. With the exception of the specimens of Group III all connectors were rolled steel channels. The sizes of the channels used are listed in Table 1. The specimens of Group III were made with connectors of special shapes: channels with the flange on the welded end cut off, plates, and bars. These shapes were chosen because the variations of the flange thickness in rolled steel channels are very small and are always accompanied by changes in some other dimension. The average cylinder strength of the concrete varied from 2300 to 5050 psi in Group II and was approximately 3000 psi in Groups III, IV and V.

The preliminary tests of small-scale specimens * indicated that a channel connector exerts high pressure on the adjacent concrete and that a triaxial state of stress exists in the concrete at such locations. Thus the deformation of the concrete under a shear connector depends on the lateral restraint as well as on the magnitude of the pressure. It was thought that locating a shear connector in a concrete fillet (Fig. 1b)

* In the following text all references to the tests of small-scale specimens are to the tests made at the University of Illinois and reported in Bulletin 396, reference 112.

might lower such restraint and thus might influence the behavior of the connector. This variable was investigated on specimens of Group VI. Connectors of this group were made of rolled steel standard channels and square bars. Strength of concrete varied from 2170 to 4690 psi.

The failures observed in the fatigue tests of small-scale T-beams suggested that the direction of load might have some influence on the behavior of a channel shear connector. Therefore two specimens of Group VII were tested with the load applied to the back face of the channel

Table 1
Outline of Push-out Tests

Group	Type of Connector	Principal Variable Investigated	Number of Specimens
I	4-in. 5.4-lb standard channel	Concrete strength	11
II	4-in. channel with web 0.25 in. thick (milled from 4-in. 7.25-lb standard channel) 4-in. 7.25-lb standard channel 4-in. 13.8-lb car building channel	Connector web thickness	10
III	4-in. 5.4-lb and 4-in. 7.25-lb standard channels with one flange cut off 4-in. 5.4-lb standard channel with a plate ½ in. thick added to one flange 4-in. x ½-in. plate 1-in. square bar 1 ¼-in. square bar	Connector flange thickness	6
IV	3-in. 4.1-lb standard channel 5-in. 6.7-lb standard channel	Connector height	5
V	4-in. 5.4-lb standard channel	Connector width	2
VI	4-in. 5.4-lb standard channel 4-in. 7.25-lb standard channel 1-in. square bar	Restraint of concrete under connector	7
VII	4-in. 5.4-lb standard channel	Direction of load	2
		Total number of specimens	43

while the specimens of all other groups were tested with the load applied to the inside face of the channel. Shear connectors of Group VII were made of 4-in. 5.4-lb rolled steel standard channels. The concrete strength was approximately 3000 psi.

5. System of Designating Specimens

Each push-out specimen was designated by two or three numbers and two capital letters as, for example 4C3C1. In these symbols the numbers and letters have the following meaning.

The first number expresses the height of the shear connector in inches.

The first letter designates the type of shear connector; *C* stands for channel, *P* for plate, and *B* for bar.

The second number gives the thickness of the connector web in sixteenths of an inch.

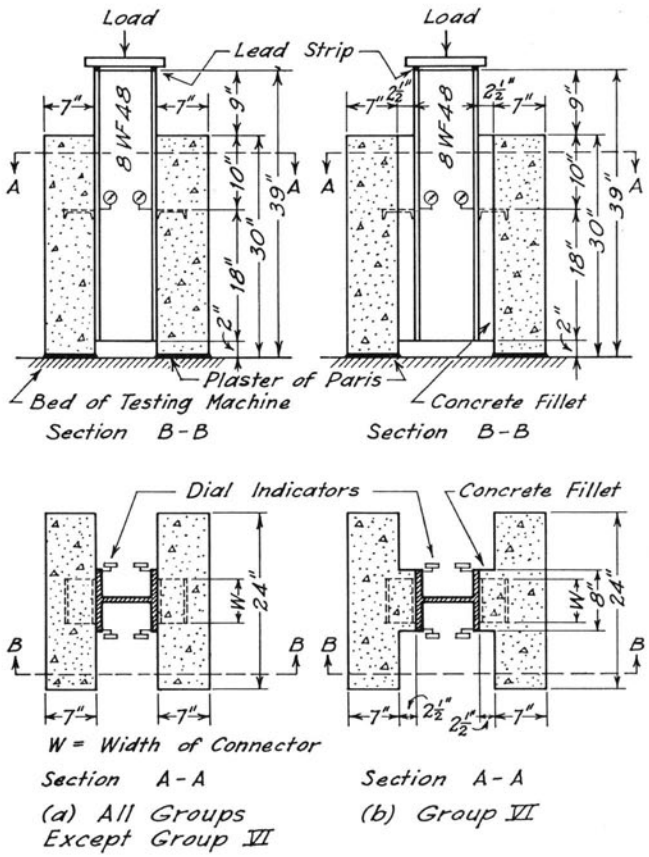

Fig. 1. Details of Push-out Specimens

The second letter designates the principle variable investigated and is the same for all specimens of one group. *C* stands for the concrete strength, *T* for the thickness of the connector web, *S* for the height of the stiff portion of the connector (thickness of the flange welded to the beam), *H* for the height of the connector, *W* for the width of the connector, *F* for the concrete fillet (variations in the restraint offered to concrete under the connector), and *D* for the direction of load.

The third number is used to distinguish between specimens of otherwise identical designations; this number is omitted when not needed.

Thus, specimen 4C3C1 had shear connectors made of 4-in. high channels with a web $\frac{3}{16}$ in. thick; this specimen was tested for the purpose of investigating the effect of concrete strength; it was the first specimen of its kind.

In some parts of the text of this bulletin it is necessary to distinguish between the two slabs of the same push-out specimen. The slab which was cast first is then called "Slab A" and the slab cast second is called "Slab B."

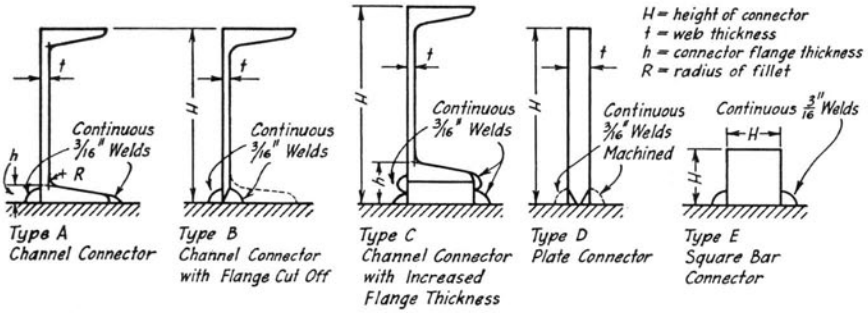

Fig. 2. Types of Shear Connectors Used in Push-out Specimens

6. Description of Specimens

The push-out specimen consists of a short steel I-beam and two concrete slabs, one attached to each flange of the beam. One or more connectors are rigidly connected to each flange of the beam and embedded in the slab. In this type of specimen both the slabs and the beam are in compression, the load being applied at the upper end of the I-beam and transmitted from the beam to the slabs through the shear connectors. The loading of the shear connectors corresponds, with some limitations, to that of similar connectors in a composite T-beam.

The types of specimens used in the tests reported herein are shown in Fig. 1. In the standard specimen (Fig. 1a) one connector was welded to each flange of the 39-in. long 8WF48 steel beam and embedded in a 24 x 30 x 7-in. concrete slab. Specimens of Group VI were made with a 8 x 28 x 2.5-in. concrete fillet between the I-beam and the slab proper as shown in Fig 1b.

Five types of shear connectors were used. Three of these (types A, B and C) were channel connectors, one (type D) was a plate connector and one (type E) was a square bar connector. Cross sections of all types are shown in Fig. 2 and a photograph of a channel connector welded to the flange of an I-beam is shown in Fig. 3. Thirty-six specimens had shear connectors of Type A—that is, rolled steel channels. Shear connectors for two specimens were machined from rolled channels by cutting off the flange on the side welded to the beam (Type B), and in one

specimen the thickness of the channel flange welded to the beam was increased by adding a steel plate 6 x 1.6 x 0.5 in. (Type C). Plate connectors (Type D) were used in one specimen, and square bar connectors (Type E) in three specimens. The dimensions of the individual shear connectors are given in Table 2. Most of the connectors were 6-in. wide pieces of 4-in. 5.4-lb and 7.25-lb rolled steel standard channels.

In all specimens, with the exception of 4C3C11 and 4C3W2, an attempt was made to destroy the bond between the beam and the slabs by covering the flanges of the I-beam with a layer of cup grease. In specimen 4C3C11 white lead was used instead of grease, and in specimen 4C3W2 no attempt was made to destroy the natural bond.

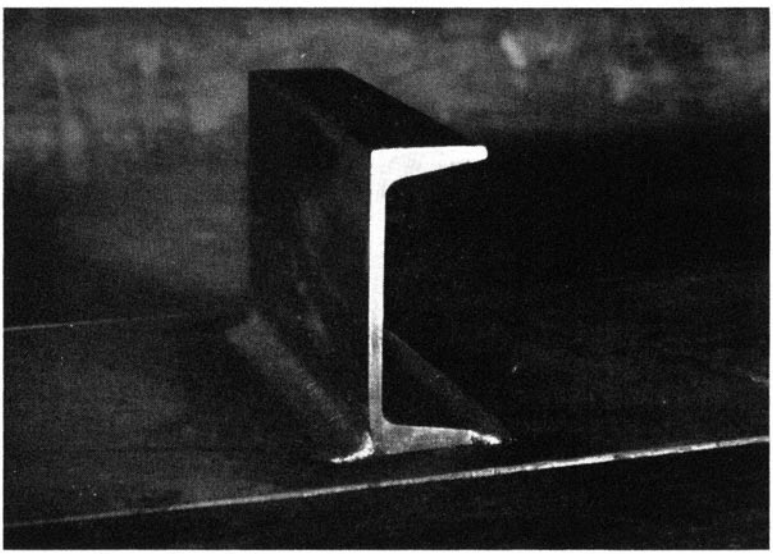

Fig. 3. Typical Channel Shear Connectors; 4-in 5.4-lb Channel

7. Materials

The concrete for the slabs was made of various standard brands of Portland cement, Wabash river torpedo sand and Wabash river gravel. Both the sand and the gravel used in the push-out specimens were the same as those used in the T-beams (Section 32). The average fineness modulus for the sand was 2.8 and the maximum size of the gravel was 1 in. The proportions of the aggregates and the cement-water ratio were varied. The results of the compression tests of five 4 x 8-in. control cylinders made with each slab are given in Table 3.

Table 2

Dimensions of Shear Connectors Used in Push-out Specimens

For explanation of headings see Fig. 2

Group	Specimen	Type	Nominal Size	Height H, in.	Width w, in.	Web Thickness t, in.	Flange Thickness h, in.
I	4C3C1-11	A	4 in. 5.4 lb	4	6	0.180	0.413
II	4C4T	A	4 in. 7.25 lb*	4	6	0.250	0.413
	4C5T1-8	A	4 in. 7.25 lb	4	6	0.320	0.413
	4C8T	A	4 in. 13.8 lb	4	6	0.500	0.531
III	4P8S	D	4 in. x 0.5 in.	4	6	0.500	.....
	4C3S1	B	4 in. 5.4 lb*	4	6	0.180	.....
	4C3S2	C	4 in. 7.25 lb +1.6 in. x 0.5 in.	4.533	6	0.180	0.944
	4C5S	B	4 in. 7.25 lb*	4	6	0.320	.....
	1.25B0S	E	1.25 in. x 1.25 in.	1.25	6	.....	.....
	1B0S	E	1 in. x 1 in.	0.938	6	.....	.....
IV	3C3H1-3	A	3 in. 4.1 lb	3	6	0.170	0.377
	5C3H1-2	A	5 in. 6.7 lb	5	6	0.190	0.450
V	4C3W1	A	4 in. 5.4 lb	4	5	0.180	0.413
	4C3W2	A	4 in. 5.4 lb	4	4	0.180	0.413
VI	4C3F1-4	A	4 in. 5.4 lb	4	6	0.180	0.413
	4C3F5	A	4 in. 5.4 lb	4	8	0.180	0.413
	4C5F	A	4 in. 7.25 lb	4	6	0.320	0.413
	1B0F	E	1 in. x 1 in.	0.938	6	.....	.....
VII	4C3D1-2	A	4 in. 5.4 lb	4	6	0.180	0.413

*Nominal size machined to desired dimensions.

Table 3

Compressive Cylinder Strength of Concrete in Slabs

Compressive strength for each slab is average of five 4 x 8-in. cylinders cast and cured together with the corresponding slab. Cylinders were moist-cured from 3 to 7 days and tested at the age of approximately 28 days.

Specimen	Concrete Strength Slab A, psi	Slab B, psi	Average, psi
	Group I		
4C3C1	2 090	2 040	2 070
4C3C2	1 800	2 800	2 300
4C3C3	2 670	2 470	2 570
4C3C4	3 090	3 190	3 140
4C3C5	3 330	3 610	3 470
4C3C6	2 750	4 250	3 500
4C3C7	3 950	4 320	4 140
4C3C8	4 340	5 200	4 770
4C3C9	5 350	5 320	5 340
4C3C10	5 950	5 530	5 740
4C3C11	6 310	6 330	6 320
	Group II		
4C4T	4 030	3 990	4 010
4C5T1	1 830	2 770	2 300
4C5T2	2 990	2 830	2 910
4C5T3	2 920	3 330	3 130
4C5T4	3 520	2 860	3 190
4C5T5	2 290	4 330	3 310
4C5T6	3 250	3 810	3 530
4C5T7	4 140	4 580	4 360
4C5T8	5 070	5 020	5 050
4C8T	2 260	3 070	2 670
	Group III		
4P8S	3 310	3 260	3 290
4C3S1	1 430	1 250	1 340
4C3S2	1 950	1 980	1 970
4C5S	2 700	2 740	2 720
1.25B0S	3 770	2 490	3 120
1B0S	3 120	3 300	3 210
	Group IV		
3C3H1	2 970	2 650	2 810
3C3H2	3 540	3 080	3 310
3C3H3	3 490	4 340	3 920
5C3H1	3 110	3 230	3 170
5C3H2	3 030	3 490	3 260
	Group V		
4C3W1	2 680	2 930	2 810
4C3W2	4 100	4 760	4 430
	Group VI		
4C3F1	3 120	2 040	2 580
4C3F2	2 360	2 940	2 650
4C3F3	4 220	4 980	4 600
4C3F4	4 380	5 000	4 690
4C3F5	3 110	3 040	3 080
4C5F	2 110	2 220	2 170
1B0F	2 410	2 040	2 230
	Group VII		
4C3D1	3 470	2 500	2 990
4C3D2	3 940	2 800	3 370

The channels, plates and bars used for the connectors were hot-rolled steel sections. Tensile tests were made on a number of coupons, some cut parallel to the direction of rolling and others perpendicular, but the tests showed no consistent differences between the two directions. The results of the tensile tests are given in Table 4.

Table 4

Tensile Properties of Steel in Shear Connectors

All coupons were cut parallel or perpendicular to the direction of rolling; as no significant difference was observed between these two types of coupons, they are not reported separately.

Specimen	Number of Test Coupons	Yield Point, psi	Ultimate Strength, psi
4C3C2, 3, 4, 6, 7 4CD1, 2	2	38 900	58 500
4C3C1, 5, 8, 4C3S1, 2	8	45 900	67 200
4C3C9, 10, 4C3F1-5 4C3W1, 2	4	39 300	55 600
4C3C11	8	42 500	61 800
4C4T, 4C5T1-8, 4C5F, 4C5S	6	37 700	61 500
3C3H1, 2, 3	2	52 500	71 400
5C3H1, 2	4	44 300	67 900
4C8T	2	39 500	64 800
4P8S	2	42 500	62 350

8. Manufacture of Specimens

The first step in the manufacture of the push-out specimens was welding the shear connectors to the beam at the locations indicated in Fig. 1. All shear connectors were welded at the front and back sides of the connector (Fig. 2). After the shear connectors were welded in place, the scale was cleaned off the welds. Next, strain gages were attached to one of the connectors and waterproofed. Finally, the flange of the beam was thoroughly covered with cup grease before the slab was cast.

The slabs were cast horizontally to simulate the conditions in a composite beam. The horizontal casting required some time delay between the casting of the two slabs of one specimen. At the beginning of the investigation the specimen was turned over and the second slab cast after the first slab has been moist cured for seven days. This procedure required adjustments in the cement-water ratio for the second slab in order to provide approximately equal strengths in the two slabs. At a later stage of the investigation the period of moist curing was reduced from seven to three days. Toward the end of the investigation only one day was allowed to elapse between casting the first and the second slab; when the second slab was one day old, the specimen was placed in the

moist room for six additional days of moist curing. During the period between the end of moist curing and the day of testing, the specimens were stored in the air of the laboratory. All specimens were tested about 28 days after the first slab was cast.

The slabs were provided with only a nominal amount of reinforcement; as a rule a single layer of wire mesh consisting of No. 10 wires at 4-in. spacing in each direction was placed at mid-depth of the slab. The five 4 x 8-in. control cylinders were cast and cured with each slab. They were tested at the end of the test of the corresponding specimen.

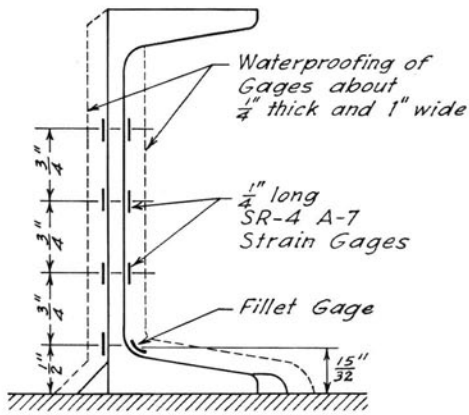

Fig. 4. Standard Location of Electric SR-4 Strain Gages on Channel Shear Connectors

9. Instruments and Loading Apparatus

Slip between the slabs and the beam was measured on all specimens, and shear connector strains were measured on all specimens except 4C3C6, 1.25B0S, 1B0S and 1B0F. No other measurements were made in these tests.

Slip was measured by four 0.001-in. dial indicators at the locations shown in Fig. 1. The dials were attached rigidly to the beam with the stem bearing against brackets glued to the slabs. To prevent errors in the slip measurements due to concrete and steel strains, the brackets and the dials were fastened to the slabs and the beam directly opposite the back faces of the connectors.

Strains were measured by means of ¼-in. long Type A-7 electric SR-4 gages. Gages were attached to one connector only. Normally, eight gages were used at the locations shown in Fig. 4; all gages were located at the midpoint of the channel width. In a few specimens 6, 7, 9, or 10

gages were used; in others, gages were placed at locations different from those shown in Fig. 4. All gages had to be waterproofed against moisture. Some difficulties due to moisture were experienced in the early stages of the investigation but later, after the method of waterproofing had been perfected, the electric gages gave very satisfactory service. The waterproofing coat was about ¼ in. thick and 1 in. wide. It was made of Petrolastic, a commercial asphaltic compound. The method of attaching and waterproofing the SR-4 gages has been described in detail in an earlier paper.* Strains were read with a Baldwin-Foxboro Portable Strain Indicator, Type K.

Specimens with concrete fillets were tested in a 3,000,000-lb capacity Southwark-Emery hydraulic testing machine; all other specimens were tested in an Olsen screw-type machine of 300,000-lb capacity. The arrangement for testing in the Olsen machine is shown in Fig. 5. The specimen was placed in the testing machine with the lower ends of the slabs bedded in plaster of paris. The load was applied to the upper end of the steel beam by the head of the testing machine through a spherical block and a steel distributing plate. To improve the distribution of the load, strips of lead were inserted between the steel plate and the flanges of the beam.

B. TESTS AND RESULTS

10. Description of Test Procedures

In the tests of push-out specimens, load was applied in increments of varying magnitude. In some tests the load was released several times before failure was reached, in others the load was increased continuously from the beginning of the test until failure occurred. Specimens 4C3C9–11, 4C4T, 4C5T7–8, 4C8T, 3C3H3, 5C3H2, 4P8S, and all specimens of Groups V and VI were tested with intermittently released loading. All other specimens were tested with continuously increasing increments.

The magnitude of the continuously increasing load increments varied from 2000 lb to 10,000 lb. The smallest increment was used until slip was recorded on all four dials; then load was increased in increments of 4000 or 5000 lb until the maximum strains in the connectors exceeded the yield point strain by a large margin. From then on 10,000-lb increments were applied.

The loading procedure for the intermittently released loading was similar except during the release and recovery of the load. The load was

* E. Hognestad and I. M. Viest, "Some Applications of Electric SR-4 Gages in Reinforced Concrete Research," Proceedings, American Concrete Institute, 1950, Vol. 46, pp. 447–450.

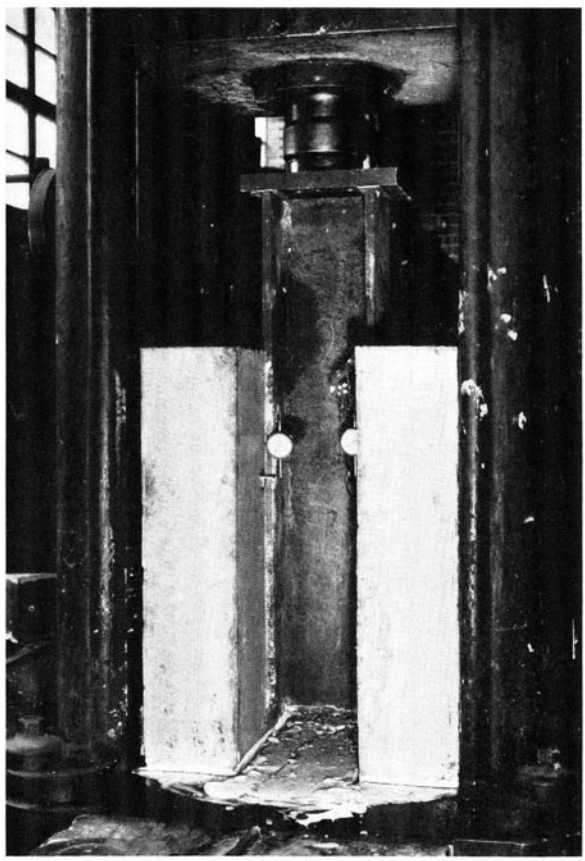

Fig. 5. Arrangement for Testing Push-out Specimens

released first after small slips were noted on all dials, and was again released and reapplied two to five times at higher loads. The load was released and recovered in steps of 10,000 to 30,000 lb.

After each increment of load, readings were taken on all slip and strain gages. The slips were read to the nearest 0.0001 in. at low loads and to the nearest 0.001 in. at high loads. Strains were read to the nearest 1×10^{-5} in. per in. Each reading of slips and strains took about 3 to 5 min. The duration of a single test varied from 1½ to 3 hr.

In addition to the push-out tests, most of the connectors with strain gages were tested as cantilevers prior to casting the slabs. This so-called bare-connector test was made to experimentally determine the moment-strain ratio for each gage and also to preload the SR-4 gages. In these tests a load was applied along the full width of the free flange of the channel in the direction perpendicular to the channel web. The load was

applied in increments of 79 or 158 lb and the maximum strains were never allowed to exceed a value of 60×10^{-5} in. per in. Only strains were measured in these tests.

11. Manner of Presentation of Test Data

Slip between the beam and the slabs, strains on one shear connector, and the ultimate load constitute the data obtained from the push-out tests. In order to interpret the behavior of shear connectors, it is desirable to find out how much of the total load was carried by the shear connectors and how much by bond or friction, how this load was distributed between the two connectors of one push-out specimen and, finally, how accurate the measured quantities are.

Load on Shear Connectors. The load applied to the top of the beam must be transferred from the beam to the slabs. There are only three ways of transfer of load from the beam to the slabs of a push-out specimen: by bond, through the connectors, and by kinetic friction. A study of the test data indicates that bond between the beams and the slabs was present in most of the tests in spite of the attempt to prevent it through oiling the flanges of the beam. This is illustrated in Fig. 6, in which the total load on a push-out specimen is plotted against slip measured by individual dials. Studies of this and of similar plots show that bond was broken at all locations at a total load varying from 0 to 30 kips. After the bond was broken most of the load had to be transferred by the shear connectors. The pressure applied to the slabs by

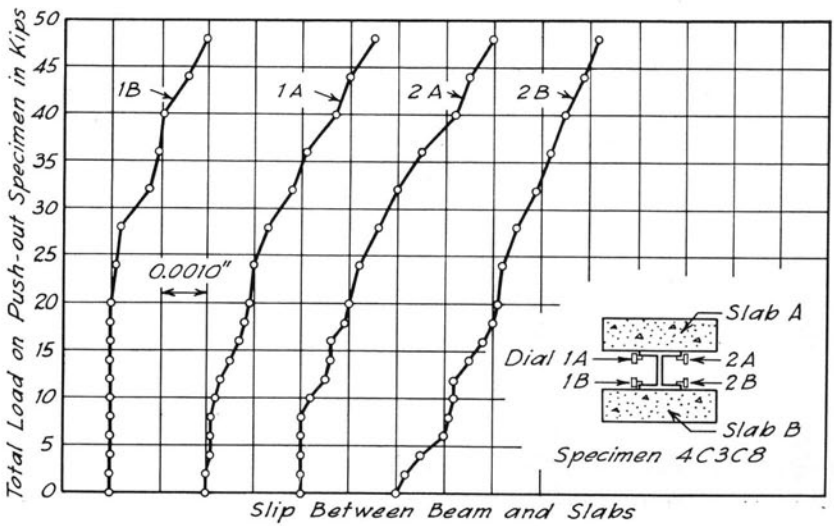

Fig. 6. Effect of Bond on Slip Between Beam and Slabs

the shear connectors is eccentric with respect to the vertical plane at mid-thickness of the slab. Owing to this eccentric loading, the slabs of the push-out specimen have a tendency to rotate and to exert normal pressure on the beam. As a result, a portion of the load is transferred from the beam to the slabs by kinetic friction. It was estimated that about 3 percent of the total load could be transferred in this way.

In all tests an attempt was made to apply the load to the beam centrally in order to achieve an equal distribution of load between the two connectors of a push-out specimen. In spite of the careful centering, eccentricities of about ¼ in. could easily be present. A ¼-in. eccentricity would result in 6 percent increase of the load on the near connector. The distribution of load would be affected in a similar manner by differences in the strength of concrete in the two slabs: a difference of 1000 psi would change the distribution of load by 2–6 percent depending upon the quality of the concrete.

It was thought that the distribution of load might have been influenced also by the presence of the waterproofing material on one of the channels. However, the data presented in Section 13 do not indicate any definite effect of the waterproofing on the distribution of load between the two connectors.

Accuracy of Measurements. Slip was measured on four sides of the beam. The differences between the individual readings were affected by the uneven breaking of bond: at an average slip of 0.0030 in. the readings differed usually by about 25 percent while at an average slip of 0.0200 in. the difference was only about 15 percent. The differences in the individual slip readings at high loads must have been caused by the lack of equal distribution of load between two connectors of one push-out specimen.

Strains were measured on one connector only. As a rule, eight strain gages were located in pairs on the opposite faces of the channel web (Fig. 4). With very few exceptions, the readings of corresponding gages were of opposite sign but of different magnitudes. The differences varied from 0 to over 100 percent. The bare-connector tests, checks on the resistances of gages and the push-out test data themselves indicated that the strain gages worked properly. Thus the differences between the strain readings on opposite sides of the web suggest that some direct stresses in addition to bending must have been present in the connectors. Bond and friction between the connector and the concrete, and the resistance of the free channel flange to the forces tending to pull the connector out of the slab might have been the causes of direct stress.

If present, bond on the surfaces of a connector would have a restraining effect on steel strains and would counteract the effects of flexure.

If present only on one side of the cross section, it would cause a reduction of strains on the bonded surface and an increase on the unbonded surface. In the absence of bond, friction is present on the surfaces which exert pressure on the adjacent concrete. The effect of such friction is similar to that of bond on one side of the cross section only. Any tendency to pull the connector out of the slab would be resisted by the free flange of channel; this would set up direct tension and additional bending stresses in the connector web.

Studies of the test data indicate that none or only a small amount of direct stresses was caused by the tendency to pull the channels out of the concrete. On the other hand, it seems probable that in the connectors tested with continuously increasing increments of load bond was present throughout the tests at least on some parts of the surface of a connector. If the bond between the surfaces of a flexible connector and the surrounding concrete is broken and the connector is loaded, the convex surface of the connector exert pressures on the concrete. As the convex surface tends to elongate, friction counteracts this tendency. Thus the presence of friction is probable, if the tensile strains in a connector are consistently numerically smaller than the compressive strains measured on the opposite surface of the connector. Such indication of the presence of friction was found in nearly all specimens tested by intermittently released loading.

The stresses in the fillet between the web and the welded flange might be influenced by the local stress concentration. It is believed that in the connectors tested the effect of this stress concentration was very small; however, its magnitude could not be determined. Furthermore, the slope of the strain distribution curve at the fillet was steep and a small accidental misplacement of the fillet strain gage may have caused large variations in the measured strains. For example, a shift in position of 0.05 in. could have caused 10 percent difference in measured strains.

Presentation of Test Data. Since it is evident that the accuracy of the push-out test data is inherently low, no great refinements are justified in presenting the data. It was decided, therefore, to present the results of these tests in the following manner. One half of the total load applied to the beam is reported as the load per connector. Reported slip is the average of the readings on all four dials. Unless consistent differences were observed in the readings of corresponding gages, only average values of strains measured on the opposing gages are reported. Fillet strains are reported as measured.

Most of the data are reported in the form of load-slip, load-maximum strain and strain distribution curves. In addition, in Table 5 loads are

Table 5

Push-out Tests: Summary of Test Results

Specimen	Load-Carrying Capacity of One Connector in Kips						Initial Failure	
	At Average Slip of			At Maximum Strain		Ultimate		
	0.0030 in.	0.0060 in.	0.0200 in.	60×10^{-5}	110×10^{-5}		Location*	Type†
4C3C1	20.3	26.8	43.3	21.2	29.1	74.8	SBO	T
4C3C2	16.8	23.8	39.7	....	....	72.5	SBO	T
4C3C3	14.0	21.8	36.9	....	....	67.5	SO	T
4C3C4	21.6	30.0	47.3	21.3	29.3	79.0	SO	T
4C3C5	22.8	31.6	52.5	24.9	35.1	91.0	SO	T
4C3C6	20.6	29.3	51.5	....	....	95.0	SO	T
4C3C7	28.7	37.7	60.0	28.6	39.5	102.5	SAO	T
4C3C8	22.0	32.0	57.2	26.0	36.0	98.2	SO	T
4C3C9	20.7	33.7	60.5	27.2	38.2	116.1	SBO	T
4C3C10	(21.8)‡	(32.1)	(60.1)	(24.0)	(35.1)	(112.1)	SBO	T
4C3C11	....	30.0	65.8	....	40.0	118.2	WCA	S + T
4C4T	....	....	57.1	....	38.8	98.8	SBO	T
4C5T1	21.9	31.2	53.1	28.4	38.4	79.0	SO	T
4C5T2	23.2	32.4	56.0	22.5	31.7	87.3	SO	T
4C5T3	25.0	35.0	59.1	26.0	37.0	90.5	SO	T
4C5T4	17.0	25.4	45.2	15.2	32.3	85.0	SO	T
4C5T5	20.0	29.0	50.5	19.1	26.4	84.8	SO	T
4C5T6	25.2	35.2	58.5	27.1	36.7	95.0	SBO	T
4C5T7	24.5	35.5	60.3	23.8	35.3	102.8	SO	T
4C5T8	30.0	42.3	72.2	26.3	40.4	131.0	SBO	T
4C8T	28.5	39.8	68.2	35.6	47.7	105.3	SO	T
4P8S	25.0	34.0	60.6	29.1	42.0	65.8	WCA	S + T
4C3S1	11.0	16.2	25.0	9.9	14.5	48.2	WCA	S + T
4C3S2	22.7	31.6	57.2	36.2	48.7	90.0	SO	T
4C5S	18.0	25.8	46.8	18.4	26.4	84.2	SBO	T
1.25B0S	35.5	46.5	65.7	....	....	82.0	SO	Sep.+C+S
1B0S	18.2	27.1	51.2	....	....	60.0	SO	Sep.+C+S

Specimen	Load-Carrying Capacity of One Connector in Kips						Initial Failure	
	At Average Slip of			At Maximum Strain		Ultimate		
	0.0030 in.	0.0060 in.	0.0200 in.	60×10^{-5}	110×10^{-5}		Location*	Type†
3C3H1	16.2	22.5	36.8	....	....	63.0	SO	T
3C3H2	19.3	26.4	45.6	18.5	25.3	75.5	SO	T
3C3H3	23.2	31.8	55.8	21.4	30.1	89.6	SBI	T
5C3H1	22.3	30.0	48.1	20.7	29.0	89.2	SBO	T
5C3H2	23.4	32.3	52.7	27.3	34.8	91.3	SBO	T
4C3W1	19.0	23.8	39.6	24.4	30.3	75.0	SBO	T
4C3W2	23.4	29.6	46.0	26.4	31.5	81.9	WCA	S+T
4C3F1	12.0	18.7	34.7	17.2	24.2	57.7	F	B+C+S
4C3F2	18.0	25.2	43.7	23.5	31.5	74.2	F	B+C+S
4C3F3	....	(25.5)	(46.5)	(20.5)	(26.5)	(91.0)	F	T
4C3F4	21.0	32.7	60.2	30.0	45.2	97.3	F	B+T+S
4C3F5	18.7	30.7	60.0	22.0	34.0	98.5	F	B+C+S
4C5F	(20.7)	(27.7)	(45.1)	30.2	38.3	67.5	F	B+C+S
1B0F	15.7	23.8	34.7	....	....	45.0	F	Sep.+C+S
4C3D1	20.0	28.5	46.1	22.4	29.1	59.4	SO	T
4C3D2	21.4	28.6	45.0	25.2	33.2	69.8	SO	T

*SBO } slab B or A respectively, outside face.
SAO }
SO—slab B or A or both simultaneously, outside face.
SBI—slab B, inside face.
WCA—welds of connector in slab A.
F—concrete fillet.

†T—tension, S—shear, B—bulging, C—crushing, Sep—separation of slabs from beam.
‡Values listed in parenthesis are of questionable accuracy.

reported at slips of 0.0030, 0.0060 and 0.0200 in. and maximum measured strains of 60 x 10^{-5} and 110 x 10^{-5}. In most of the tests the maximum measured strain was that at the fillet gage, but in a few instances it was that at the gage located approximately opposite the fillet gage.

Slips and strains in Table 5 were selected to correspond approximately to what might be considered the working and yield loads for the connectors. At working loads a slip of about 0.0030 in. and strain of 60 x 10^{-5} may be expected. Strain of 110 x 10^{-5} was selected as a nominal yield value; the corresponding slip was about 0.0060 in. Slip of 0.0200 in. was reached in all tests only after extensive yielding of the shear connectors and was chosen as a basis for comparison at high loads.

Ultimate loads per connector and the locations and types of initial failure also are listed in Table 5. It can be seen that, as a rule, failure was caused by tensile cracking of the slabs. The tensile failure of the slab is characteristic of push-out specimens and probably would not occur in a composite T-beam. Therefore the ultimate loads found from the tests of push-out specimens do not bear any real relation to the ultimate capacities of the same types of connectors used in composite T-beams. A partial exception to this observation is the specimens made with concrete fillets. Several of these specimens failed by shearing off a wedge of concrete under the connector. It is probable that a similar type of failure may occur in a composite T-beam with similar fillets.

For some of the specimens in Table 5 data are missing or are unreliable due to various experimental difficulties encountered during the tests. Strains were not measured in specimen 4C3C6 and the strain gage was omitted from the fillet of specimen 4C3C3. The strain indicator was defective during the test of specimen 3C3H1. Specimens 4C3C11 and 4C4T were accidentally preloaded; for these specimens, only the readings at high loads are reliable. Brackets were not attached properly on specimen 4C5F so that the reliability of slip readings is questionable. Finally, specimens 4C3C10 and 4C3F3 were loaded eccentrically; the results of these tests are entirely unreliable.

12. Effect of Variation of Properties of Connectors and Slabs

The previous tests of small-scale push-out specimens indicated that the behavior of channel connectors depends on the dimensions of the channels and on the quality of the concrete. It was decided, therefore, to investigate the effects of the following variables in the full-scale push-out tests: concrete strength, thickness of the channel web, thickness of the channel flange, height of the connector and width of the connector. The investigation included also studies of the effects of a concrete fillet between the steel beam and the concrete slab.

Concrete Strength. The effects of this variable on the behavior of channel shear connectors were investigated with specimens of Groups I and II. The results are shown in Figs. 7–11. In Group I the average concrete strength varied from 2070 to 6320 psi and in Group II from 2300 to 5050 psi.

The effect of the concrete strength on slip between the beam and the slabs is shown in Figs. 7 and 8. For reasons of simplicity load-slip curves in Fig. 7a, b are plotted for only a few representative specimens of Groups I and II respectively. They were selected to include wide variations of concrete strength and to give a fair picture corresponding to that indicated by all test data. In the figure, load-slip curves are plotted up to loads approaching the ultimate; the initial parts of the curves are distorted by the presence of bond and are therefore omitted from the graphs. The most important portions of the load-slip curves correspond to loads from about 20 to 40 kips per connector. They are plotted on an enlarged scale in Fig. 7a, b. The curve for connector 4C5T4, shown on Fig. 7b as a dotted line, lies outside the band of curves for other similar specimens. It is not known why the load-slip curve for this connector exhibited this irregularity, but it is suspected that either the specimen may have been damaged during handling or the concrete was not properly placed around the connector during casting. Similar deviations were observed in the data on specimens 4C3C3 and 4C5T5, which were not included in Fig. 7.

The load-slip curves for specimens of Groups I and II show a significant influence of the concrete strength on the load-slip characteristic of channel connectors. The amount of slip increases with decreasing concrete strength and the differences are more pronounced at high than at low loads. This point is illustrated clearly in Fig. 8, in which the load per connector is plotted against the concrete strength at a slip of 0.0030, 0.0060 and 0.0200 in. for all connectors. The loads required to cause a certain slip on various specimens are grouped fairly close together and follow an increasing trend with increasing strength of concrete. Lines drawn through the test data emphasize this tendency. The test data plotted in Fig. 8 show a 40–80 percent increase of the load-carrying capacity of connectors when the concrete strength increases from 2000 to 6000 psi. The exact magnitude of the increase in capacity depends on the magnitude of slip and to a lesser degree also on the web thickness.

The effects of the strength of concrete on strains in a channel shear connector are illustrated in Figs. 9–11. In Fig. 9 the distribution of strain along the channel web is plotted for several connectors of Groups I and II at maximum measured strains of 60×10^{-5} and 110×10^{-5}. The differences between the curves for individual connectors are small. It may

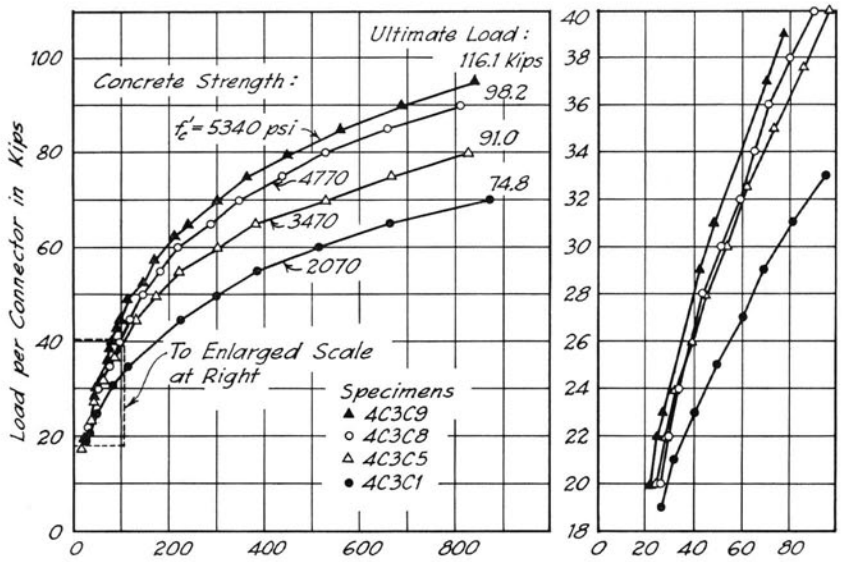

(a) Group I – All Connectors 4in. – 5.4 lb. Channels

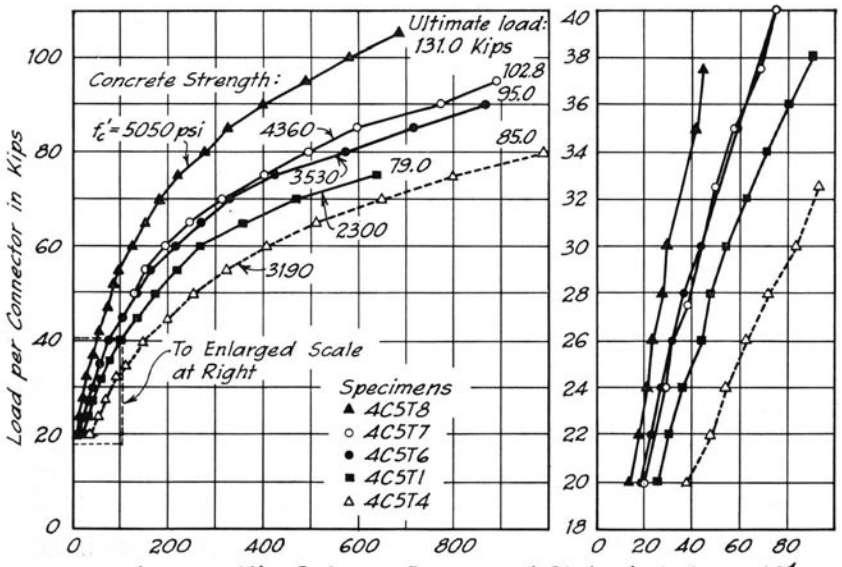

(b) Group II – All Connectors 4in. – 7.2 lb Channels

Fig. 7. Representative Load-Slip Curves, Group I and Group II

be concluded that the distribution of strain along the web of a channel connector is not affected significantly by the strength of the concrete.

The effect of concrete strength on the maximum strain in a channel connector is shown in Figs. 10 and 11. In Fig. 10 maximum strain is plotted against load for several connectors. For connectors with web $\frac{3}{16}$ in. thick a fairly definite effect of concrete strength may be observed, but for connectors with web $\frac{5}{16}$ in. thick the data are erratic. A somewhat better picture of the effect of concrete strength on the maximum connector strains may be gained from Fig. 11 in which load per connector at maximum steel strains of 60×10^{-5} and 110×10^{-5} is plotted against concrete strength. In spite of considerable scatter, there is a definite trend: the higher the concrete strength the higher is the load required

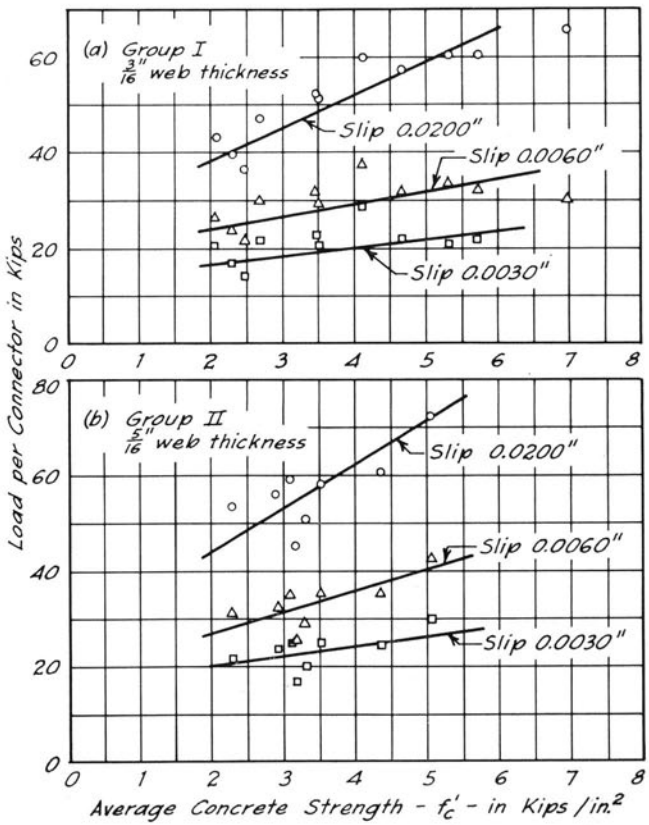

Fig. 8. Effect of Concrete Strength on Connector Load Capacity at Constant Slip

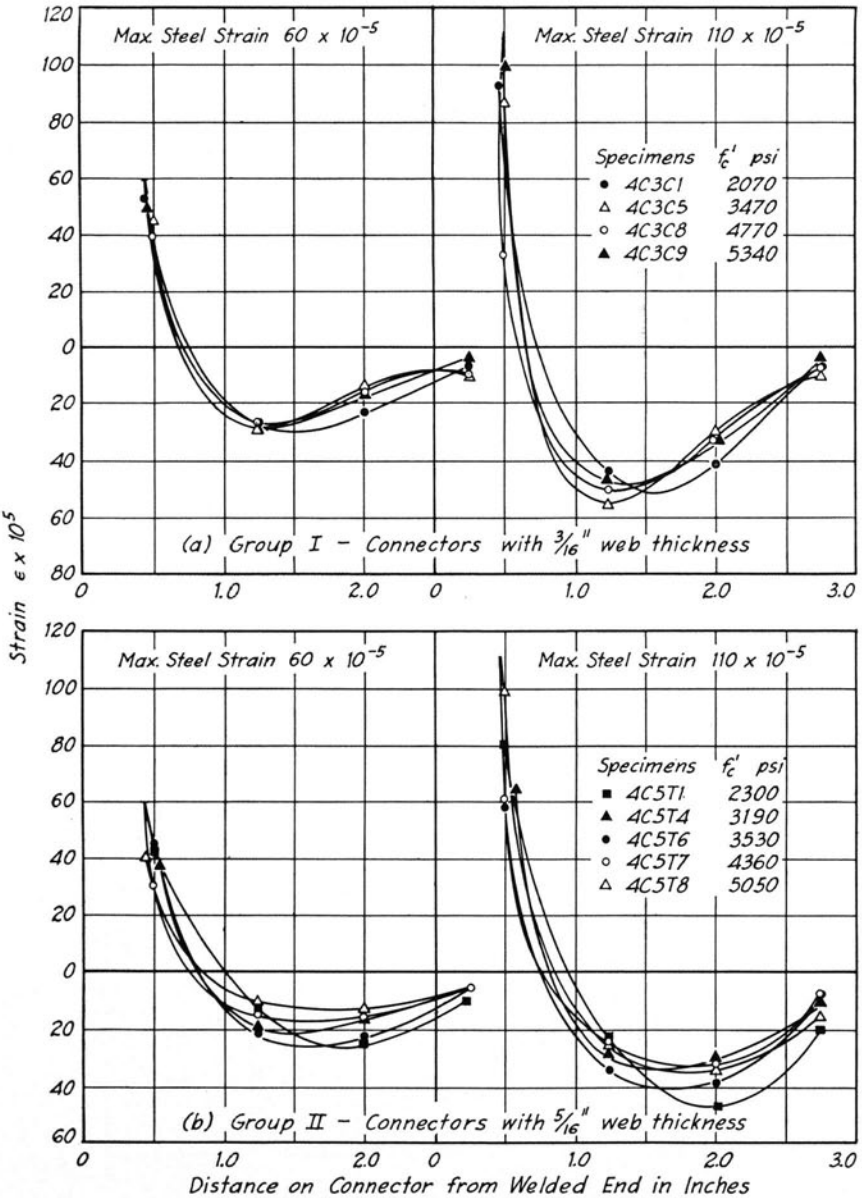

Fig. 9. Distribution of Strain in Webs of Channel Connectors at Constant Maximum Steel Strain

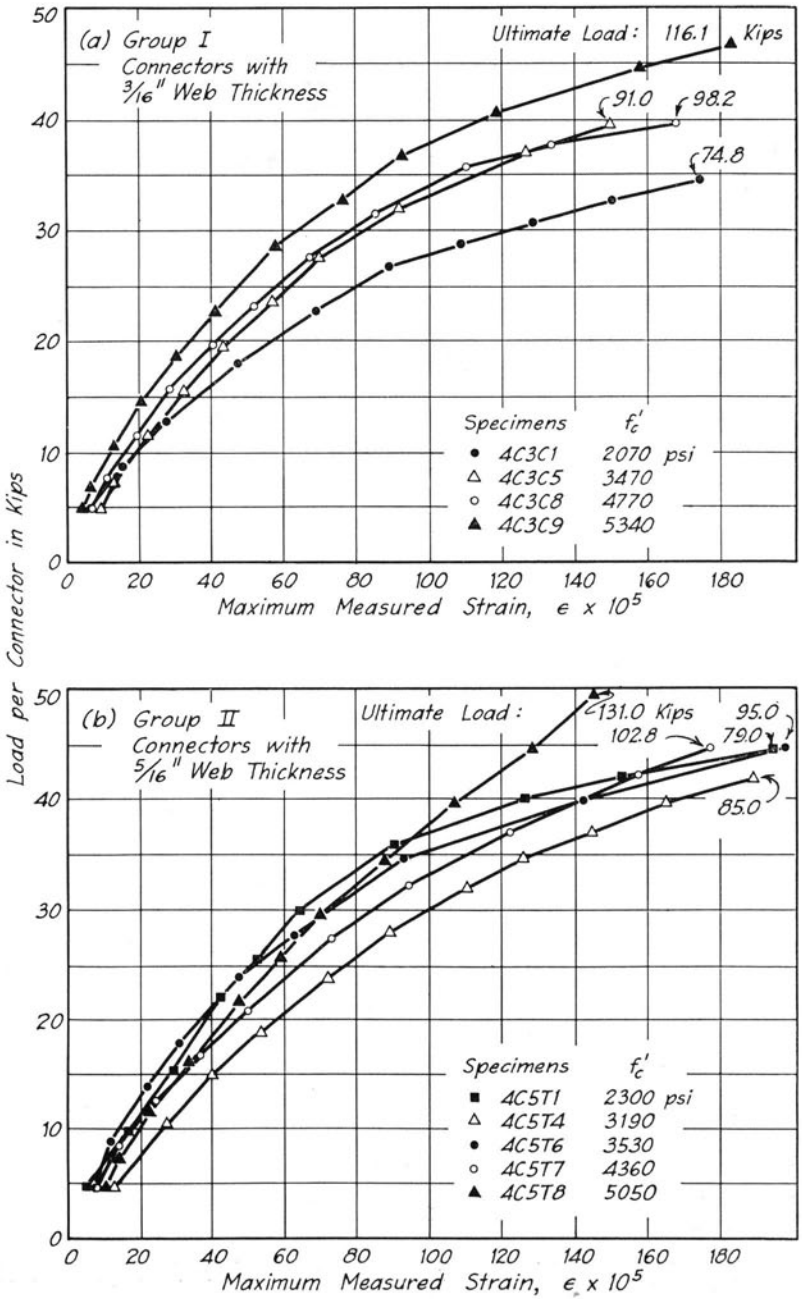

Fig. 10. Representative Load-Maximum Strain Curves, Group I and Group II

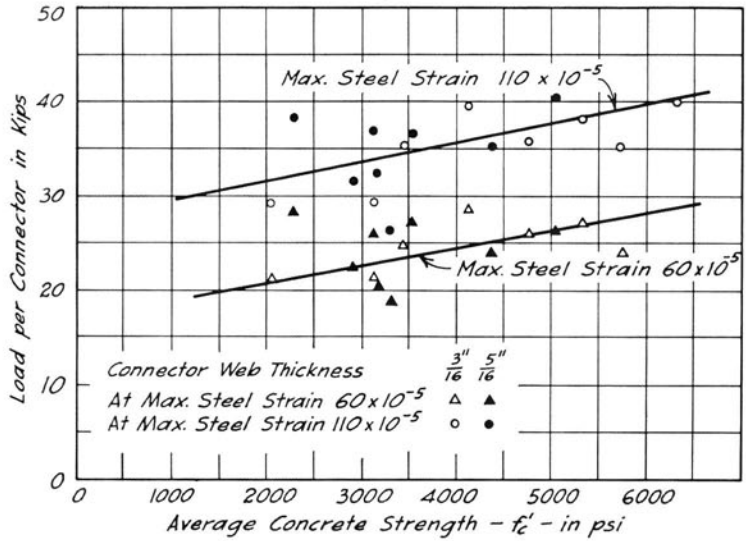

Fig. 11. Effect of Concrete Strength on Connector Load Capacity at Constant Maximum Steel Strain

to produce a given maximum strain. For the connectors included in Fig. 11 an increase of the concrete strength from 2000 to 6000 psi corresponds roughly to 30–40 percent increase in the load-carrying capacity. The capacity based on maximum strains seems to vary with the web thickness only slightly or not at all.

Thickness of Channel Web. Channel connectors with webs of four thicknesses were tested: $\frac{3}{16}$, $\frac{4}{16}$, $\frac{5}{16}$ and $\frac{8}{16}$ in. Connectors with $\frac{3}{16}$-in. and $\frac{5}{16}$-in. thick webs were made from 4-in. 5.4-lb and 4-in. 7.25-lb standard channels, connectors with $\frac{4}{16}$-in. webs were machined from a 4-in. 7.25-lb standard channel, and connectors with $\frac{8}{16}$-in. thick web were made from a 4-in. 13.8-lb car-building channel. The only variable in the first three types of connectors was the web thickness; the car-building channel differed also in the thickness of the flange. The effects of the web thickness on the behavior of channel connectors are illustrated in Figs. 12–14.

The load-slip curves for four push-out specimens with different web thicknesses are shown in Fig. 12. A decrease of slip with increasing web thickness is apparent from this figure. The rather large difference between the load-slip curves for specimens 4C5T6 and 4C8T was probably caused by combined effects of increased thickness of web and flange. The effect

of web thickness on slip is also illustrated in Fig. 13a, in which the loads per connector are plotted against web thickness at three values of slip. At a constant slip the load per connector increases with increasing web thickness. However, the increase of load is small: a 166-percent increase of web thickness corresponds to a load increase of only 30–40 percent.

The effect of web thickness on strain distribution is illustrated in Fig. 14 and its effect on maximum strain is shown in Fig. 13b and in Table 6. Connectors with thicker webs have a flatter strain distribution curve. At equal maximum strain, connectors with thicker webs carry more load than connectors with a smaller web thickness. It should be noticed, however, that a 166-percent increase of web thickness corresponds to only a 40-percent increase of load. Fig. 13b illustrates the reason why practically no effect of the web thickness on the load required to produce a certain maximum strain could be observed in Fig. 11: The difference between capacity of the connectors with $\frac{3}{16}$-in. and $\frac{5}{16}$-in. thick web is only of the order of 20 percent or less. Such a difference can easily be obscured by the scatter of the test results.

Thickness of Channel Flange. How the flange thickness affects slip and maximum strain of a flexible connector is shown in Figs. 15 and 16.

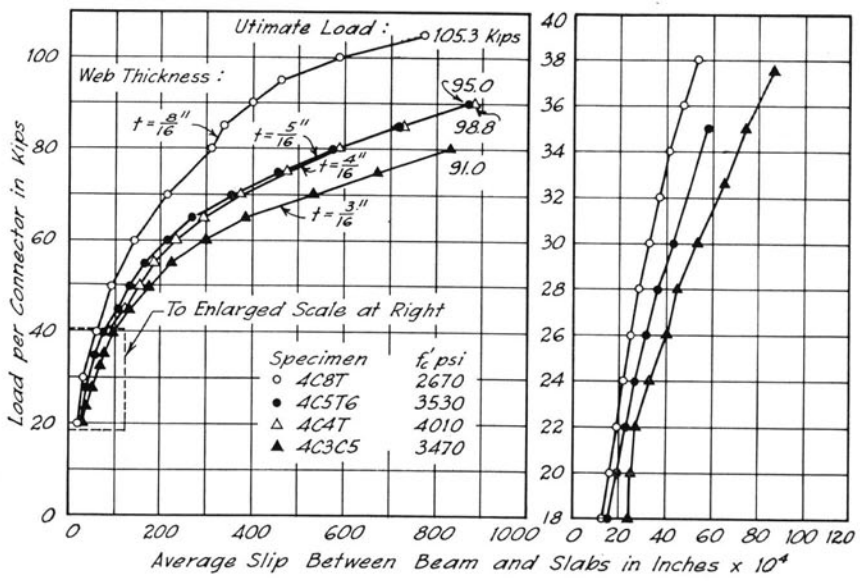

Fig. 12. Load-Slip Curves for Connectors with Various Web Thicknesses

In order to investigate the effects of this variable, special connectors were made of standard channels, plates or bars. Specimens 4C3S1 and 4C5S were made from standard channels by cutting off the flange on the side to be welded to the beam (Fig. 2, Type B). In these specimens comparatively large welds had a stiffening effect which is accounted for

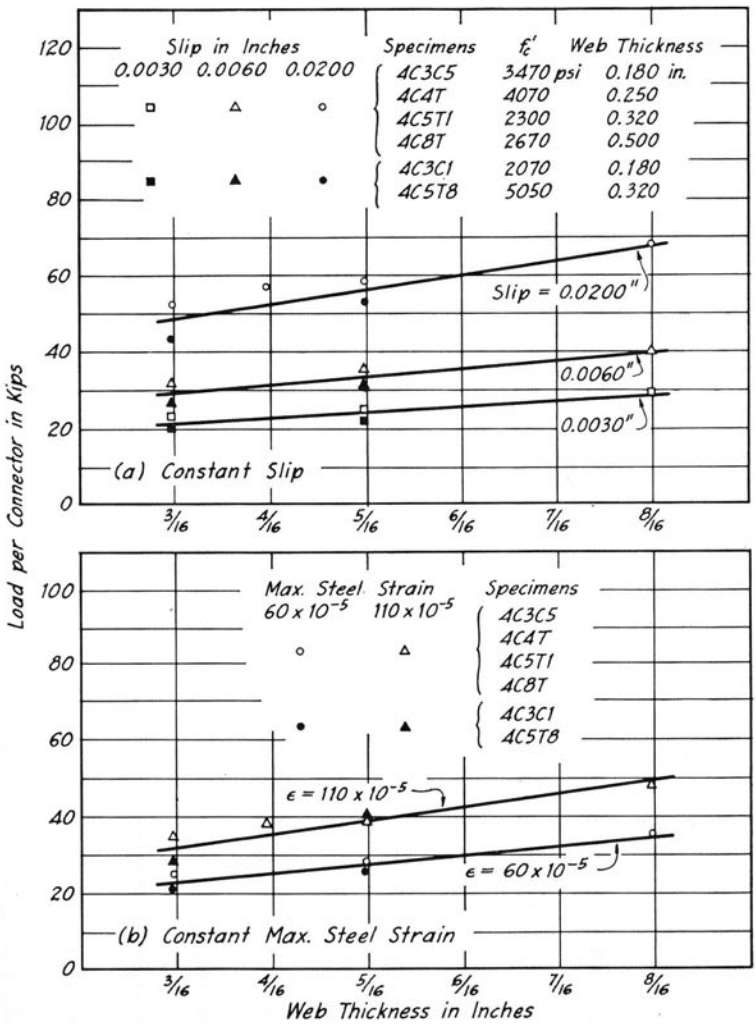

Fig. 13. Effect of Web Thickness on Connector Load Capacity at Constant Slip and Constant Maximum Steel Strain

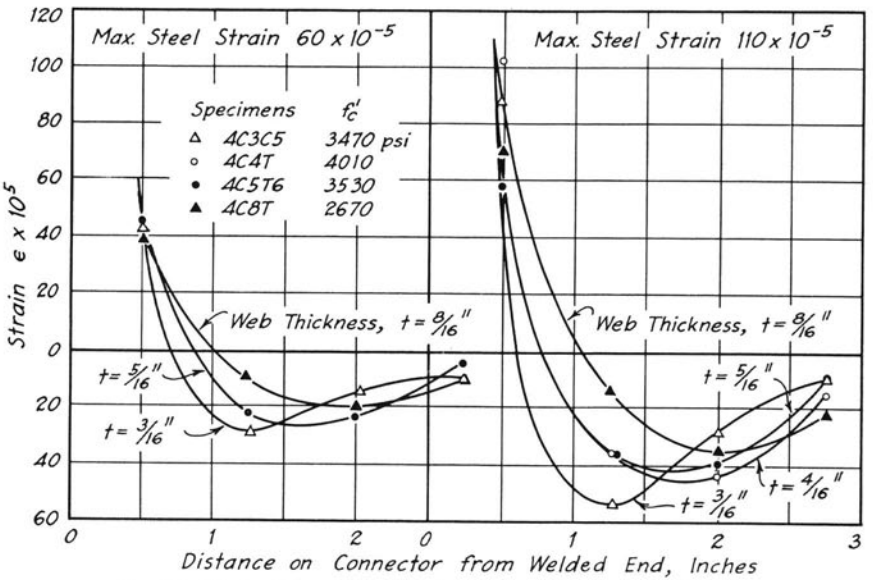

Fig. 14. Effect of Connector Web Thickness on Distribution of Strain

in Figs. 15 and 16 by assuming an effective flange thickness of 0.15 in. In specimen 4C3S2 the flange thickness was increased by adding a ½-in.-thick plate to a standard channel connector (Fig. 2, Type C). Connectors of one specimen were made from 0.5-in. plate and for two specimens from square steel bars.

The effect of the flange thickness on slip between the beam and the slabs is illustrated best in Figs. 15a and 16a, and the effect on maximum

Table 6
Load-Carrying Capacity of Connectors at Working and Yield Strains; Variation with Web Thickness

Specimen	Web Thickness, in.	Flange Thickness, in.	Av Concrete Strength, psi	Load per Connector in Kips at ϵ_{max} 60 x 10^{-5}	110 x 10^{-5}
4C3C5	0.180	0.413	3 470	24.9	35.1
4C4T	0.250	0.413	4 010	...	38.8
4C5T6	0.340	0.413	3 530	27.1	36.7
4C8T	0.500	0.531	2 670	35.6	47.7
4C3C9	0.180	0.413	5 340	27.2	38.2
4C5T8	0.320	0.413	5 050	26.3	40.4
4C3C8	0.180	0.413	4 770	26.0	36.0
4C5T7	0.320	0.413	4 360	23.8	35.3
4C3C4	0.180	0.413	3 140	21.3	29.3
4C5T3	0.320	0.413	3 130	26.0	37.0

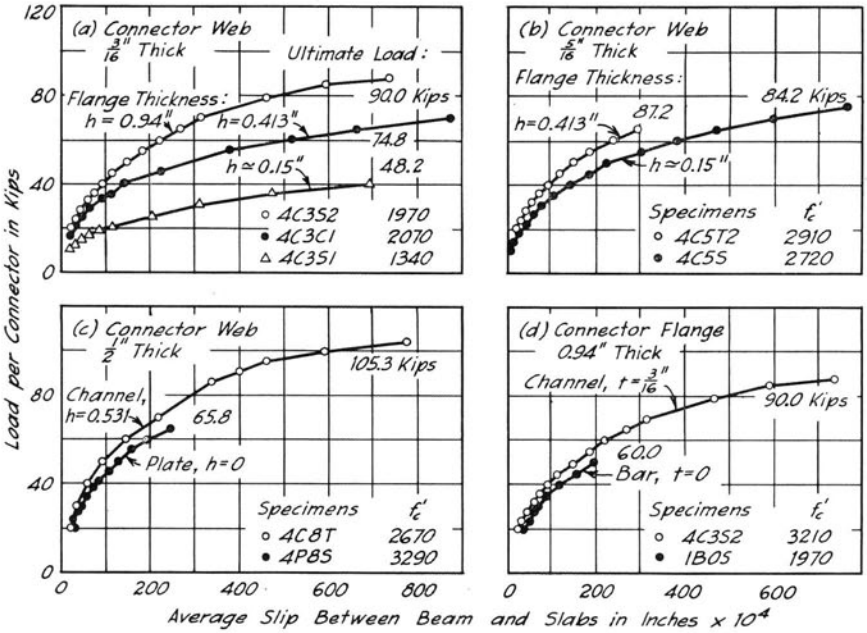

Fig. 15. Effect of Connector Flange Thickness on Load-Slip Curves

strain is shown in Fig. 16b. When the load is kept constant, an increase of the flange thickness causes a definite reduction of both slip and strain. The increase of flange thickness has a more pronounced effect on strain than it does on slip.

It is obvious that an increase of the thickness of the stiff flange results in a stronger connector. The magnitude of the strengthening effect depends, however, not only on the thickness of the flange but also on the thickness of the connector web. Comparison of the data in Fig. 15a and 15b illustrates this point. The effect of increasing the flange thickness is appreciably greater for connectors with webs $\frac{3}{16}$ in. thick (Fig. 15a) than for connectors with webs $\frac{5}{16}$ in. thick (Fig. 15b).

The effects of the flange and web thicknesses are interrelated. When the web is relatively thick the effect of the flange is rather small; on the other hand, when the flange is relatively thick the effect of the web is small. This is illustrated in Fig. 15c and 15d, in which load-slip curves for channel connectors are compared with similar curves for a plate and a bar connector respectively.

Height of Connector. The tests of small-scale shear connectors indicated very strongly and the strain readings in the full-scale tests (Figs. 9 and 14) confirmed the idea that the behavior of a channel connector is similar to that of a dowel embedded in an elastic medium. Some doubt remained, however, whether connectors of practical sizes may be investi-

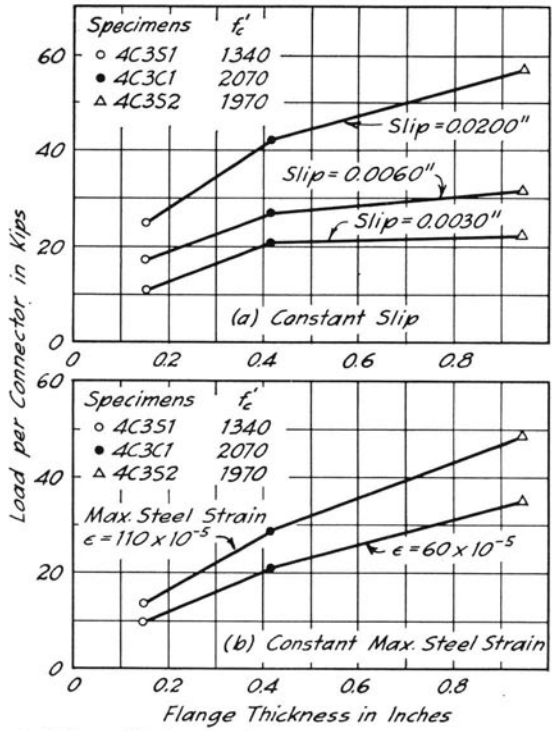

Fig. 16. Effect of Flange Thickness on Connector Load Capacity at Constant Slip and Constant Maximum Steel Strain

gated as infinitely long dowels or whether the height of the connector must be taken into account. Connectors of three heights were investigated for this purpose. The results of tests on specimens with shear connectors made from 3-in. 4.1-lb, 4-in. 5.4-lb and 5-in. 6.7-lb channels are shown in Figs. 17 and 18 and in Table 7. It should be noted that in these connectors the height was not the only variable; both the thicknesses of the web and of the flange increased slightly with increasing height.

In the upper part of Fig. 17 load-slip curves are given for several specimens for each height of connector. One specimen of each height was chosen on the basis of these curves and the load-slip curves for the selected specimens are compared in the lower part of Fig. 17. These load-slip curves differ only slightly and are in accord with the increases of the web and flange thicknesses. The strain distribution curves for connectors of different heights are compared in Fig. 18 and the load-carrying capacities at equal maximum strains are given in Table 7. Both the strain distribution curves and the load-carrying capacities are practically the same for the 4-in. and 5-in. connectors and consistently slightly different for the 3-in. connectors. The load-carrying capacities seem to be somewhat lower for the 3-in. connectors than for the two larger sizes.

These small differences might have been caused by the effect of the height of connector. Thus the strain data seem to indicate that the 3-in. connectors represent an approximate limit below which the effect of the connector height might be important.

Width of Connector. It was shown by the tests of small-scale shear connectors that the load-slip characteristics of a channel connector vary linearly with the width of the connector. If the channel acts as a dowel, a linear variation of slips and strains with connector width can be expected only for wide connectors. Since most of the specimens were 6 in. wide, specimen 4C3W1 with 5-in. wide connectors was tested to

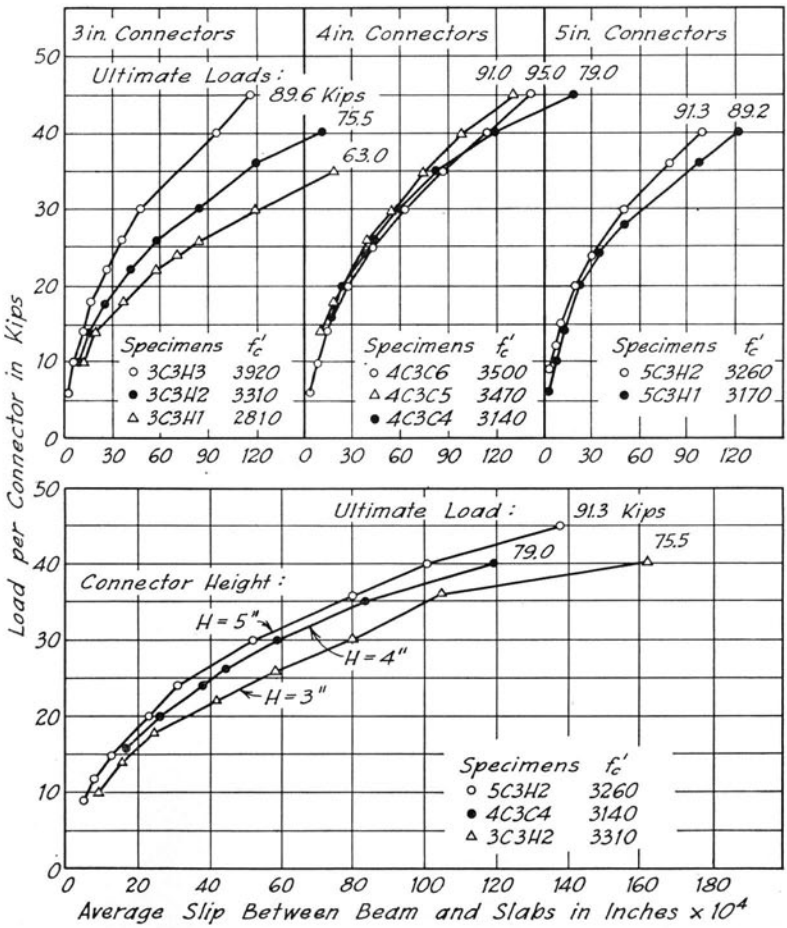

Fig. 17. Load-Slip Curves for Connectors of Various Heights

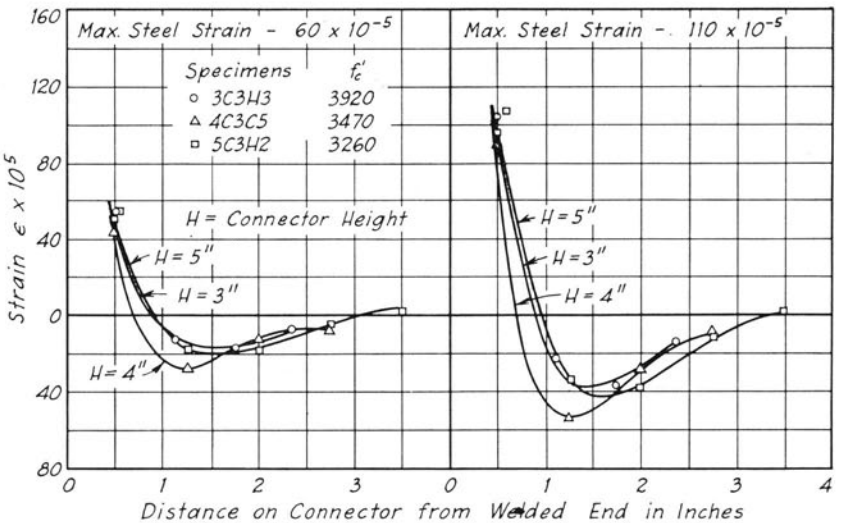

Fig. 18. Effect of Connector Height on Distribution of Strain

determine whether the connectors in these tests fall in the category of wide connectors. The results of the test of specimen 4C3W2 with 4-in.-wide connectors, tested as an auxiliary specimen for composite beam B21W, are also included in the study of the effects of connector width.

Load-slip and load-strain curves for specimen 4C3W1 are compared with corresponding curves for specimen 4C3C4 in Fig 19. In this figure the load per connector was divided by the connector width. The load-slip curves are practically equal for both connectors; therefore slip seems to be linearly proportional to the connector width.

On the other hand, there is a noticeable difference between the load-strain curves for connectors 4C3W1 and 4C3C4. That the strains do not

Table 7

Load-Carrying Capacity of Connectors at Working and Yield Strains; Variation with Connector Height

Specimen	Height of Connector, in.	Web Thickness, in.	Flange Thickness, in.	Av Concrete Strength, psi	Load per Connector in Kips at ϵ_{max} 60 x 10^{-5}	110 x 10^{-5}
3C3H2	3.0	0.170	0.377	3 310	18.5	25.3
3C3H3	3.0	0.170	0.377	3 920	22.6	32.2
4C3C4	4.0	0.180	0.413	3 140	21.3	29.3
4C3C5	4.0	0.180	0.413	3 470	24.9	35.1
5C3H1	5.0	0.190	0.450	3 170	20.7	29.0
5C3H2	5.0	0.190	0.450	3 260	27.3	34.8

seem to vary linearly with the connector width is brought out also in Table 8, in which test data for specimens 4C3W1 and 4C3W2 are compared with corresponding data for specimens 4C3C4 and 4C3C8. In both comparisons the unit load required to produce a certain maximum strain is larger for the narrower connectors. The differences are on the order of 20–30 percent. Whether these differences were accidental or were caused by the relatively small width of connector cannot be said on the basis of the data available.

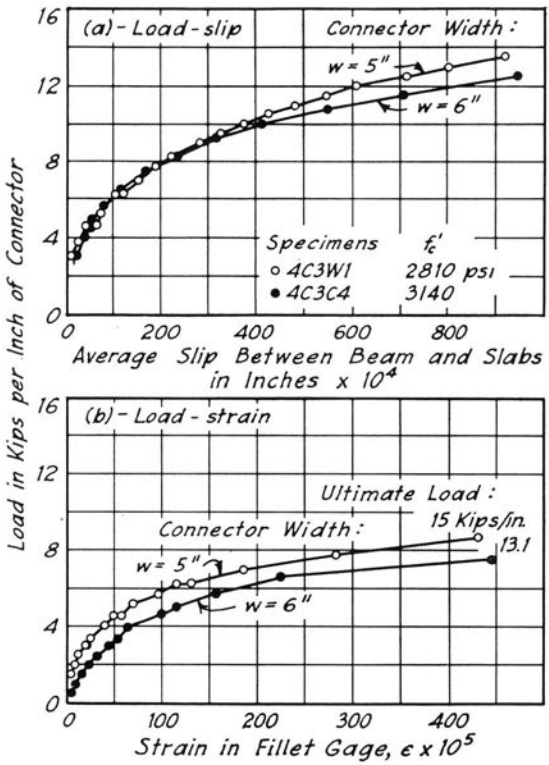

Fig. 19. Effect of Connector Width on Load-Slip and Load-Strain Curves

Concrete Fillet. Specimens of Group VI were tested to determine whether a lowering of the restraint of concrete adjacent to a shear connector affects the behavior of a channel connector. An attempt was made to decrease the restraint by placing a concrete fillet between the flanges of the steel beam and the main body of the concrete slabs (Fig. 1b). Shear connectors in five specimens were made from 4-in. 5.4-lb standard

Table 8
Unit Load-Carrying Capacity of Connectors at Working and Yield Strains; Variation with Connector Width

Specimen	Width of Connector, in.	Av Concrete Strength, psi	Load per one inch of Connector Width in Kips at ϵ_{max} 60×10^{-5}	110×10^{-5}
4C3W1	5.0	2 810	4.9	6.1
4C3C4	6.0	3 140	3.6	4.9
4C3W2*	4.0	4 430	6.6	7.9
4C3C8	6.0	4 770	4.3	6.0

*In this specimen no attempt was made to destroy natural bond between slabs and beam.

channels, in one specimen from 4-in. 7.25-lb standard channels, and in one specimen from 1-in. square steel bar. In specimen 4C3F5 the shear connectors extended throughout the width of the fillet; in all other specimens the connectors had a 1-in. concrete cover on each side.

The test results are presented in Figs. 20–22 and in Table 9. Load-slip curves for 4C3F1, 4C3F2 and 4C3F4 are shown in Fig. 20. Specimen 4C3F3 was omitted from all comparisons for reasons discussed in Section 11. The remaining specimens of Group VI had some additional variables and therefore could not be compared directly. Figure 20 illustrates that the effect of concrete strength on the load-slip characteristics of the channel connectors of Group VI was similar to that for specimens without the concrete fillet. The range of load-slip curves for fillet specimens is compared with a corresponding range for standard specimens in Fig. 21. There seems to be no significant difference between the load-slip curves for the two types of specimen.

The strain distribution for connectors embedded in a concrete fillet is shown in Fig. 22. In this figure, curves are plotted separately for gages on the front and back sides of the channel. The strains on the front side of the channels were tensions at locations close to the welded

Table 9
Load-Carrying Capacity of Connectors at Working and Yield Strains; Effect of Concrete Fillet

Specimen	Type of Concrete Slab	Av Concrete Strength, psi	Load per Connector in Kips at ϵ_{max} 60×10^{-5}	110×10^{-5}
4C3F1	with fillet	2 580	17.2	24.2
4C3C1	no fillet	2 070	21.2	29.1
4C3F4	with fillet	4 690	30.0	45.2
4C3C8	no fillet	4 770	26.0	36.0
4C5F	with fillet	2 170	30.2	38.3
4C5T1	no fillet	2 300	28.4	38.4

end of the connectors and compressions at locations further removed from the welded end; on the back side of these channels compressive strains were measured at locations close to the welded end while tensile strains were measured at locations further removed from the welded end. To make the visual comparison easier, however, these strains are plotted

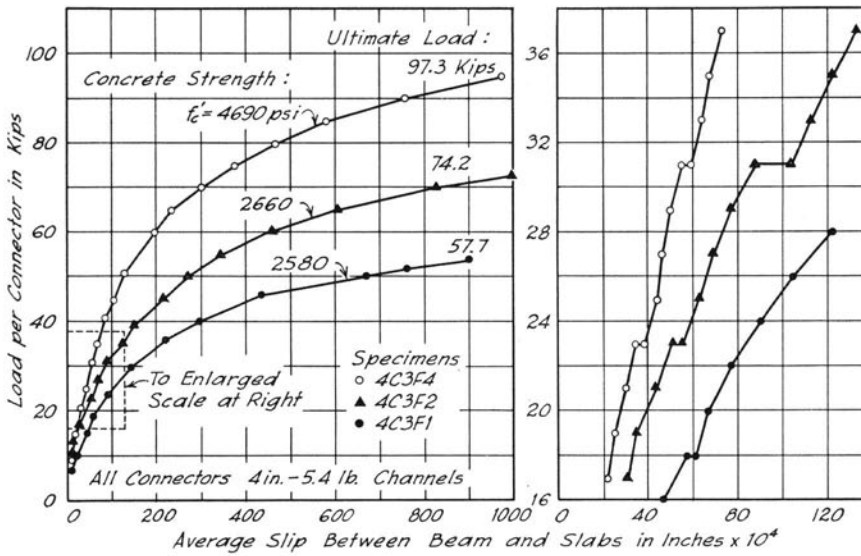

Fig. 20. Representative Load-Slip Curves, Group VI (Specimens with Concrete Fillet)

as if the corresponding strains on two sides of the channels were of the same sign. The curves for strains measured at the front side lie consistently below those for the strains at the back side. This phenomenon seems to be typical of all specimens tested with intermittently released loading—not only for specimens with the concrete fillets. The reasons for the differences between the strains on the front and the back sides of the channel are discussed in Section 13.

Average strain distribution curves for fillet specimens are also shown in Fig. 22 and loads at equal maximum strain are compared in Table 9. When compared with corresponding specimens without fillets, no consistent effects of the concrete fillet on average strains can be observed.

The only fairly consistent differences found between the specimens with and without fillets were in the magnitudes of ultimate loads (Table 5) and the manner of failure (Table 5 and Section 15).

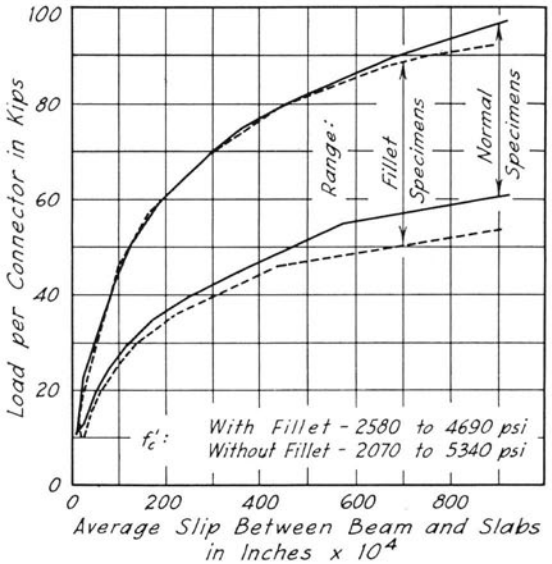

Fig. 21. Effect of Concrete Fillet on Range of Load-Slip Curves due to Variations of Concrete Strength

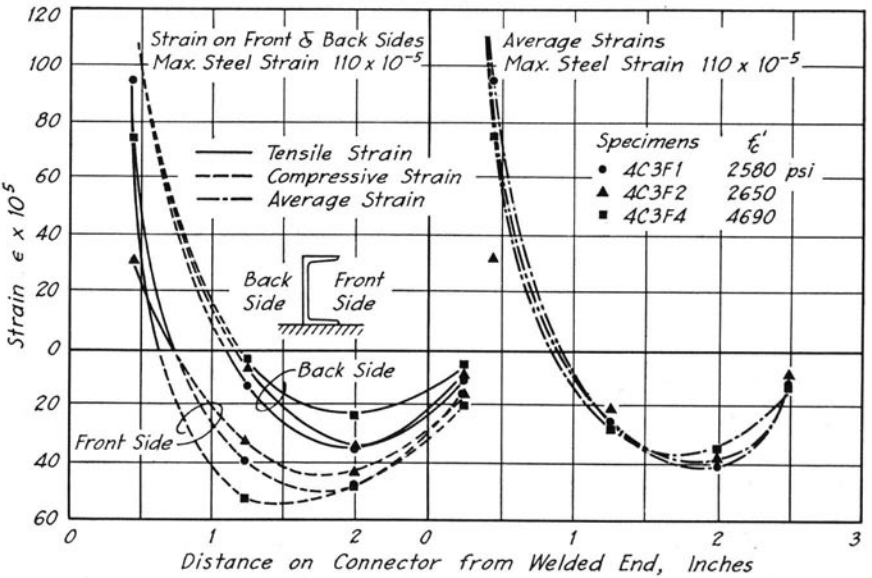

Fig. 22. Distribution of Strains in Connectors Embedded in Concrete Fillet

13. Effects of Testing Techniques

Most of the push-out specimens had applied to them continuously increasing increments of load, the load being applied to the front face of the channel (Fig. 1). It seemed important to investigate whether either an intermittently released loading or the orientation of a channel connector with respect to the load has any effect on the test results. It was also desired to find whether the presence of the waterproofing material on the loaded side of the channel had any significant effect. Several specimens were made in order to investigate such effects; the test results are reported in this section.

Intermittently Released Loading. Nineteen specimens were tested with intermittently released loading. The effects on the load-slip and the load-strain characteristics were consistent for all tests. For this reason the results from only two tests are reported.

Complete load-slip and load-maximum strain curves as well as residual slips and strains for specimen 4C8T are presented in Fig. 23. In this figure practically no residual slip or strain can be observed for the first two removals of the load. Some larger residuals are indicated for the next three removals of load; and a very marked increase of residuals is shown for the last removal of load. This behavior is in complete agreement with the results of the tests of the small-scale push-out specimens and may be explained by the following hypothesis. At low loads both the stresses in the steel and the concrete are elastic; at intermediately high loads some permanent deformations take place in the concrete, whereas the steel stresses are still elastic. Thus up to first yielding of the connectors, friction between the beam and the slab is responsible for the residual slip and strain. As soon as yielding occurs in the shear connectors large residuals are to be expected.

A comparison between the results of tests with intermittently released and continuously increased loading is shown in Fig. 24. In this figure load-slip and load-strain curves for connectors 4C3C9 with intermittently released loading are compared with corresponding curves for specimen 4C3C8 with continuous loading. The virgin curves, that is the curves connecting points representing first loading for each particular load, for specimen 4C3C9 are slightly higher than the curves for 4C3C8. The slight difference may be attributed to the higher strength concrete used in specimen 4C3C9.

This intermittently released loading has noticeable influence on the strain distribution along the channel web. While the differences between the strains measured on the two faces of the web were inconsistent in the tests of specimens loaded with continuously increasing increments of load, a consistent difference was observed for most of the specimens

loaded with intermittently released loading (Fig. 22). It is believed that this different behavior was due to the presence of bond on both sides of the connector web in the first type of test and the presence of friction on one side only in the case of intermittently released loading. However, it is important that no significant differences between the average strain distribution curves were found.

Orientation of Channel with Respect to Direction of Load. In specimen 4C3D2 the channel connectors were welded to the beams with flanges turned up so that the load was applied to the back side of the connectors; this represents a condition exactly opposite to that of the

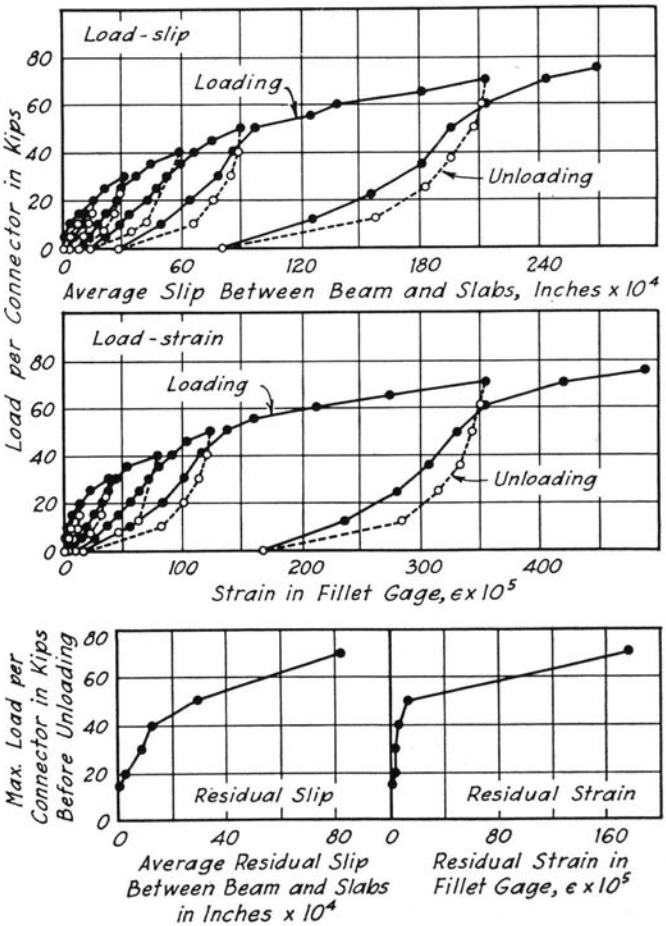

Fig. 23. Load-Slip and Load-Strain Curves for Connector 4C8T Subjected to Intermittently Released Loading

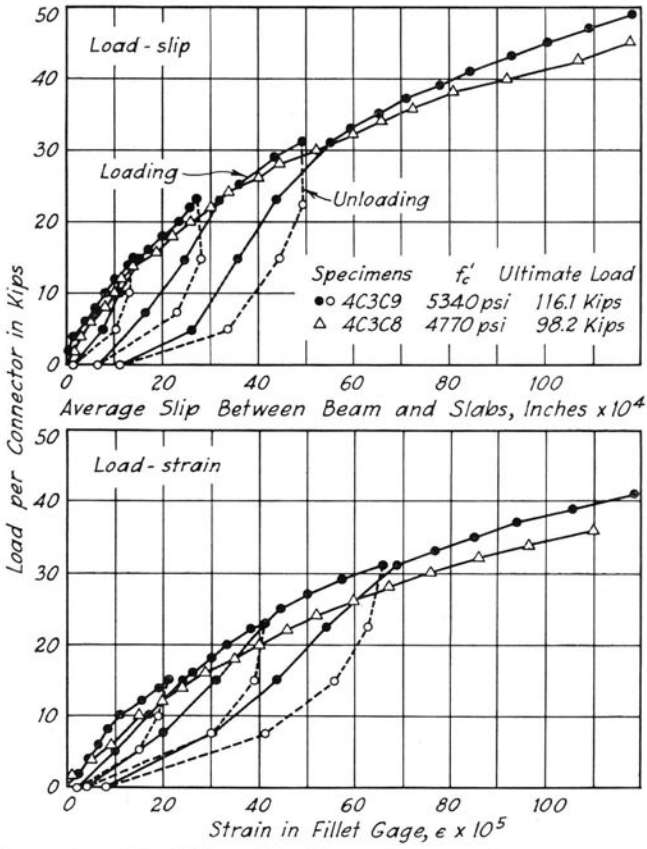

Fig. 24. Comparison of Load-Slip and Load-Strain Curves for Continuously Increased and Intermittently Released Loading

usual specimen. The load-slip and the load-maximum strain curves for this specimen are plotted in Fig. 25 and compared with corresponding curves for connectors 4C3C4 and 4C3C5, in which connectors were loaded on the fillet side. Such differences as exist between these curves are small and well within the range of experimental inaccuracies. The distribution of strain, not shown in this bulletin, was not affected by the reversed direction of load.

Waterproofing of Strain Gages. The waterproofing material covered one-sixth of the channel surface. Specimen 4C3D1 was built with strain gages on the unloaded side of the web only, to find out whether the presence of the waterproofing material had any significant effect on the

behavior of channel connectors. Specimen 4C3D1 was loaded in the same manner as specimen 4C3D2. The load-slip and load-maximum strain curves for these two specimens are compared in Fig. 26. Up to a load of about 55 kips per connector the load-slip curves for both specimens are practically identical. The load-strain curve for the connector with gages on the unloaded side only is consistently lower than the corresponding curve for the connector with gages on both sides of the channel. However, the difference is not large; moreover, it would be expected that the presence of waterproofing material would have just the opposite effect. The strain distribution curves, not shown in this bulletin, also indicate that the strain readings on the fillet gage of specimen 4C3D1

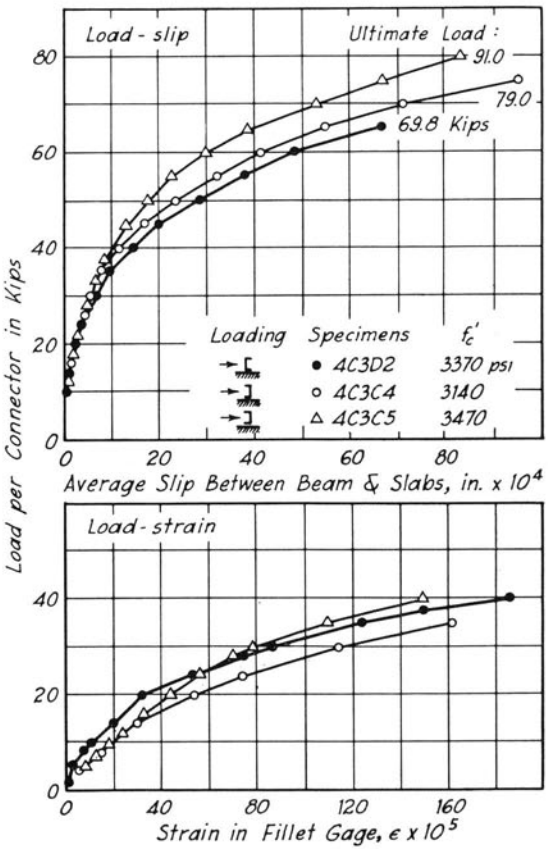

Fig. 25. Effect of Orientation of Channel on Load-Slip and Load-Strain Curves

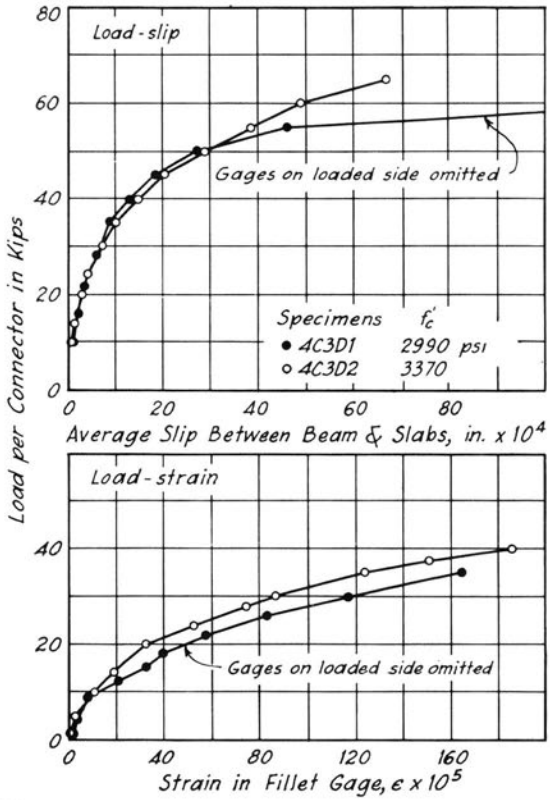

Fig. 26. Effect of Waterproofing Material on Load-Slip and Load-Strain Curves

were low, but the general shape of the strain distribution curves for specimens 4C3D1 and 4C3D2 were in good agreement. It may be concluded that the presence of the waterproofing material on the loaded side of the connector web did not have any significant effect on test results.

14. Distribution of Load on Channel Shear Connectors

The strain distribution curves and the quantitative studies of the test results reported in the previous sections confirmed the hypothesis that the behavior of a channel shear connector is similar to that of a dowel embedded in an elastic medium. It seemed desirable at this point to find out how the reaction of the concrete is distributed along the channel and how the total load transferred by a channel connector is apportioned to the flexible web and the stiff flange respectively.* This was done on the basis of measured strains as follows.

* In the following discussion the flexible web of a channel connector is called "flexible portion" and the stiff flange welded to the beam is called "stiff portion of the connector."

For twelve representative push-out specimens strains measured at two or three loads were converted to moments with the aid of the moment-strain ratios determined from the bare-connector tests of the particular specimens (Section 10). Then a cut-and-try analysis was made separately for every load and specimen. The connector was considered as a cantilever loaded with a continuously varying distributed load. Moments were computed from an assumed continuously varying distributed load by a step-by-step procedure * and compared with the moments determined from the measured strains. When the two sets of moments did not agree, the assumed load was changed to give a better approximation and moments were computed again. This procedure was repeated until a satisfactory agreement was obtained between the computed and known moments.† The load for the last cycle of computations was assumed as the reaction exerted by the concrete on the channel.

Reaction, shear, moment and strain distribution curves for connectors 4C3C8 and 4C8T determined in the described manner are shown in Fig. 27. It can be seen from this figure that the reaction of the concrete is distributed nonuniformly and has both positive and negative values. The reaction has the largest absolute values at locations close to the end welded to the beam, and its magnitude decreases rapidly toward the free flange of the connector.

The area under the reaction curve represents the load transmitted by the flexible portion of the connector. The difference between the total load on the connector and the load on the flexible portion must then be carried by the stiff portion. The total load and the loads apportioned to the flexible and stiff portions are presented in Table 10 for all twelve connectors for which such analyses were made. It can be seen that in all cases listed in Table 10 the load carried by the stiff portion is considerably greater than that carried by the flexible portion. The percentage of the load carried by the flexible portion increases with increasing load and with increasing web thickness; it decreases with increasing concrete strength and with increasing flange thickness. If it is assumed that the reaction is distributed uniformly over the stiff portion, the magnitude of the reaction for the listed connectors varies from 1.3 to 4.7 times the compressive cylinder strength of the concrete. As failure of the concrete in compression was not observed at those loads, a triaxial state of stress must have been present in the concrete adjacent to the stiff portion. All these results are in agreement with the observations which were made directly from the test data.

* N. M. Newmark, "Numerical Procedure for Computing Deflections, Moments and Buckling Loads," Trans. ASCE, 1943, Vol. 108, pp. 1161–1234.

† An inverse procedure—that is, computation of the load from the known moments—could not be used with confidence because it would have required two numerical differentiations which are very sensitive to the errors in the moment distribution curves.

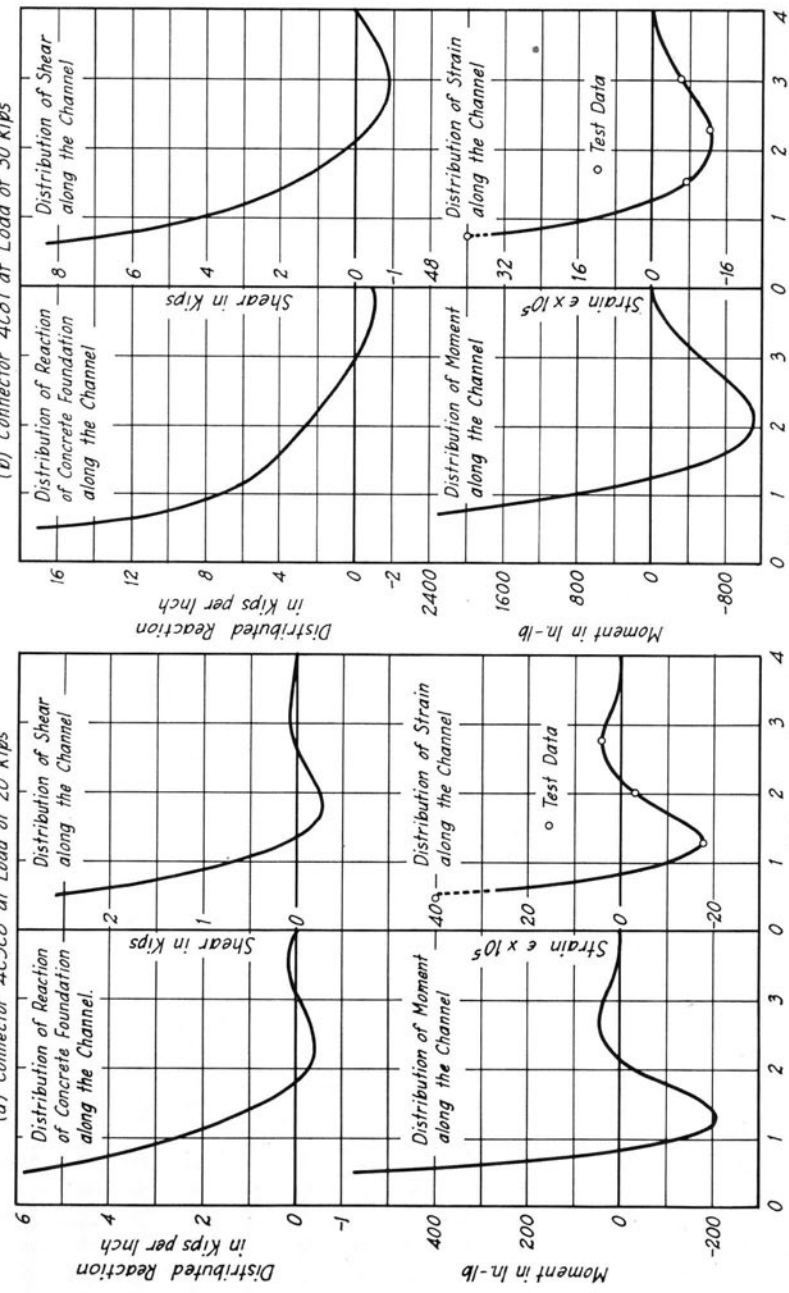

Fig. 27. Reaction, Shear, Moment, and Strain Distribution Curves for Connectors 4C3C8 and 4C8T

Table 10
Apportionment of Load on Shear Connector Between Flexible and Stiff Portions

Specimen	Total Load on Shear Connector, lb	Load on Flexible Portion, lb	Load on Flexible Portion, % of Total	Load on Stiff Portion, lb	Load on Stiff Portion, % of Total
4C3C1	20 000	3 480	17.4	16 520	82.6
	30 000	6 880	22.9	23 120	77.1
4C3C5	20 000	2 650	13.2	17 360	86.8
	30 000	5 470	18.2	24 530	81.8
4C3C8	20 000	2 270	11.3	17 730	88.7
	30 000	3 800	12.7	26 200	87.3
4C3C9	20 000	1 860	9.3	18 140	90.7
	30 000	3 170	10.6	26 830	89.4
	40 000	6 840	17.1	33 160	82.9
4C5T1	20 000	4 750	23.7	15 250	76.3
	30 000	6 900	23.0	23 100	77.0
	40 000	13 100	32.7	26 900	67.3
4C5T2	20 000	5 850	29.2	14 170	70.8
	30 000	9 840	32.8	20 160	67.2
4C5T6	20 000	3 590	18.0	16 410	82.0
	30 000	7 070	23.6	22 930	76.4
	40 000	12 380	30.9	27 620	69.1
4C5T8	20 000	3 560	17.9	16 440	82.1
	30 000	6 320	21.1	23 680	78.9
	40 000	10 300	25.7	29 700	74.3
4C8T	30 000	7 850	26.2	22 150	73.8
	40 000	12 320	30.8	27 680	69.2
3C3H3	20 000	2 100	10.5	17 900	89.5
	30 000	4 640	15.5	25 360	84.5
5C3H2	20 000	2 510	12.5	17 490	87.5
	30 000	4 340	14.5	25 660	85.5
4C3S2	30 000	2 240	7.4	27 760	92.6
	40 000	3 830	9.5	36 170	90.5
	50 000	5 850	11.8	44 150	88.2

15. Manner of Failure of Push-out Specimens

The manners of failure of the push-out specimens and the ultimate loads for the individual shear connectors are listed in Table 5. With exception of four, all specimens with flexible connectors and with slabs cast flush with the flanges of the I-beam, failed by tensile cracking of the slabs. As a rule, one horizontal and one vertical crack appeared first at the outside faces of slabs and then spread toward the inside slab surfaces. Some separation of the slabs from the beams was noted in all specimens prior to failure, but no crushing of concrete could be detected. After each test, the slabs were broken from the beam, and a subsequent inspection revealed crushed concrete at locations immediately under the connectors and adjacent to the beam. The crushed zone was limited to a very small area under the welded flange of the connector. It was impossible to determine directly whether the concrete was crushed before or after the tensile failure occurred, but from the shapes of the load-slip curves it seemed certain that this crushing must have taken place either at loads just slightly lower than the ultimate or just after the ultimate load had been reached.

The tensile failure of the slab is characteristic of push-out specimens without any reinforcement or with weak reinforcement; and it cannot take place in the slab of a composite T-beam. Hence the ultimate loads for specimens failing by tensile cracking of the slabs have little significance and can be regarded only as some lower limit which this type of shear connector can undoubtedly develop.

Four specimens with concrete slabs cast flush with the I-beam flanges and with flexible connectors failed in the connecting welds. In specimen 4C3C11 with 6-in. wide channel connectors and concrete strength of 6320 psi and in specimen 4C3W2 with 4-in. wide channel connectors and concrete strength of 4430 psi, the welds failed on one channel only. The upper weld, subject to shear and compression, failed on a vertical plane flush with the surface of the beam flange; the failure plane of the lower weld, subject to shear and tension, was that of the minimum weld cross-section. It seems obvious that the upper weld failed in shear and the lower one in tension. Other specimens which failed by shearing of the welds of one connector were 4P8T and 4C3S1. In these specimens the connectors had no flange on the welded end, and the failure occurred by shear. The ultimate capacities of the welded connections were computed on the basis of an ultimate shearing strength of 59,000 psi and an ultimate tensile strength of 80,000 psi.* The computed maximum loads compare favorably with the measured ultimate loads:

	Ultimate Loads in Kips	
Specimen	Computed	Measured
4C3C11	130.4	118.2
4C3W2	86.9	81.9
4P8T	66.4	65.8

The ultimate load for specimen 4C3S1 could not be computed because the weld areas were not known.

All three specimens with stiff shear connectors failed by separation of the slabs from the beam followed by the shearing of a wedge of concrete from under the connectors. The concrete under the connectors was crushed. The distribution of pressure under the connector must have been uniform or close to it. The following pressures at failure were computed on the basis of a uniform pressure distribution:

* Values of the ultimate shearing and tensile strengths were taken from the Univ. of Ill. Eng. Exp. Sta. Bul. 380, "Fatigue Strength of Fillet-Weld, Plug-Weld, and Slot-Weld Joints Connecting Steel Structural Members," by W. M. Wilson, W. H. Munse and W. H. Bruckner, pp. 32 and 89, Table 48.

Specimen	Pressure on Concrete at failure, f'_{co} psi	Ratio f'_{co}/f'_c
1.25B0S	10 930	3.5
1B0S	10 660	3.3
1B0F	8 000	3.6

It is believed that the failure would not have occurred even at these loads if the separation of slabs from the beam had been prevented.*

Concrete fillets between the slabs and the beam had a profound effect on the manner of failure of push-out specimens. All specimens made with concrete fillets, except specimen 4C3F3, failed by shearing of a wedge of concrete from under the connector. This final failure was preceded by a slight separation of the concrete slabs from the beam, by bulging of the concrete on the sides of the fillets just below the location of the shear connectors, and by appearance of several inclined cracks on the fillet side faces. In one specimen horizontal tensile cracks appeared on the inside faces of the slabs proper. The ultimate loads for specimens with fillets, however, were on the average only 6.5 percent lower than the ultimate loads of corresponding specimens without fillets.

C. DISCUSSION OF TEST RESULTS

16. Dowel-like Behavior of Channel Shear Connectors

Tests of 43 push-out specimens were made for the purpose of investigating the behavior of channel shear connectors. The results of the small-scale tests indicated that a channel shear connector acts as a dowel.† This finding was fully confirmed by the full-scale tests reported in this bulletin. According to the dowel concept the pressure, shear, and moment distribution curves have the form of a wave with rapidly diminishing amplitude. The maximum values of these curves are located at the welded end of the channel connector, so that the critical concrete pressure and the maximum moment are located at this section. However, because of the shape of the channel, the critical moment section is at the fillet between the channel web and flange welded to the beam. Furthermore, the dowel concept brings out the fact that the largest part of the load transmitted by a channel connector is carried by the sections

* That the concrete under a shear connector is capable of resisting stresses several times larger than the cylinder strength of the concrete has been shown by Roš, reference 29, p. 41, Fig. 15, and by Graf, reference 93, p. 209, Table 1.

† Reference 112, pp. 56–59, Section 20.

adjacent to the welded end; consequently the major portion of the web and free flange are unimportant for the transfer of load.

17. Maximum Stresses in Channel Shear Connectors

Maximum stress in a channel shear connector occurs at the fillet between the web and the welded flange. Its magnitude depends on the apportionment of the total load carried by the connector to the flexible web and the stiff flange. Thus the maximum stress is affected appreciably by the thickness of the stiff flange and to a lesser degree by the web thickness and the strength of the concrete.

The distribution of the load transmitted by the flexible web also influences the magnitude of the maximum stress but this effect is less pronounced than that of the apportionment of load. The distribution of the load carried by the flexible web is nonuniform and its nonuniformity increases with decreasing thickness of web and with decreasing strength of concrete. The more nonuniform the distribution, the closer the resultant is located to the critical moment section; in other words, the smaller is the moment causing the maximum stress. The decrease of the critical moment with decreasing web thickness offsets partly the decrease of the section modulus. Similar reasoning applies to the effect of the strength of concrete: the higher the concrete strength the larger the critical moment but at the same time the smaller the load carried by the flexible web. As a result, the maximum stress is affected very little by the strength of concrete.

18. Stresses in Concrete Adjacent to Channel Connector

The dowel-like action of a channel connector and the presence of the stiff flange next to the beam result in a large concentration of pressure on the adjacent concrete. Because the pressure decreases very rapidly toward the free flange, only the stresses in the concrete located next to the beam are of practical interest. It has been shown in the previous sections that concrete at this location is capable of carrying stresses several times larger than its compressive cylinder strength. These high stresses can exist because a state of triaxial compression is present in the concrete under the connector. The lateral restraint is offered on three sides by the surrounding concrete and one side by the flange of the beam. The slab thickness will always be sufficient to offer the needed restraint.

In a fillet the concrete cover on the two sides of a connector might prove to be the point of weakness. With one exception, all specimens with

concrete fillet failed at that location. In these specimens the concrete cover was 1 in. thick. Thus it seems desirable that the minimum cover should be thicker than 1 in. How much thicker, cannot be determined from the results of these tests.

From the standpoint of lateral restraint, it is also important that the slab and the beam be held firmly together since the tests of push-out specimens indicate that a separation of those two elements leads eventually to failure of concrete. It is imperative, therefore, that the slab be anchored to the beam in the direction normal to the contact surfaces of the two elements.

19. Connection of Channel Connectors to Beam

For channel connectors connected to the beam by welds in the same way as in the reported tests, the welded connection will seldom be critical. The loads actually carried by the welded connections used in these tests were approximately six times greater than the allowable loads for these welds as computed from the current specifications for welded highway bridges.*

20. Effect of Shape of Channel on Load-Carrying Capacity of Connectors

Most of the push-out specimens failed by tensile cracking of the slabs. Since such failures were functions of the dimensions of the slabs rather than of the shape of channel, the effect of the dimensions of various parts of a channel on the ultimate load-carrying capacity of a channel connector could not be established from these tests. Therefore these effects had to be determined from comparisons based on loads producing equal slip and equal maximum strains. It was found that the load-carrying capacity of a channel connector of practical dimensions is affected by the strength of concrete, by the channel web thickness, by the thickness of the channel flange welded to the beam, and by the width of the connector. It is not affected by the height of the channel. The effect of the concrete strength is discussed in Section 22. The effects of the other variables are discussed in the following paragraph.

As would be expected, the effect of the width of a channel connector on its load-carrying capacity may be considered linear for all practical purposes. The quantitative effects of the web and flange thicknesses depend on the ratio of these two dimensions and on the stiffness of the

* "Standard Specifications for Welded Highway and Railway Bridges," Fourth Edition, American Welding Society, 1947, p. 10, Article 209c.

flexible web relative to that of the surrounding concrete. Therefore they have to be determined individually for each specific case. Nevertheless, the qualitative effect of these variables was well brought out by the tests of push-out specimens. A comparison of Figs. 13a and 16a shows that on the basis of equal slip the load-carrying capacity of a channel connector is affected by both the web and flange thickness in about the same manner. On the other hand, a comparison on the basis of equal maximum strains (Figs. 13b and 16b) shows that the increase of the flange thickness increases the load-carrying capacity of a channel connector more effectively than an increase of the web thickness.

In addition, the tests indicated that the presence of the free flange was effective in delaying the tendency of the slabs to separate from the beam and thus must have delayed the failure. The slip measured at the last load increment before failure was about 0.1 in. or more for all specimens with anchored shear connectors. On the other hand, the corresponding slip for bar connectors, which did not have any anchorage, did not exceed 0.05 in. The shape of the load-slip curves for the bar connectors indicate also that if separation had not occurred the specimens probably would have carried a higher load.

21. Characteristics of Desirable Shapes of Flexible Connectors

On the basis of the foregoing discussion certain conclusions may be drawn regarding the desirable shape of a flexible connector. The most effective flexible connector will have a very thick flange welded to the beam. This flange does not need to be long, but it is imperative that it be stiff enough to prevent bending. The web of a flexible connector does not contribute much to the load-carrying capacity directly; it should be, therefore, as thin as practicable. A free flange is a "must" of a good connector; it should be fairly long and must be connected rigidly to the web. This flange may be fairly light. The height of a flexible connector should be large enough to extend well into the body of the slab.

Among the steel shapes rolled at the present time, the lightest types of bulb angles might give the most effective shear connectors of the flexible type. However, no tests were made with bulb angles. From rolled steel channels the lightest shapes are very effective and at the same time economical shear connectors.

22. Effect of Concrete Strength on Load-Carrying Capacity of Connectors

The load-carrying capacity of a channel shear connector increases with increasing concrete strength. This observation is based on comparisons at equal slips and at equal strains. Whether the same would be true

for the ultimate capacity cannot be said conclusively on the basis of the test data. The results of the tests of specimens with concrete fillet indicate, however, that the beneficial effect of an increased strength of concrete will be retained up to the ultimate loads.

The quantitative effect does not depend directly on the concrete strength but rather on the relative stiffnesses of the concrete and the connector web, and also on the relative dimensions of the connector web and flange. Thus the quantitative effect of the concrete strength on the load-carrying capacity must be determined individually for each specific type of connector.

23. Effect of Manner of Loading on Behavior of Channel Shear Connectors

Tests of several specimens with intermittently released and reapplied loading proved that the load-slip and load-strain characteristics are not influenced by this manner of loading. Furthermore, residual slips and strains remain small as long as the steel connectors do not begin to yield. Once the virgin curves, that is the curves for first loading, are known both slip and strain may be determined approximately at all stages of loading.

The effect of orientation of a channel connector with respect to the direction of load was also investigated. No significant effect of the orientation was found on either the load-slip or load-strain curves.

D. THEORETICAL ANALYSIS FOR CHANNEL SHEAR CONNECTORS

24. Forces Acting on Channel Connector

A channel shear connector is a cantilever beam supported on a continuous concrete foundation. Owing to its shape, method of attachment, and embedment in concrete, it is subject to a complex system of forces which are discussed in this section. This discussion is preliminary to an approximate theoretical analysis which, in connection with the test results, leads to semi-empirical formulas for predicting maximum stresses and slips for a channel shear connector.

The forces applied to a channel connector may be divided into three categories: (1) external forces transmitted to the connector directly from the steel beam, (2) reacting forces exerted on the connector by the surrounding concrete, and (3) additional forces owing their existence to the characteristics of the type of specimen (push-out specimen or T-beam).

The external force transmitted from the beam to the slab through the shear connector is a shearing force applied at the welded connection of the connector. In the push-out specimens shown in Fig. 1 the known

total force applied to the beam is transmitted to two concrete slabs. After the breaking of bond between the contact surfaces of the steel beam and the concrete slabs occurs, this force can be transmitted only by the connectors and by friction. The friction depends on the magnitude of a force acting in a direction normal to the contact surfaces of the beam and the slab and is always small (Section 11). The major portion of the applied load is transmitted as vertical shear to the two connectors through the welds.

The forces applied to the connector are transmitted through the connector to the surrounding concrete. The connector web and the flange welded to the beam exert vertical pressure on the concrete; this pressure is distributed nonuniformly in the form of a rapidly diminishing wave with both positive and negative values and with the highest values under the welded flange. The free flange fully embedded in the concrete may exert a small nonuniformly distributed horizontal pressure on the surrounding concrete.

In addition to the contact pressures, the surfaces of the connector may be subjected to the restraining forces of bond or friction between the concrete and the steel. It is believed that the bond between the connector and the surrounding concrete is broken at working stresses. But as deformation takes place the convex surfaces of the deformed connector remain in contact with the concrete and friction restrains the stretching of the extreme convex fibers of the connector.

The vertical shear applied to the connector and the forces acting on the surfaces of the connector set up internal moments at all sections of the connector and the welded end tends to rotate. Owing to the stiffness of the welds the angle between the connector and the beam remains fixed at the welded end and, as a result, a fixed-end moment will be present in addition to the vertical shear at this location.

The third category includes forces which tend to separate the slabs of a push-out specimen from the beam. Since the load applied to the beam and the vertical reactions on the bottom surfaces of the slabs are not concurrent, internal moments are set up in the specimen. These moments tend to rotate the slabs about a horizontal axis and are resisted by the bedding between the slabs and the testing machine on one end and by the shear connectors and direct bearing of the slabs against the beam on the other end. Thus these internal moments cause direct tension in the connectors and, at the same time, friction between the beam and the slabs. The direct tension may be transmitted to the slab either through friction between the channel surfaces and the concrete or by the

free flange which would exert horizontal pressure on the surrounding concrete. The friction between the beam and the slabs causes a decrease of the magnitude of vertical shear transmitted through the welds.

The forces acting on a horizontal channel shear connector in a vertical push-out specimen may be summarized as follows.

1. Shear Q transmitted to the connector through the welds at the toe and the heel of the flange attached to the beam.
2. Moment M_o holding the welded end of connector fixed.
3. Vertical pressure of the concrete foundation q distributed non-uniformly along the welded flange and the web.
4. Horizontal pressure of the concrete foundation q' distributed non-uniformly along the free flange.
5. Friction f restraining the horizontal surfaces of the connector.

25. Simplifying Assumptions of Theoretical Analysis

The tests of push-out specimens have shown conclusively that the behavior of a channel shear connector is similar to that of a semi-infinite dowel embedded in an elastic medium. The following analysis is basically a modification of the well-known theory for semi-infinite beams on elastic foundation.* In order to make such an analysis possible, a number of simplifying assumptions must be made regarding the system of forces applied, the shape of the channel and the characteristic properties of materials.

1. Forces. Of the forces acting on a channel shear connector, the load Q, moment M_o, and the reaction of the foundation q are the most important. Effects of the remaining forces are neglected in the analysis. The magnitude of the moment M_o is controlled by the condition that the welded end of connector remains fixed against rotation.

2. Shape of Connector. In the theoretical analysis the actual shape of the channel connector is replaced by the idealized shape shown in Fig. 28a. This idealized connector consists of an infinitely rigid stiff portion and an infinitely long flexible portion. The height of the stiff portion is equal to the thickness of the flange of the corresponding channel connector and the thickness of the flexible portion is equal to the thickness of the web.

3. Materials. The analysis is limited to elastic behavior in the steel of the channel connector. Consequently the only property of the steel required for the purpose of the analysis is the modulus of elasticity.

* See, for instance, S. Timoshenko, "Strength of Materials, Part II," D. Van Nostrand Co., New York, 1948, p. 12 and following. (The beam on an elastic foundation and the dowel in an elastic medium are identical problems in the theory of elasticity.)

Where numerical values are needed, the value of 30,000,000 psi is used. The second material involved is concrete, which forms the foundation for the channel connector. Its properties enter the analysis in the form of the so-called foundation modulus. This modulus is defined as the unit pressure per full width of the connector required to produce a unit deflection of the foundation. In the ordinary elastic analysis the foundation modulus is assumed to be constant. If the foundation modulus of concrete were constant, however, the load-slip curves for channel connectors would have to be straight lines. It has been shown in previous

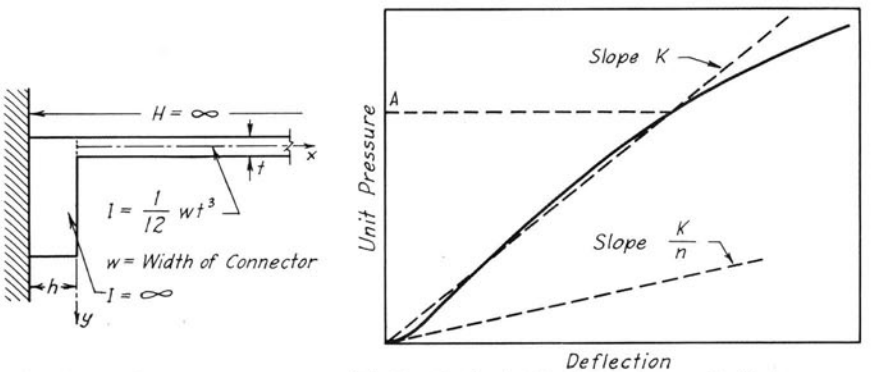

(a) Idealized Shape of Channel Connector

(b) Hypothetical Relation Between Unit Pressure and Deflection for Concrete Foundation

Fig. 28. Assumptions of Theoretical Analysis

sections that the slope of the load-slip curves varies with the load. Thus the foundation modulus for concrete actually varies with the pressure exerted on the concrete by the connector.

The foundation modulus for the concrete under the channel connectors could not be determined by direct measurements, but studies of the push-out test data and of the literature pertaining to this question * lead to the hypothetical relation between the unit pressure and deflection shown in Fig. 28b. The deflection increases rapidly at first but above some load or deflection the rate of increase becomes smaller and remains approximately constant. At intermediately high loads the rate of the deflection increase begins to increase continuously.

* F. E. Richart, A. Brandtzæg and R. L. Brown, "A Study of the Failure of Concrete Under Combined Compressive Stresses," Univ. of Ill. Eng. Exp. Sta. Bul. 185, 1928, p. 54, Fig. 17.
M. D. Shaffer and F. M. Williams, "Investigation of the Strength of the Connection Between a Concrete Cap and the Embedded End of a Steel H-Pile," Research Report No. 1, State of Ohio Dept. of Highways, 1947, pp. 22–28, Figs. 29–55.

Since the stiff portion of the idealized connector is assumed to be infinitely stiff and to undergo no rotation at the attached end, the deflection of this portion can consist only of a translation: that is, the deflection is uniform over the length h (Fig. 28a). For this condition of constant deflection, it follows from Fig. 28b that the load per unit length, and also the foundation modulus, must be constant over the length of the stiff portion. It has been observed in the preceding sections that large pressures exist only under the stiff portion and under a very short length of the web of a channel connector immediately adjoining the stiff portion. If the hypothetical curve in Fig. 28b represents the actual conditions, the foundation modulus will have very small values at most sections of the web. This observation suggests an assumption regarding the foundation moduli which greatly simplifies the theoretical analysis. If it is assumed that at any particular load on the connector the foundation modulus is constant under the whole length of the web, the theoretical analysis may be based on two constant and independent moduli of foundation. Such moduli are indicated in Fig. 28b. For a unit pressure A on the stiff portion the modulus under the stiff portion is taken as K; the unit pressures on the flexible portion will be very much smaller than A and the modulus under this section is assumed to be K/n, as shown in Fig. 28b.

In the following theoretical analysis of channel shear connectors the properties of the concrete foundation are expressed by means of these two foundation moduli, K and K/n. Their numerical values depend on the magnitude of the load and on several other variables. Semi-empirical formulas for both moduli have been derived from the push-out test data and are given in Section 26.

The assumptions of the analysis may be summed up as follows.

(1) The connector consists of an infinitely rigid stiff portion of height h and of an infinitely long flexible portion of thickness t and width w.

(2) The connector is made of steel, the stresses in which remain below the yield point.

(3) The connector is embedded in concrete which is characterized by two foundation moduli: modulus K for the part under the stiff portion of the connector and modulus K/n ($n>1$) for the part under the flexible portion. Both K and n vary with the total load on the connector, but they are constant for any particular load.

(4) The connector and the foundation deflect alike at all points.

(5) The deflection of the foundation is equal to the pressure exerted on the foundation divided by the foundation modulus at that point.

(6) The external load is applied to the end of stiff portion in the direction of the y-axis (Fig. 28a).

(7) The stiff portion has only one degree of freedom; it can be translated in the direction of the y-axis, but cannot be translated in the direction of the x-axis or rotated.

26. Theoretical Analysis of Channel Connectors

Notation. The following notation is used in the theoretical analysis of channel shear connectors.

h, t, w, H = dimensions of connector, in. (Fig. 28a)
I = moment of inertia of flexible portion of connector, in.^{4}
E = modulus of elasticity of the connector material (steel), psi
K = modulus of foundation under the stiff portion of the connector, lb/in.^{2}
K/n = modulus of foundation under the flexible portion of the connector, lb/in.^{2}
$\beta = \sqrt[4]{\frac{K}{4nEI}}$, in.$^{-1}$
Q = external load applied to the connector, lb
Q_f = part of the external load carried by the flexible portion of the connector, lb
Q_s = part of the external load carried by the stiff portion of the connector, lb
V = shear at any section of the connector, lb
M = moment at any section of the connector, in.-lb
q = reaction of the foundation, lb/in.
y = deflection of the connector, in.
ϵ = strain in the connector, in./in.
f_{co} = unit pressure exerted by the stiff portion of the connector on the adjacent concrete, psi
f_{max} = maximum steel stress in connector, psi
x = distance along the connector; $x = 0$ at the junction of the stiff and flexible portions

Subscript $_o$ denotes quantities at $x = 0$.

Derivation of Formulas. On the basis of assumptions (4), (5) and (6) of the previous section the deflections of the stiff portion of a channel connector may be expressed as

$$y_o = \frac{}{K\ h} \tag{1}$$

and the deflections of the flexible portion may be expressed in the form

$$y = \frac{q\ n}{K} \tag{2}$$

According to the ordinary theory of flexure of beams

$$\frac{d^4y}{dx^4} = -\frac{q}{EI} \tag{3}$$

If q is eliminated from Eqs. 2 and 3 a differential equation for deflections of the flexible portion of the connector is obtained in terms of the physical properties of the connector and of the foundation:

$$EI\frac{d^4y}{dx^4} + \frac{K}{n}y = 0 \tag{4}$$

Since the modulus K/n is constant for a particular load Q, the general solution of Eq. 4 is

$$y = e^{\beta x}\ (A\ \cos\ \beta x + \mathrm{B}\ \sin\ \beta x) + e^{-\beta x}\ (\mathrm{C}\ \cos\ \beta x + \mathrm{D}\ \sin\ \beta x)$$

where the expression

$$\beta = \sqrt[4]{\frac{K}{4nEI}}$$

is introduced for convenience.

The constants of the general solution, A, B, C, and D, may be determined from the four end conditions

$$\text{at } x = \infty,\ y = 0 \text{ and } \frac{dy}{dx} = 0$$

$$\text{at } x = 0,\ y = y_o \text{ and } \frac{dy}{dx} = 0$$

The deflections of the flexible portion of the connector are given by the expression

$$y = y_o\ e^{-\beta x}\ (\cos\ \beta x + \sin\ \beta x). \tag{5}$$

The deflection y_o may be determined from Eq. 1 and from the conditions of statical equilibrium. The total load carried by the connector is

$$Q = Q_s + Q_f \tag{6}$$

The load carried by the flexible portion Q_f is numerically equal and opposite in sign to the shear V_o at $x = 0$; hence

$$Q_f = -V_o$$

From the ordinary theory of flexure of beams

$$V_o = -EI\left[\frac{d^3y}{dx^3}\right]_{x=0}$$

If the third derivative of y is evaluated from Eq. 5 and substituted in the expression for V_o, the load carried by the flexible portion is determined as

$$Q_f = \frac{y_o K}{n\beta} \tag{7}$$

After substituting from Eqs. 1 and 7 into Eq. 6, the deflection y_o may be expressed as

$$y_o = \frac{n\beta Q}{K(1 + n\beta h)} \tag{8}$$

Equations 5 and 8 represent the theoretical solution for deflections of a channel shear connector.

Expressions for moment, shear, and reaction of the foundation may be found for the flexible portion as derivatives of Eq. 5:

$$M = -EI\frac{d^2y}{dx^2} = -\frac{Q}{2\beta(1 + n\beta h)}e^{-\beta x}(\sin \beta x - \cos \beta x) \tag{9}$$

$$V = -EI\frac{d^3y}{dx^3} = -\frac{Q}{(1 + n\beta h)}e^{-\beta x}\cos \beta x \tag{10}$$

$$q = -EI\frac{d^4y}{dx^4} = -\frac{\beta Q}{(1 + n\beta h)}e^{-\beta x}(\cos \beta x + \sin \beta x) \tag{11}$$

The reaction of the foundation under the stiff portion may be found from Eq. 8:

$$q_o = K y_o = \frac{n\beta Q}{1 + n\beta h} \tag{12}$$

Strain on both surfaces of the connector may be computed from Eq. 9:

$$\epsilon = \pm \frac{3Q}{E\beta(1 + n\beta h)wt^2}e^{-\beta x}(\sin \beta x - \cos \beta x). \tag{13}$$

Evaluation of Constants K, n, and β. The quantities K, n, and β in Eqs. 5 and 8–13 are unknown; however, they can be evaluated from the data obtained from the push-out tests. To evaluate the quantities K and n, two equations involving measured quantities are needed. Slip and strain data may be used for this purpose.

Slip between the slabs and the beam is equal to the deflection of the stiff portion. Hence Eq. 8 provides one equation for the evaluation of K and n. The interpretation of strain data is more difficult than that of slip data. Only the strains measured at the fillet of the channel connectors are large enough to serve as a fairly accurate basis for a direct numerical evaluation of K and n. All other strains measured along the web are so small that serious errors might be introduced if they were used directly. Unfortunately, strains measured at the fillet are also undesirable in some ways, since the basic assumptions of the theory do not agree with the actual conditions at this location. Hence an indirect approach through the load on the stiff portion Q_s, evaluated in Section 14, seems to be best. The loads Q_s, carried by the stiff portion of the connector were determined on the basis of all measured strains and therefore represent an average quantity.

After eliminating y_o from Eqs. 1 and 8 the following expression is obtained for Q_s

$$Q_s = \frac{n\beta h}{1 + n\beta h} Q \tag{14}$$

The parameter β is related to K and n by

$$\beta^4 = \frac{3K}{Enwt^3} \tag{15}$$

With the help of Eqs. 8, 14 and 15 the quantities K, n, and β were evaluated for the 12 specimens listed in Table 10. The resulting values are listed in Table 11. It should be noted in this table that the foundation modulus K is listed in terms of the full width of the connector. If expressed in terms of a unit width its value would range from 0.52×10^6 to 3.18×10^6 lb per cu in. The value of the modulus K decreases with increasing load and with increasing connector flange thickness, and increases with increasing concrete strength and with increasing connector web thickness. The ratio n of the foundation moduli under the stiff and flexible portions of a channel connector has values from 5.30 to 18.17. The value of the foundation modulus under the flexible portion, expressed per unit width of connector, varies from 0.068×10^6 to 0.467×10^6 lb per cu in.

Table 11

Values of K, n, β, and c Computed from Push-Out Test Data

All values computed with data from Tables 2 and 10

Specimen	Total Load on Shear Connector Q, lb	Foundation Modulus K, 10^6 lb/in.^{2}	Ratio of Foundation Moduli n	β, 1/in.	Correction Coefficient $c = \frac{\epsilon_o}{\epsilon_{max}}$
4C3C1	20 000	13.32	7.71	1.49	2.18
	30 000	7.32	5.91	1.37	2.22
4C3C5	20 000	16.80	11.00	1.44	2.16
	30 000	10.98	7.66	1.42	2.51
4C3C8	20 000	16.50	13.91	1.24	2.55
	30 000	11.04	13.47	1.24	2.06
4C3C9	20 000	18.84	18.17	1.31	2.21
	30 000	14.04	16.37	1.25	2.12
	40 000	9.90	8.75	1.34	2.35
4C5T1	20 000	14.22	7.93	0.97	2.10
	30 000	10.14	9.40	0.86	2.05
	40 000	6.36	5.70	0.87	1.95
4C5T2	20 000	14.94	5.36	1.09	1.72
	30 000	9.90	5.30	0.98	1.64
4C5T6	20 000	20.88	11.19	0.98	1.67
	30 000	12.60	8.47	0.93	1.72
	40 000	8.82	5.73	0.99	1.39
4C5T8	20 000	27.00	10.41	1.07	1.32
	30 000	19.08	8.82	1.02	1.42
	40 000	13.08	7.08	0.94	1.72
4C8T	30 000	8.34	8.94	0.59	2.22
	40 000	8.52	6.56	0.56	2.08
3C3H3	20 000	21.60	15.22	1.48	1.64
	30 000	14.04	9.73	1.48	1.86
5C3H2	20 000	18.48	10.84	1.42	2.41
	30 000	10.98	10.36	1.27	2.14
4C3S2	30 000	5.52	12.32	1.06	2.82
	40 000	4.02	9.54	1.05	2.88
	50 000	3.12	7.70	1.04	2.80

A comparison of the measured strains with the theoretical values is shown in Fig. 29. For this figure measured and computed strains multiplied by the factor

$$\frac{E\beta(1+n\beta h)\,wt^2}{3Q}$$

are plotted against βx so that all results should fall on one theoretical curve (Eq. 13). The test results, reduced with the n- and β- values given in Table 11, are compared with the theoretical curve at loads of 20,000 and 30,000 lb per connector. When considering all assumptions made at the outset of the development of the theory, the results are gratifying. Average strains measured at various points along the web of the connector follow the theoretical line as closely as can be expected. Strains measured at the fillet are consistently much smaller than the theoretical values; this is reasonable because the actual thickness of the channel at these gages was larger than t.

To make possible the numerical evaluation of the deformations of a channel connector, mathematical formulas were needed for K and n. Such formulas were developed from Figs. 30a, b. In Fig. 30a the modulus

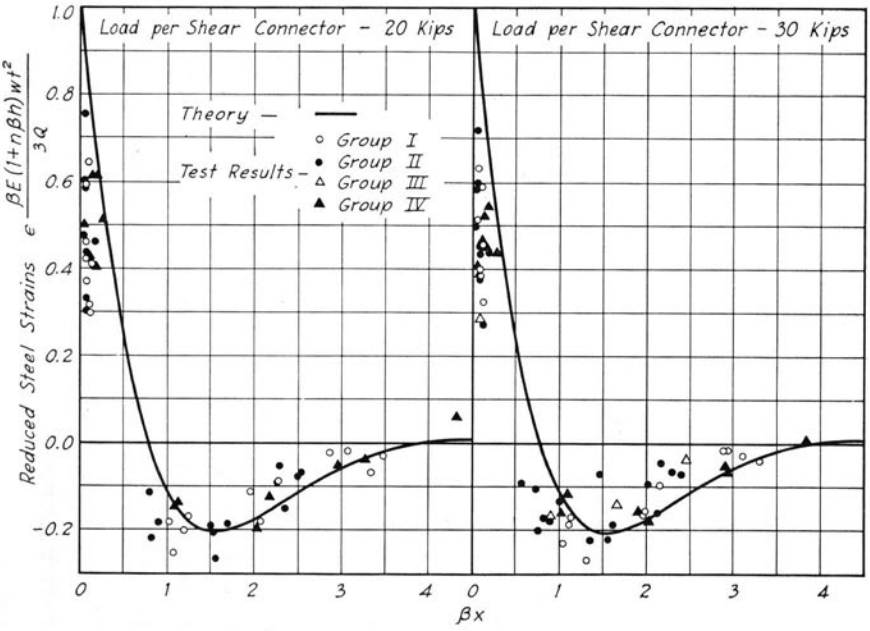

Fig. 29. Comparison of Theoretical and Measured Strains in Channel Shear Connectors

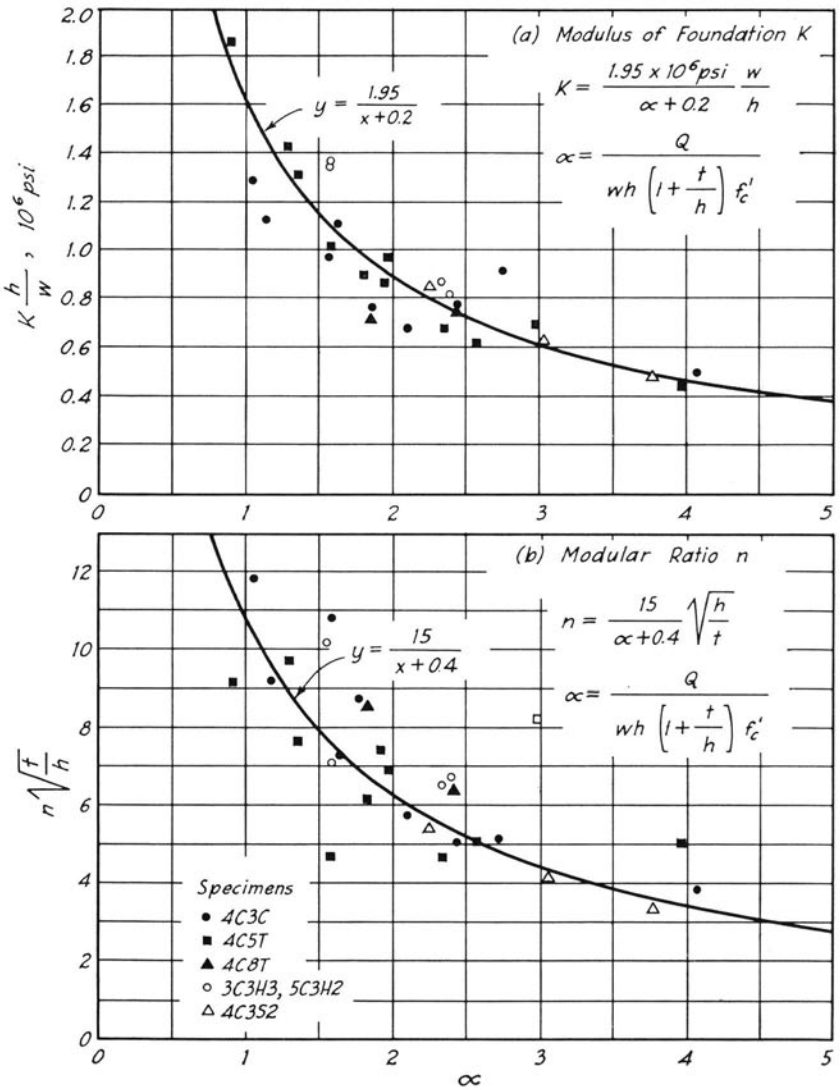

Fig. 30. Empirical Evaluation of Modulus of Foundation K and of Modular Ratio n

K multiplied by h/w is plotted against a parameter denoted as α (Eq. 17); a fairly good correlation was obtained. An average line was drawn through the plotted points. The equation of the average line gives the empirical formula for K:

$$K = \frac{1.95 \times 10^6 \text{ psi}}{\alpha + 0.2} \quad \frac{w}{h} \tag{16}$$

where

$$a = \frac{Q}{wh(1 + \frac{t}{h}) f'_c} \tag{17}$$

in which f'_c denotes the cylinder strength of concrete. An empirical formula for the ratio n was determined from Fig. 30b in a similar manner. The resultant formula is

$$n = \frac{15}{a + 0.4} \sqrt{\frac{h}{t}} \tag{18}$$

Maximum Strain. Maximum strain in a channel connector occurs at the fillet between the flexible web and the stiff flange. Computation of the maximum strain is complicated by three factors: (1) The exact location of the maximum strain is unknown and will vary from one type of connector to another. (2) The thickness at the location of maximum strain will generally be larger than that of the web; because the location is unknown, the thickness is also unknown. (3) Some stress concentration of unknown magnitude may occur at the point of maximum stress, because of the fairly sharp curvature of the fillet.

In order to obtain a relatively simple expression for maximum strains, it has been assumed that the maximum strain occurs at the theoretical junction of the flexible and stiff portions (at the height h as shown on Fig. 2). The expression for strain at this location may be obtained from Eq. 13 as

$$\epsilon_o = \frac{3Q}{E\beta(1 + n\beta h)\, wt^2} \tag{19}$$

To account for the increased thickness, the web thickness t must be replaced by some larger value t_{max}, which is defined as

$$t_{max} = t + A$$

or

$$t_{max} = (1 + \frac{A}{t})\, t$$

where A is a parameter expressed in inches. The maximum strain may then be expressed as

$$\epsilon_{max} = \frac{3Q}{E\beta(1 + n\beta h)\, wt^2\, (1 + \frac{A}{t})^2} = \frac{\epsilon_o}{c} \tag{20}$$

in which

$$c = (1 + \frac{A}{t})^2 \tag{21}$$

Numerical values for c were determined from Eqs. 20 and 21, in which values of ϵ_o were computed from Eq. 19 and values of ϵ_{max} were taken as the largest measured strains. It was found that for the specimens which were tested, satisfactory values of c may be obtained from the empirical expression.

$$c = (1 + \frac{0.093 \text{ in.}}{t})^2 \tag{22}$$

Values of c for the 12 specimens which served as a basis for Eq. 22 are shown in the last column of Table 11.

Comparison of Theory with Test Results. Sixteen standard push-out specimens were selected for comparing the theory with the test data. The selected specimens represent large variations in the strength of concrete, the thicknesses of the connector web and flange, and the height of connector, as well as a small variation in the width of the connector.

For each specimen two loads were selected so as to give comparisons approximately at maximum connector strains of 60×10^{-5} and 110×10^{-5}. Slips and maximum strains were computed from Eqs. 8, 15–20, and 22 and are compared with the test results in Table 12.

Slips are compared in columns (3), (5) and (6) of Table 12. The ratios of computed to measured slips for all specimens average 1.013, with maximum deviations of +34 and −19 percent and an average deviation of 10.8 per cent. The 16 specimens are divided into three groups: the first group includes specimens with connectors made of 4-in. 5.4-lb standard rolled steel channels, the second group specimens with 4-in. 7.25-lb channels, and the third miscellaneous specimens. It is important that no large consistent variations of the ratio of computed to measured slips can be observed within any single group and that the averages for all three groups differ by only a few percent.

Strains are compared in columns (8), (10) and (11) of Table 12. The ratios of computed to measured maximum strains for all specimens average 1.063. Ratios for individual specimens show maximum deviations of +30 and −19 percent from the total average and an average deviation of 9.8 percent. The strain ratios do not show any important consistent variations with any of the variables investigated.

The pressure on the concrete under the stiff portion may be calculated from Eq. 12:

$$f_{co} = \frac{q_o}{w} = \frac{n\beta Q}{(1 + n\beta Q)w} \tag{23}$$

Pressures so computed are listed in column (13) of Table 12. At the lower of the two loads included for each specimen, corresponding roughly

Table 12
Comparison of Theory with Results of Push-out Tests

Specimen	Load on Connector	Slip					Maximum Strain					Maximum Pressure on Concrete	
		Theory*	Simplified Formula†	Test Data	Ratio (3)/(5)	Ratio (4)/(5)	Theory*	Simplified Formula†	Test Data	Ratio (8)/(10)	Ratio (9)/(10)	Theory*	Simplified Formula†
(1)	lb (2)	10^{-4} in. (3)	10^{-4} in. (4)	10^{-4} in. (5)	(6)	(7)	10^{-6} (8)	10^{-6} (9)	10^{-6} (10)	(11)	(12)	psi (13)	psi (14)
					3/16-in. Channels								
4C3C1	20 000	40	45	30	1.33	1.50	62	69	55	1.13	1.25	6 530	6 630
	30 000	82	96	76	1.08	1.26	123	137	117	1.05	1.17	9 030	9 940
4C3C4	20 000	29	32	26	1.12	1.23	45	54	54	0.83	1.00	6 920	6 630
	30 000	60	67	59	1.02	1.14	91	103	115	0.79	0.90	9 790	9 940
4C3D2	20 000	28	31	25	1.12	1.24	43	52	36	1.19	1.44	6 900	6 630
	30 000	57	63	67	0.85	0.94	87	98	87	1.00	1.13	9 930	9 940
4C3C5	25 000	40	44	36	1.11	1.22	62	72	60	1.03	1.20	8 520	8 280
	35 000	73	82	75	0.97	1.09	111	124	109	1.02	1.14	11 330	11 600
4C3C8	25 000	31	35	37	0.84	0.95	49	61	56	0.88	1.09	8 840	8 280
	35 000	57	63	69	0.83	0.91	88	102	103	0.85	0.99	11 910	11 600
4C3C9	25 000	29	32	32	0.91	1.00	45	56	45	1.00	1.24	8 930	8 280
	35 000	52	57	64	0.81	0.89	81	96	85	0.95	1.13	12 090	11 600
				Av	0.999	1.114				0.977	1.140		
					5/16-in. Channels								
4C5T1	25 000	40	58	40	1.00	1.45	74	75	52	1.42	1.44	7 120	7 270
	35 000	70	92	76	0.92	1.21	127	132	89	1.43	1.48	9 030	10 180
4C5T2	25 000	34	41	36	0.94	1.14	63	65	70	0.90	0.93	7 530	7 270
	35 000	60	75	71	0.85	1.06	110	112	140	0.80	0.80	9 690	10 180
4C5T3	25 000	33	38	30	1.10	1.27	60	63	57	1.05	1.10	7 650	7 270
	35 000	57	70	60	0.95	1.17	105	107	96	1.09	1.11	9 890	10 180
4C5T6	25 000	30	35	29	1.03	1.21	56	58	52	1.08	1.12	7 830	7 270
	35 000	53	64	59	0.90	1.08	97	99	94	1.03	1.05	10 200	10 180
4C5T8	25 000	23	27	22	1.05	1.23	44	49	56	0.79	0.88	8 280	7 270
	35 000	41	48	41	1.00	1.17	77	81	88	0.88	0.92	10 290	10 180
				Av	0.974	1.199				1.047	1.083		

Specimen	Load on Connector	Slip					Maximum Strain					Maximum Pressure on Concrete	
		Theory*	Simplified Formula†	Test Data	Ratio (3)/(5)	Ratio (4)/(5)	Theory*	Simplified Formula†	Test Data	Ratio (8)/(10)	Ratio (9)/(10)	Theory*	Simplified Formula†
(1)	lb (2)	10^{-4} in. (3)	10^{-4} in. (4)	10^{-4} in. (5)	(6)	(7)	10^{-5} (8)	10^{-5} (9)	10^{-5} (10)	(11)	(12)	psi (13)	psi (14)
Miscellaneous Channels													
4C3S2	35 000	78	80	73	1.07	1.10	64	55	50	1.28	1.10	5 660	5 640
	45 000	124	128	115	1.08	1.11	101	83	90	1.12	0.92	7 130	7 250
4C8T	35 000	48	59	47	1.02	1.26	77	72	60	1.28	1.20	7 540	7 470
	45 000	72	93	80	0.90	1.16	115	108	103	1.12	1.05	9 020	9 600
4C3W1	20 000	44	49	34	1.29	1.44	67	77	36	1.86	2.14	7 980	7 950
	30 000	90	103	96	0.94	1.07	136	150	107	1.27	1.40	11 120	11 930
5C3H2	25 000	40	46	34	1.18	1.35	60	68	49	1.22	1.39	7 870	7 790
	35 000	73	84	78	0.94	1.08	106	117	111	0.95	1.05	10 500	10 900
3C3H3	20 000	26	29	22	1.18	1.32	43	55	50	0.86	1.10	7 660	7 220
	30 000	53	56	48	1.10	1.17	87	103	98	0.88	1.05	10 920	10 820
				Av	1.070	1.206				1.184	1.240		
			Av All Specimens		1.013	1.169				1.063	1.153		
3/16-in. Channels, Specimens with Concrete Fillet													
4C3F1	20 000	34	38	68	0.50	0.56	53	60	84	0.63	0.71	6 740	6 630
	30 000	70	79	141	0.50	0.56	106	117	149	0.71	0.79	9 450	9 940
4C3F2	20 000	33	37	39	0.85	0.95	52	59	45	1.16	1.31	6 770	6 630
	30 000	68	78	83	0.82	0.94	104	115	95	1.09	1.21	9 500	9 940
4C3F4	25 000	32	35	42	0.76	0.83	50	61	49	1.09	1.24	8 820	8 280
	35 000	58	64	67	0.87	0.96	90	103	72	1.25	1.43	11 860	11 600
				Av	0.716	0.80				0.988	1.115		

*Equations 8, 20, and 23.
†Equations 26, 25, and 24.

to a working load, the pressure on the concrete is 1.64 to 3.27 times the compressive strength of control cylinders. At the higher load, corresponding approximately to a nominal yield load, the pressure is 2.18 to 4.36 times the compressive cylinder strength. The pressure on the concrete increases only slightly with increasing strength of the concrete, so that a lower concrete strength gives a higher pressure-strength ratio.

A group of three specimens with concrete fillets is added at the end of Table 12. The data for the fillet specimens was included in order to show whether the decreased restraint to the concrete under the stiff portion would invalidate the applicability of the empirical formulas 16–18 and 22. It can be seen from Table 12 that the computed values of slip are somewhat low while those of maximum strain are in good agreement with the test data.

27. Simplified Formulas for Channel Connectors

It is shown by the comparisons listed in Table 12 that the semi-empirical procedure developed in the preceding section can be used for predicting the behavior of a channel shear connector with satisfactory accuracy. However, this procedure is rather cumbersome. Additional simplifications presented in this section decrease the accuracy of the formulas, but at the same time result in very simple expressions. It is felt that the resulting simplicity outweighs the decrease in accuracy. Maximum steel strain, maximum pressure on the concrete, and slip are the quantities of primary interest. Therefore only these three quantities are dealt with in this section.

It can be shown that in the range of variables encountered in the tests of push-out specimens, Eqs. 8, 20 and 23 for slip, maximum steel-strain and pressure on concrete may be written, without undue loss of accuracy, in the forms

$$f_{co} = \frac{Q}{\gamma w} \tag{24}$$

$$f_{\max} = \frac{Q}{k_1 \gamma w} \tag{25}$$

$$y_o = \frac{Q}{k_2 \gamma} \tag{26}$$

where

$$\gamma = \frac{1}{2} t + h \tag{27}$$

and k_1, k_2 are parameters which must be evaluated from the test data. It can be seen from comparison of Eqs. 8, 20 and 23 with Eqs. 24–27 that the simplified expressions were obtained by substituting $n\beta t = 2$, $k_1 = \frac{1}{3} cn(\beta t)^2$, and $k_2 = K$.

Before evaluating the parameters k_1 and k_2, it should be noticed that k_1 and k_2 are related directly to n and K respectively. It seems reasonable, therefore, to expect that the general form of the empirical formulas for k_1 and k_2 will correspond roughly to the form of Eqs. 16–18. Furthermore it should be noticed that in the parameter a (Eq. 17)

$$\frac{Q}{wh\ (1+\frac{t}{h})} \cong f_{co}$$

so that

$$a \cong \frac{f_{co}}{f'_c}$$

In Fig. 31a and 31b, k_1 and k_2 h/w are plotted against the ratio f_{co}/f'_c. The scatter in this figure is larger than the scatter in the corresponding Fig. 30a, b, but the plotted points show definite trends. If safe values of maximum pressure, maximum stress and slip are desired, the parameters k_1 and k_2 must be smaller than the average quantities. Both curves shown in Fig. 31a, b, were drawn with this point in mind. The empirical formulas for k_1 and k_2 are

$$k_1 = \frac{1.6}{\frac{f_{co}}{f'_c} + 1.8} \tag{28}$$

$$k_2 = \frac{2.3 \times 10^6 \text{ psi}}{\frac{f_{co}}{f'_c} + 0.6} \frac{w}{h} \tag{29}$$

The simplified formulas 24–26 are compared with the test data and with the more exact theory in Table 12. The simplified formulas give higher values for both strain and slip than those measured in the tests of the push-out specimens or those computed from the more exact theory. On the average, computed slips are 16 percent higher and computed maximum strains 15 per cent higher than those obtained from the test data. The maximum pressures on the concrete computed from Eq. 24 are practically the same as those computed from the more exact theory.

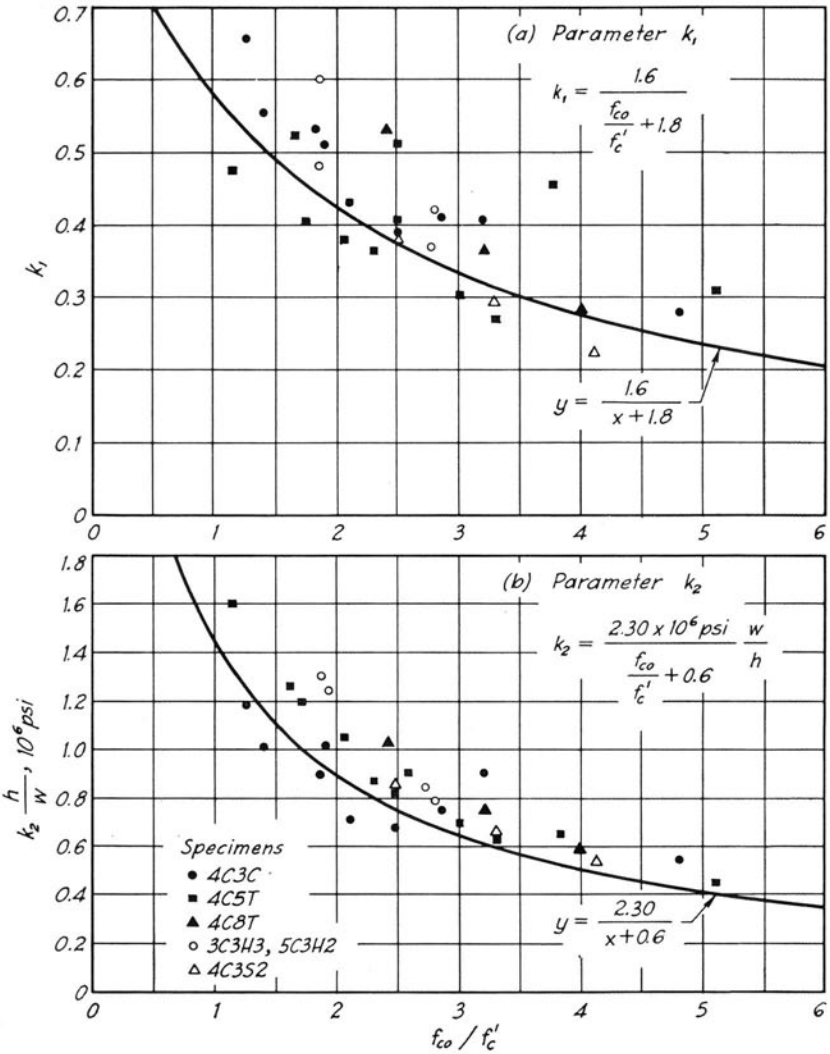

Fig. 31. Empirical Evaluation of Parameters k_1 and k_2

28. Range of Applicability of Theory and Simplified Formulas

Limitations. The simplified formulas as well as the more exact theoretical formulas presented in the previous sections are based on several assumptions and contain empirical parameters. Thus the applicability of the formulas derived in Sections 26 and 27 is limited by both the assumptions of the theory and the scope of the tests. The important limitations may be summarized as follows:

(1) The formulas are applicable only to steel channels forming flexible connectors and only in the range of elastic steel stresses.

(2) The dimensions of the channel connectors must fall within these limits:

$$1.0 \leq \frac{h}{t} \leq 5.5$$

$$\frac{H}{t} \geq 8.0$$

$$\frac{w}{h} \geq 6.0$$

$$0.5 \leq \frac{R}{t} \leq 1.6$$

in which

h = connector flange thickness, in. (Fig. 2)
t = connector web thickness, in. (Fig. 2)
H = height of connector, in. (Fig. 2)
w = width of connector, in. (Fig. 1)
R = radius of the fillet between the web and the welded flange of the connector, in. (Fig. 2)

Dimensions of the steel channels rolled in the United States are such that all channels suitable for shear connectors fall within these limits.

(3) The formulas apply for loads and concrete strengths for which

$$a \geq 0.9$$

or

$$\frac{f_{co}}{f'_c} \geq 1.0$$

in which

$$a = \frac{Q}{wh\,(1 + \frac{t}{h})\,f'_c}$$

Q = external load applied to the connector, lb
f'_c = cylinder strength of concrete, psi
f_{co} = unit pressure exerted by the stiff portion of the connector on the adjacent concrete, psi
w, h, t = the same as defined under condition (2)

For loads causing maximum steel stresses of 12,000 psi or larger, concretes of cylinder strength 6000 psi or lower will comply with the above requirements for a and f_{co}/f'_c provided that both conditions (1) and (2) are also satisfied.

Channel Connectors for Composite T-Beams. The empirical parameters for the simplified and theoretical formulas were determined on the basis of the results of push-out tests. Thus the formulas are directly applicable to the shear connectors for composite T-beams only if the results of push-out and T-beam tests are in agreement. It is shown in Section 46 that for channel shear connectors such agreement does exist.

Flexible Connectors Other than Channels. It is probable that the formulas are applicable also to flexible shear connectors made of rolled sections other than channels provided that the conditions (2) and (3) are satisfied. However, tests of shapes other than channels are needed to prove or disprove this hypothesis.

III. TESTS OF COMPOSITE T-BEAMS

A. SPECIMENS AND APPARATUS

29. Outline of Test Program

Four composite steel and concrete T-beams were tested for the purpose of investigating the behavior of composite T-beams. All four beams are shown in Fig. 32 and described in Section 31. The variables included in this series of tests were the size of the steel I-beam and the stiffness of the shear connection. Connectors for all beams were made from 4-in. 5.4-lb. channels, the width and spacing being varied. In three beams the shear connections had a stiffness comparable to that for practical design, while the shear connection of the fourth was made extremely weak.

All tests were made with a static concentrated load simulating the effects of a truck wheel load. The load was located at one of three positions—(1) midspan, (2) quarter-point, (3) close to the support. The first two locations were chosen primarily for investigating the effects of bending, while the loading close to the support was chosen to investigate the effects of high shear.

30. System of Designating Specimens

The four T-beams were designated by symbols B24W, B24S, B21S and B21W. In this notation the letter B stands for "Beam," the number 24 or 21 indicates the depth of the steel I-beam in inches, and the letter S or W indicates whether the T-beam was built with or without shoring.

31. Design and Description of T-beams

Each of the four T-beams consisted of a wide-flange steel I-beam and a 6-ft. wide reinforced concrete slab cast on top of the steel beam. Each specimen may therefore be considered as a section cut from an I-beam bridge having the steel beams spaced at 6 ft. Beams B24W and B21S were designed for the loads they would theoretically carry in an I-beam bridge with beams spaced at 6 ft and loaded with a single rear axle of an H-20 truck. According to the design procedure proposed by N. M. Newmark, the proportion of a wheel load to be considered in the design of a beam is equal to the beam spacing divided by 5.3 ft.* On

* Reference 59, pp. 1020–21.

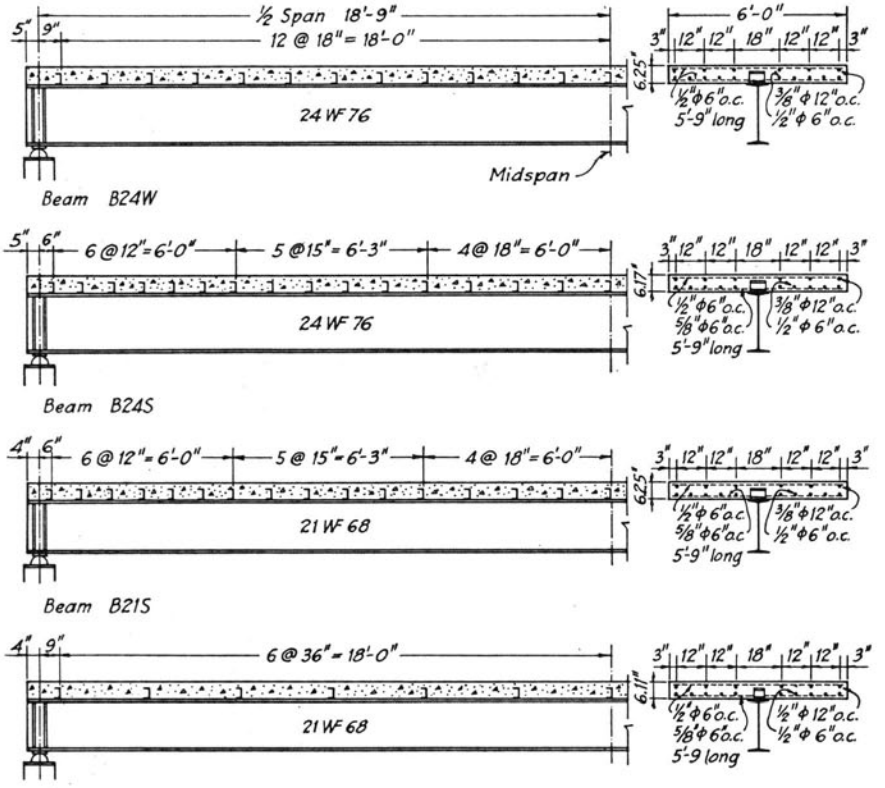

Notes:
Shear connectors for all beams are 6" long 4"-5.4# channels, except for beam B21W which has 4" long 4"-5.4# channels.
Transverse reinforcing bars have 1" concrete cover.
All beams are symetrical about the midspan, except that the shear connectors all face the same direction.

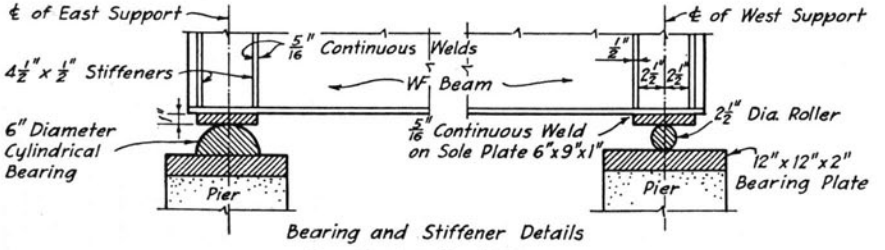

Fig. 32. Details of T-Beams

the basis of these assumptions, and including an impact allowance of 30 percent in accordance with the AASHO Specifications,* the design wheel load was found as follows:

$$\frac{6.0}{5.3} \times 16{,}000 \times 1.30 = 23{,}600 \text{ lb}$$

Beams B24W and B21S were then designed for a load of this magnitude at midspan. The design was based on a working stress for steel of 18,000 psi and a modular ratio of ten for the concrete.

The shear connection was made of rolled steel channels welded to the top flange of the steel beams. They were proportioned for the design load placed at midspan using the procedure recommended by C. P. Siess.† This procedure was modified for beam B21S in that a minimum end-spacing of 12 in. was used instead of the 7-in. spacing required by the calculation.

The reinforcement in the slab was designed by the procedure recommended by N. M. Newmark‡ for a rear wheel load of 12,000 lb and 30 percent impact. Slight changes in the reinforcing steel were needed to provide at least 2 in. of clearance between the reinforcing bars and shear connectors.

The difference in the beam sections for B24W and B21S was caused by the provision of the AASHO Specifications which allows consideration of the effect of temporary supports on the design stresses.¶ Beam B24W was designed and built without any intermediate supports, so that in accordance with the specifications the dead load had to be assigned to the I-beam alone, and only the live load could be considered as carried by the full composite section. On the other hand, beam B21S was designed and built with shoring so that both the dead and live loads were assigned to the full composite section.

Beam B24S was similar to B24W except for the spacing of the shear connectors and the use of shoring in its construction. Because of the shoring, the shear connection was made the same as for B21S.

Beam B21W was the same in section as B21S but its shear connection was designed to permit simultaneous yielding in the steel beam and in

* "Standard Specifications for Highway Bridges," American Association of State Highway Officials, Washington, D. C., 1944, p. 134, Article 32.2.12.

† Reference 61, pp. 1043-44.

‡ Reference 59, pp. 1012-19.

¶ "Standard Specifications for Highway Bridges," American Association of State Highway Officials, Washington, D. C., 1944, p. 195, Article 3.9.3.

the shear connectors. The design of shear connectors for B21W was based on the data obtained from the tests of push-out specimens.

The actual dimensions of all four beams are given in Fig. 32. With the exception of the slab thicknesses and the reinforcement of the slab for beams B24W and B21W, all actual dimensions were the same as those obtained from the design. The design thickness of the slab for all beams was 6 in.; the actual average slab thickness was 2 to 4 percent larger. The bottom transverse reinforcement in B24W was made of ½-in. bars instead of ⅝-in. bars, and in B21W ½-in. bars were used for longitudinal reinforcement instead of ⅜-in. bars. Both of these changes were made because the required sizes were not at hand during the construction of these specimens and it was felt that these changes would have no measurable influence on the behavior of the T-beams.

It can be seen from Fig. 32 that all four specimens were simple beams with a span length of 37.5 ft, supported at one end on a half cylinder and at the other end on a roller. The steel beams for B24W and B24S were standard rolled sections 24WF76, and for B21S and B21W standard rolled sections 21WF68. The beams were stiffened above each support by two vertical plates welded to each side of the web. The slabs for all beams were approximately 6 ft wide and 6 in. thick. The shear connectors were made of 4-in. 5.4-lb. channels; 6-in. wide connectors were used in all beams except B21W, in which the connectors were only 4 in. wide. In beam B24W the connectors were spaced at 18 in. and in beam B21W at 36 in. A nonuniform spacing of 12, 15 and 18 in. was used in beams B24S and B21S.

To prevent bond between the steel beam and the concrete slab, the top flanges of three I-beams were covered with a thick layer of white lead. No attempt was made to prevent natural bond in the beam B21W.

32. Materials

The concrete for the slabs was made of a standard brand of Portland cement, Wabash river torpedo sand, and Wabash river gravel. The results of the sieve analysis of sand and gravel are listed in Table 13. The average fineness modulus of sand was 2.80; the maximum size of gravel, 1 in. Only three samples were taken for the sieve analysis, as those aggregates have been used in this laboratory for several years; a large number of sieve analyses made over that period have given uniform results.

The concrete was mixed in a Kwik-Mix 6S nontilting drum mixer of 6.5-cu ft capacity. Materials were batched by weight. The proportions, the water-cement ratio and the average slump for the individual slabs are given in Table 14.

From twenty-four to thirty 6 x 12-in. control cylinders were made with each slab and tested at the beginning, in the middle, and at the end of the test period of the corresponding slab. The compressive strength and modulus of elasticity were measured on each cylinder. The average compressive strengths and moduli of elasticity are also listed in Table 14.

The tensile properties of the steel in the I-beams were measured on coupons cut after the test from portions of the beams at which yielding did not occur. The coupons were made in accordance with the ASTM Designation A7-46, with the middle portion 9 in. long and 1½ in. wide. The thickness was left as rolled. For each beam two coupons were cut

Table 13

Grading of Sand and Gravel

All figures are averages for three samples

Sieve Size	Percent Retained	
	Sand	Gravel
1½″	....	0
1″	....	2.9
¾″	....	17.0
½″	....	42.2
⅜″	....	77.5
No. 4	0.4	92.9
8	3.2	....
16	13.1	....
30	70.3	....
50	94.4	....
100	98.9	....
Fineness Modulus	2.80	6.87

from both the top and the bottom flanges and three coupons from the web. The results of the tests are reported in Table 15. The results for the corresponding specimens were uniform for each beam; therefore only average values are reported. It should be noted that the coupons cut from the webs always gave higher yield points and ultimate strengths than those cut from the flanges. With the exception of the ultimate strength for the material in the flanges of B24S, B21S, and B21W the requirements of ASTM Designation A7-46 were met.

The tensile properties of the steel in the channel shear connectors are given in Table 16. They were measured on coupons cut both parallel and perpendicular to the direction of rolling. The coupons were ½ in. wide and 4 in. long. The thickness was left as rolled. The test results were uniform; only the averages are listed in Table 16.

The slab of the beam B24W was reinforced with steel on hand, and therefore consisted of several types of new deformed bars. The slabs of the remaining three beams were reinforced with intermediate grade deformed Hi-Bond bars satisfying the minimum requirements of ASTM Designation 305-47T.

Table 14
Physical Properties of Concrete in Slabs of T-Beams

Specimen	Concrete Mixture			Concrete Cylinders‡			
	Proportions by Weight*	w/c Ratio by Weight†	Slump, in.	Age at Test, Days	Number	Compressive Strength, psi	Modulus of Elasticity,¶ psi
B24W	1:2.12:3.52	0.59	5.5	34	10	5 230	4 140 000
				49	10	5 500	4 190 000
				61	10	5 700	4 160 000
						Av 5 500	4 160 000
B24S	1:2.12:3.52	0.57	5.0	39	8	5 630	4 200 000
				52	9	5 570	4 120 000
				62	11	5 670	4 120 000
						Av 5 620	4 150 000
B21S	1:1.46:2.44	0.42	6.0	33	8	6 430	4 370 000
				42	8	6 470	4 590 000
				58	8	6 530	4 780 000
						Av 6 480	4 580 000
B21W	1:2.0:3.10	0.49	4.5	35	10	5 520	4 470 000
				41	10	5 470	4 290 000
				57	10	5 750	4 600 000
						Av 5 580	4 450 000

*Cement: sand: gravel.

†Slabs for B24W and B24S made from Medusa Portland Cement. Slabs for B21W and B21S made from Alpha Portland Cement.

‡All cylinders moist cured for 7 days under wet burlap. Cylinders for B24W, B24S, and B21S coated with white paint after 7 days of moist curing and then allowed to cure in air of laboratory. Cylinders for B21W remained uncoated, otherwise same as other cylinders. Size of cylinders: 6 x 12 in.

¶Initial modulus of elasticity.

33. Construction of T-Beams

The steel beams were delivered with the end stiffeners and bearing plates welded in place. The first step in the laboratory was to arc-weld the shear connectors to the top flange of the beams. This was accomplished with continuous welds on the front and back sides of the channel with Lincoln No. 7 electrodes. The welding proceeded from one end of the beam to the other. The size of the welds was $\frac{3}{16}$ in. Connectors welded to the beam are shown in Figs. 33 and 34.

Table 15

Tensile Properties of Steel in Beams

Test coupons were about 1½ in. wide. Thickness of coupons was same as flange and web thickness respectively.

Specimen	Location of Test Coupons	Number of Test Coupons	Yield Point, psi	Ultimate Strength, psi	Modulus of Elasticity, psi	Percent Elongation in 8 in.	Percent Reduction in Area
B24W	Flanges	4	35 800	61 300	31 100 000	31	59
	Web	3	38 700	64 400	30 400 000	30	57
B24S	Flanges	4	35 200	59 200	30 600 000	32	60
	Web	3	37 900	61 200	30 700 000	29	59
B21S	Flanges	4	35 100	58 300	29 400 000	33	57
	Web	3	41 800	60 400	29 900 000	28	50
B21W	Flanges	4	34 300	57 900	29 200 000	29	52
	Web	3	41 400	61 800	29 600 000	24	51

Table 16

Tensile Properties of Steel in Shear Connectors

Test coupons were about ½ in. wide. Thickness was same as channel web thickness.

Specimen	Direction of Coupons to Direction of Rolling	Number of Test Coupons	Yield Point, psi	Ultimate Strength, psi	Percent Elongation in 2 in.
B24W and B24S	Parallel	4	44 400	67 250	26
	Perpendicular	4	47 000	67 150	25
B21S	Parallel	4	42 200	60 500	25
	Perpendicular	4	42 700	63 000	33
B21W	Parallel	2	38 900	54 500	..
	Perpendicular	2	39 700	56 600	40

The forms for casting (also shown in Figs. 33 and 34) were suspended from the steel beams. They were constructed of plywood and lumber supported by Junior I-beams. The bottom slab form was made of $\frac{5}{8}$-in. plywood placed flush with the top flange of the I-beam.

The reinforcement was wired together in a continuous mat. The longitudinal bars had to be spliced by butt welds located about 1 ft from midspan. The reinforcing mat removed from the forms is shown in Fig. 33, and in place and ready for casting the slab in Fig. 34.

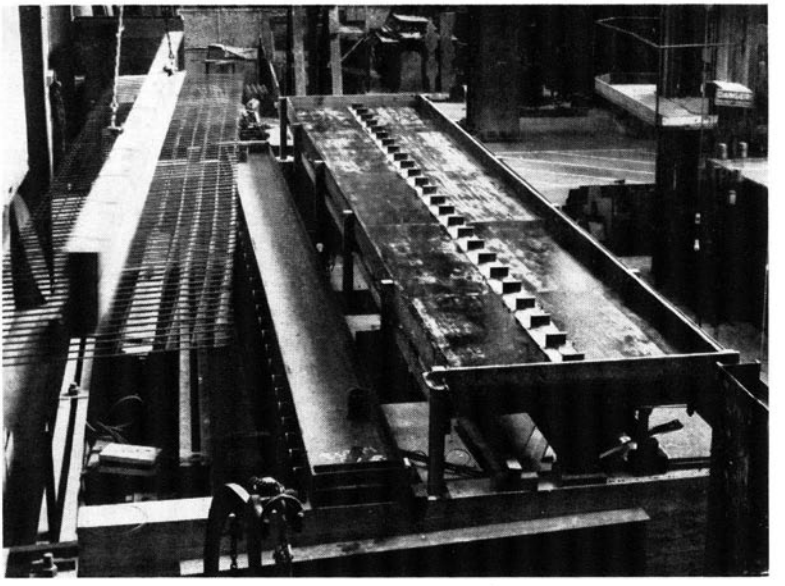

Fig. 33. Forms for B24W

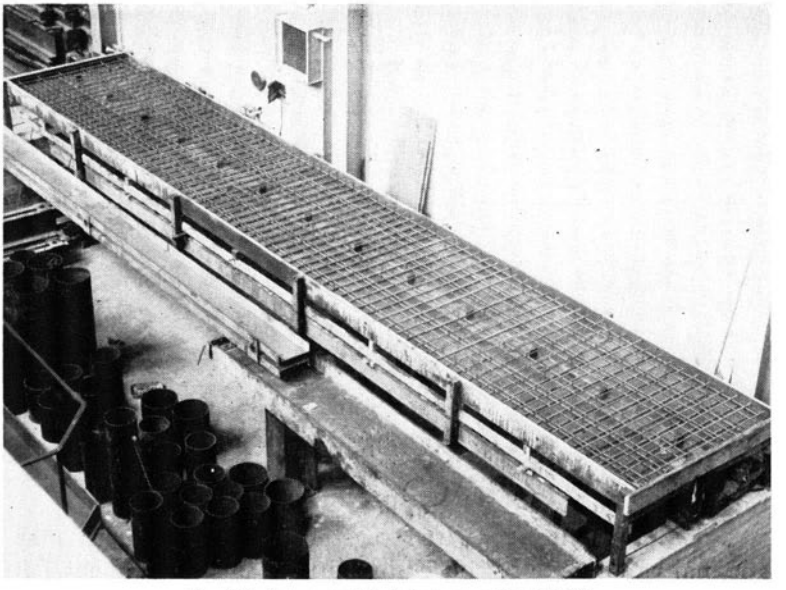

Fig. 34. Forms and Reinforcement for B21W

Beams B24S and B21S were built with one temporary support placed under the beam after the forms and reinforcement were in place. For beam B24S a reaction computed for a two-span continuous beam loaded only with the weight of the I-beam, forms, and reinforcing was jacked in 12 in. off center with a screw jack. An elastic ring dynamometer was used to measure the load. A support was then provided at midspan and the dynamometer removed. For beam B21S a slightly different procedure was followed in that the reaction was jacked in at a location 18 in. from midspan and the dynamometer and support left in place at this location.

Before the slab was cast, the forms were oiled and the top flange of the I-beam was covered with a heavy coat of white lead in order to destroy the bond between the slab and the beam. An exception to this procedure was beam B21W, in which no attempt was made to destroy the natural bond.

Each slab was made from 22 batches of concrete cast continuously. The concrete was vibrated externally with a vibratory screed consisting of a steel channel and a Viber Model No. 1 internal vibrator operating at more than 9000 rpm. After the first set took place, the surface of the slab was smoothed with steel trowels. The slab was moist-cured for 7 days. At the end of the moist-curing period the forms were removed, and after a few days of drying the slab was painted with a white enamel paint to prevent excessive shrinkage. The paint was omitted from beam B21W. A finished slab is shown in Fig. 35.

In B21S the shoring reaction was adjusted every day so as to keep the intermediate support at a constant elevation. No such adjustment was needed for B24S, since in this beam the intermediate support was rigid. The shoring was removed 20 days following the casting of the slab on B21S and 46 days on B24S.

Before testing began, all exposed surfaces of the I-beams were painted with aluminum paint. This coating reflects light and aids in the detection of yield lines.

For each slab three of the 6 x 12-in. control cylinders were made from every other batch. Steel forms placed on a machined steel base were used. The forms were filled in three layers and each layer was vibrated with a Viber Model No. 1 internal vibrator. The cylinders were cured and treated in the same way as the corresponding slab.

34. Instruments and Loading Apparatus

Instruments. The following measurements were made on each beam: strains on the beam and on the slab surface, deflections of the beam,

strains on the shear connectors, and slips between the slab and the beam. On beam B21W vertical movements of the slab with respect to the beam were also measured. With few exceptions, gages were located symmetrically about midspan as well as about the longitudinal centerline of the beam. In this way several check readings could be obtained. The locations of gage lines are shown in Fig. 36 for the east halves of beams.

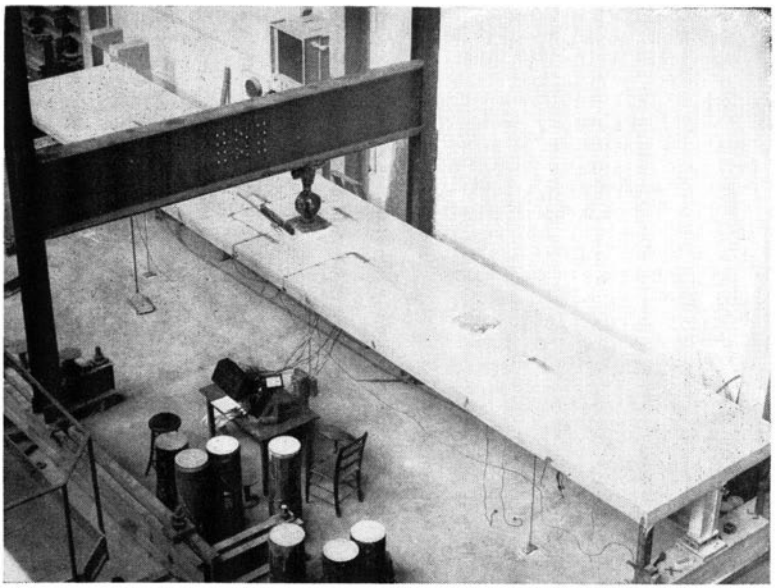

Fig. 35. B21W Ready for Testing

Strains on the steel beams were measured with 1-in. long Type A-11 SR-4 strain gages and with portable mechanical Berry gages, the latter gages being used only at midspan. A 5-in. gage with a multiplication ratio of 5.05 was used in the tests of B24W and B24S. An 8-in. gage with a multiplication ratio of 5.30 was used in the tests of B21S and B21W. Both Berry gages were equipped with 0.001-in. dial indicators. In addition, large inelastic strains on B21W were measured by a direct reading gage of 8-in. gage length. This gage also was equipped with a 0.001-in. dial indicator.

Strains on the slabs were measured with 6-in. long Type A-9 SR-4 strain gages. It was felt that a 6-in. gage length was needed to compensate for the heterogeneous character of concrete. Strains on the shear

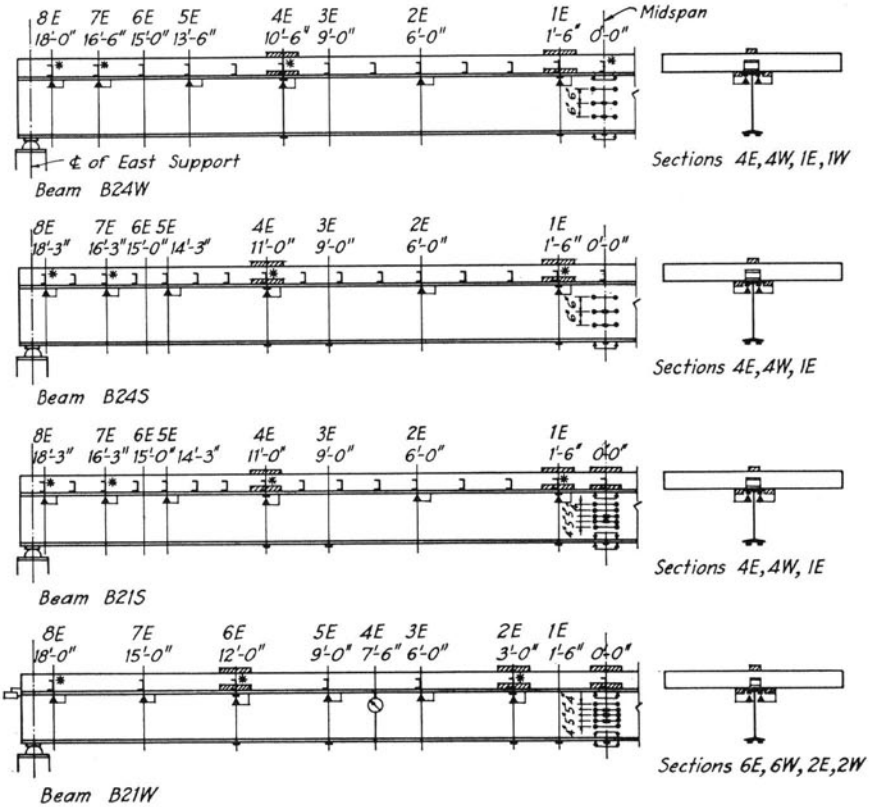

Symbols for Gage Locations

Note: All gages are symetrical about mid-span, except as noted for Type A-9 gages.

- 1" SR-4, Type A-11 Gages – at each location, one on each side of web.
- 6" SR-4, Type A-9 Gages – at each location on top of slab, one only, except at midspan of B21W where two gages are located 4'-0" apart, and except on top of slab at sections 1W on B21S and B24S where five gages are located 1'-3" on center; at each location on bottom of slab, one gage on each side of beam.
- Mechanical Gage Lines – at each location on web, one gage line each side; on flanges, three on outside and two on inside faces. (Gage lines are 5" long on B24W and B24S, and are 8" long on B21W and B21S.)
- Slip Gages – at each location on flange and slab, one on each side of beam.
- Slip Dials – one at each end of beam.
- Uplift Dials – one on each side of web.
- * 1/4" SR-4, Type A-7 Gages – on connectors indicated; detailed below.

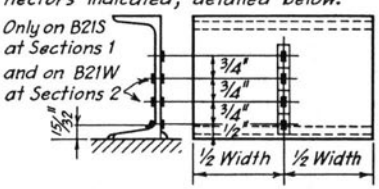

Fig. 36. Location of Gage Lines on T-Beams

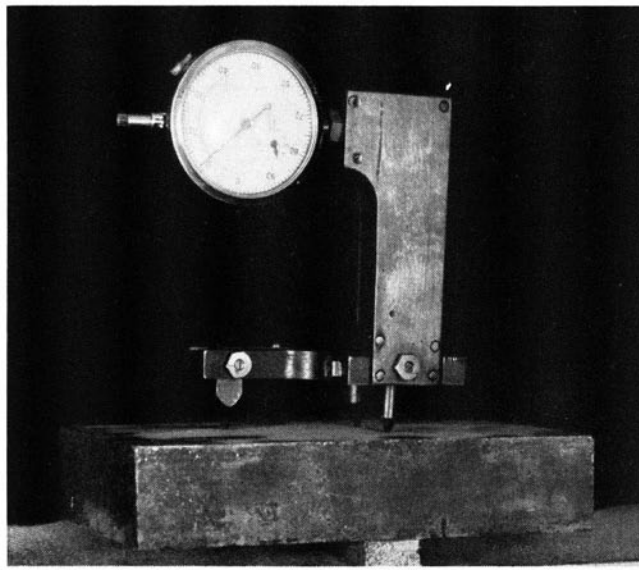

Fig. 37. Portable Slip Gage

connectors were measured with ¼-in. long Type A-7 SR-4 gages. These gages had to be attached and waterproofed before casting the slab. The manner of attaching electric strain gages and of waterproofing has been described in an earlier paper.*

All SR-4 gages were connected to a Baldwin Foxboro Type K Portable Strain Indicator having a least reading of 1×10^{-5} in. per in. The individual gages were connected to the indicator through a 100-point switch box. The wires were No. 22 tinned copper wire with plastic insulation.

Deflections were measured at midspan and at Sections 4E, W on the beams B24W, B24S, and B21S and at Section 6E, W on B21W (Fig. 36). Deflection measurements were made on the centerline of the I-beam with deflectometers bearing against the concrete floor of the laboratory and against the bottom flange of the beam. The deflectometers were equipped with 0.001-in. dial indicators. In the tests to failure deflection readings were made also with a 6-ft rule graduated in $\frac{1}{16}$ in.

Slips between the slab and the beam were measured with a portable mechanical gage designed on the principle of the Berry gage. The gage is shown in Fig. 37. In use, one of the three legs of this gage was seated in a hole drilled in a metal plug embedded in the slab and the remaining two legs were seated in two gage holes drilled in the top flange of the I-beam. The slip gage was equipped with a 0.001-in. dial indicator and

* E. Hognestad and I. M. Viest, "Some Applications of Electric SR-4 Gages in Reinforced Concrete Research," Proceedings, American Concrete Institute, 1950, Vol. 46, pp. 447–50.

had a multiplication ratio of 2.88. In the tests of B21W, slips at both ends of the beam were also measured by 0.0001-in. dial indicators.

The vertical movements of the slab with respect to the beam were measured in the tests of beam B21W by four 0.0001-in. dial indicators.

In addition to the instruments described above, mechanical and electric strain gages were used for measuring residual stresses in the I-beams. The instruments and locations of gage lines are described in Section 37.

The moduli of elasticity of the control cylinders were determined from measurements with a 6-in. gage length compressometer equipped with a 0.001-in. dial indicator. The multiplication ratio of the compressometer was 2.

Loading Apparatus. Load was applied to the beams by means of a screw jack bearing against a steel frame which was anchored to the floor of the laboratory. The load was measured with an elastic ring dynamometer of 125,000-lb capacity. A steel plate 14 x 14 x 2 in. was placed between the dynamometer and the slab. The plate was grouted in place on the slab with high strength gypsum plaster. The load from the T-beams was transmitted to two supporting concrete piers through a steel sole plate 6 x 9 x 1 in., a 6-in.-diam half cylinder at one end and a 2½-in. diam roller at the other end, and a steel bearing plate 12 x 12 x 2 in. The concrete piers were 4 ft 3 in. high, to permit access to the underside of the beam.

In the tests to failure the screw jack of 100,000-lb capacity was replaced by a 200,000-lb hydraulic jack. The arrangement for testing beam B21W is shown in Fig. 35. A similar arrangement was used for all four T-beams.

The control cylinders were tested in an Olsen screw-type testing machine of 300,000-lb capacity.

B. TESTS AND RESULTS

35. Description of Test Procedures

To meet the objectives of the investigation, three types of tests were performed: tests of the T-beams in flexure, tests of the shear connection, and capacity tests. All three types of tests were made with a single concentrated load. In the flexural tests load was applied at midspan and at the quarter-points. In the tests of shear connectors load was applied at locations close to the supports. The capacity tests were carried out with the load applied at midspan.

The sequence of the different types of loading and the magnitudes of loads are summarized in Table 17. All beams were tested first in flexure, twice with load at midspan and once with load at each quarter-point. In all these tests, strains were kept below yielding. With the exception of

Table 17
Outline of Tests of Composite T-Beams

Test Number	Age of Slab Days	Position of Load*	Load Increments, Kip	Maximum Load, Kip
		B24W		
1	39	Midspan	10	40
2	41	3E	10, 5	70
3	43	Midspan	10	60
4	47	3W	10	70
5	49	6W	10	50
6	61	Midspan	20, 10, 5	100
7	64	6W	20	100
8	70	Midspan†	40, 10	111
9	71	6E	25	100
		B21S		
1	20	Shore Removed		
2	34	Midspan	10	50
3	36	3E	15	60
4	40	Midspan	10	50
5	41	3W	15	60
6	43	Midspan	20, 10, 5	75
7	47	6W	30, 20	100
8	48	6E	30, 20	100
9	57	Midspan†	20, 10, 5, 2	102
		B24S		
1	46	Shore Removed		
2	47	Midspan	10	60
3	48	3E	20	80
4	49	Midspan	20, 5	65
5	55	3W	20	80
6	71	Midspan†	30, 10, 5	115
7	63	6W	30	120
8	63	6E	30, 16	[106
		B21W		
1A	33	Midspan	10, 5	40
		11 Repetitions of Load 40 Kips		
1B	34	Midspan	10	40
2	36	5E	10, 5	30
3	37	Midspan	10, 5	40
4	39	5W	5	30
5A	40	Midspan	15, 5, 3, 2	50
5B	41	Midspan	10	50
6	54	Midspan†	15, 5, 4	79

*3E, 3W, 5E.5W—9 ft from midspan. 6E. 6W—15 ft from midspan.
†Capacity test.

B24W, the next test was again with load at midspan, the objective being to find the load corresponding to the first yielding of the steel beam. The yield test was followed by two shear connector tests with loads near the supports, and by the capacity test. The tests with load close to the supports were omitted for beam B21W, because in this beam all shear connectors had already yielded during the yield test. The ultimate capacity of the structure was reached only in the tests of beams B21S and B21W. Capacity tests of beams B24W and B24S were stopped at loads of 111 and 115 kips respectively, because of danger of damage to the connections of the loading frame.

In all tests a set of readings of all instruments was taken before application of the first load increment. Then load was applied in increments of 5 to 40 kips and a set of readings was taken after each increment of the load. After the maximum load had been reached and a set of readings were taken, the load was released and the no-load readings were then repeated.

Readings were taken a few minutes after applying the load, so that the beam was allowed to become stable. In general, loads below yielding were stable. After the yield load was exceeded, and especially as the loads were approaching the ultimate, the load dropped off an appreciable amount after each increment. The maximum drop-off was about 10 percent. As a rule, no attempt was made to keep the load at a certain value. Instead the tests were so conducted that the deformation induced by each load increment was held constant during the measurements.

Each test was completed within a period of 2 to 5 hr, in order to avoid complications due to various time effects, such as temperature changes, drift of electric strain indicators, etc.

A few special tests were made in addition to the tests with a concentrated static load. In specimens built with shoring, the first test was the removal of the shore. In the specimen B21W bond between the steel beam and the concrete slab had to be broken first. Since the static test with a load of 40 kips at midspan did not break the bond this load had to be removed and reapplied eleven times. The only measurements which were made during this repeated loading were the occasional checks of slips and deflections.

36. Manner of Presentation of Test Data

The results of the tests of composite T-beams are presented in Figs. 38–59 and Tables 19–28. The data obtained are very uniform for all tests. It is considered sufficient to present the results for a few typical tests only.

The data on the behavior of composite T-beams are divided into two sections: (1) behavior at loads lower than those causing yielding of the I-beams and (2) behavior at loads causing yielding of the I-beams. The yield and ultimate loads are discussed separately.

The test data on the behavior of T-beams are compared with theoretical values. For the loads below yielding three different theories are included in the comparisons: the theory for complete interaction between

Table 18
Properties of T-Beams

Section Properties	B24W	B24S	B21S	B21W
I-BEAM				
Area, A_b, in.^{2}	22.37	22.37	20.02	20.02
Moment of Inertia, I_b, in.^{4}	2096	2096	1478	1478
Modulus of Elasticity, E_b, 10^6 psi	30.7	30.6	29.6	29.4
SLAB				
Area, A_s,* in.^{2}	469.6	463.8	467.1	461.1
Moment of Inertia, I_s,† in.^{4}	1529	1471	1521	1434
Modulus of Elasticity, E_s, 10^6 psi	4.16	4.15	4.58	4.45
COMPOSITE SECTION				
Modular Ratio, $n = E_b/E_s$	7.38	7.38	6.46	6.61
Moment of Inertia, I, in.^{4}	5943	5943	4652	4580
Distance of Neutral Axis from Centerline of Steel I-beam, $\bar{y}$, in.	10.97	10.97	10.72	10.58
Ratio of Horizontal Shear per Unit Length at the Contact Slab and Beam Surface to the Vertical Shear, q'_c/V, in.$^{-1}$	0.0413	0.0413	0.0462	0.0463
Ratio of Connector Modulus to Connector Spacing, k/s, 10^6 psi	0.374	0.513	0.366	0.0907
Weight, lb per ft	567	552	565	551

*A_s includes transformed steel area.
†I_s is based on A_s.

the slab and the beam, the theory for incomplete interaction, and the theory for no interaction. The theories for complete interaction and no interaction represent limiting values for the behavior of a composite T-beam; their application does not require any explanation. The theory for incomplete interaction used in connection with this report was that developed by N. M. Newmark.* The values of the stiffness of the shear connection used in this theory were computed from the measured slips by a method given in the Appendix of Bulletin 396.† All theoretical calculations were based on the data given in Table 18.

For loads beyond first yielding the test data were compared with theories for complete interaction and no interaction only, the assumptions

* Reference 112, Appendix, pp. 115-33.
† Reference 112, pp. 132–33.

and methods used for computing the theoretical values being outlined in Appendix A of this bulletin.

The behavior of the shear connectors in composite T-beams is compared with the behavior of corresponding connectors in push-out specimens in Section 46, in which complete test histories are presented for several connectors because of the influence of pre-loading on the succeeding tests. Finally, the semi-empirical formulas for analysis of channel shear connectors derived from the push-out test data are compared with the results of the tests of composite T-beams in Section 46.

37. Auxiliary Tests

In order to be able to determine total stresses in the steel beams measurements were made of the residual stresses due to welding of the shear connectors, shrinkage of the slabs and rolling of the I-beams.

Residual stresses due to welding of the shear connectors were measured at midspan on beams B24W and B24S, and about 5 ft from one support on beams B21S and B21W. Strains were measured on both flanges and on the web with a Berry strain gage. Although erratic, the readings indicated that welding of the shear connectors set up tensile stresses on the order of 1000 psi in the bottom flange of the beam. An exception was beam B21W in which practically no stresses due to welding of the connectors could be measured at any gage line.

A part of the shrinkage stresses was measured together with the dead load and shoring strains. Total shrinkage stresses were measured as a part of the residual stresses in the beams.

After the test to failure, residual stresses in the beams were determined on sections of beams cut out approximately 5 ft from one support. This location was chosen in order to obtain a section at which yielding did not occur during testing. Residual strains were measured on several gage lines (Fig. 38) by a mehanical 8-in. Berry gage; on B21W all mechanical gage readings were checked by A-11 SR-4 gages of 1 in. length. Residual stresses were relieved as follows: first the concrete slab was removed, then a 12-in. wide section was cut out of the beam, and finally each gage line was separated by saw cuts. Readings were taken before and after each step. In B21W satisfactory agreement was found between the mechanical gages and electric strain gages, the latter being used on this beam only.

The shrinkage strains measured at the conclusion of the tests are shown in Fig. 38. In this figure measured strains are plotted as full circles;

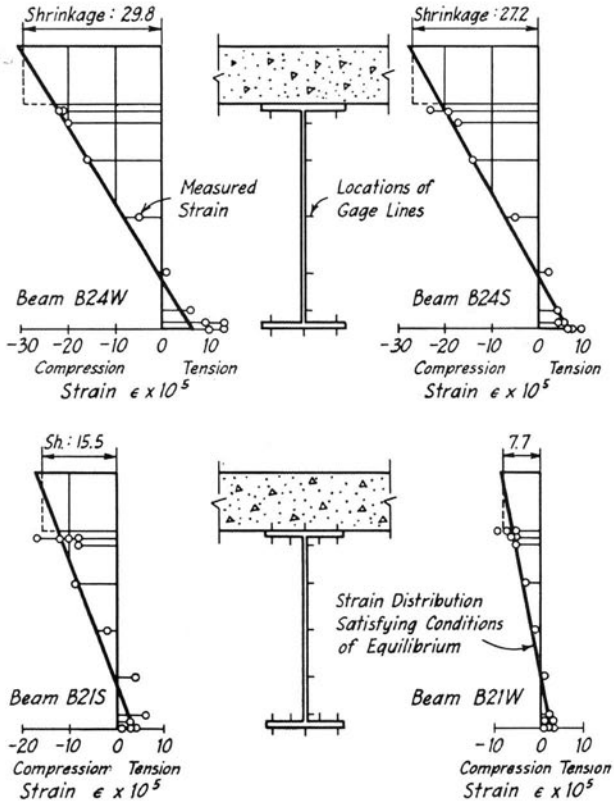

Fig. 38. Shrinkage Strains in Composite T-Beams

a strain distribution satisfying conditions of equilibrium is drawn for each beam. Although individual readings are erratic, the test data give a reasonable distribution of strains due to shrinkage. The following amounts of shrinkage in the concrete slab were found for the individual beams:

Beam	Shrinkage, in. per in.
B24W	0.000298
B24S	0.000272
B21S	0.000155
B21W	0.000077

These values correspond to some restraint to the shrinkage because of the shear connectors. In the test to failure of beam B21W several shear connectors were broken off in the vicinity of residual-strain gage lines. Therefore it is probable that a large portion of the shrinkage strain was relieved before the slab was removed. This explains the low value of shrinkage for beam B21W.

The shrinkage strains in the bottom flange of the beam range from 5 to 10 x 10^{-5}, corresponding to tensile stresses of 1500 to 3000 psi.

Residual strains which were set up in the I-beams due to rolling and which were relieved after the tests by successive cutting operations are shown in Fig. 39. With the exception of B24S the shapes of the strain

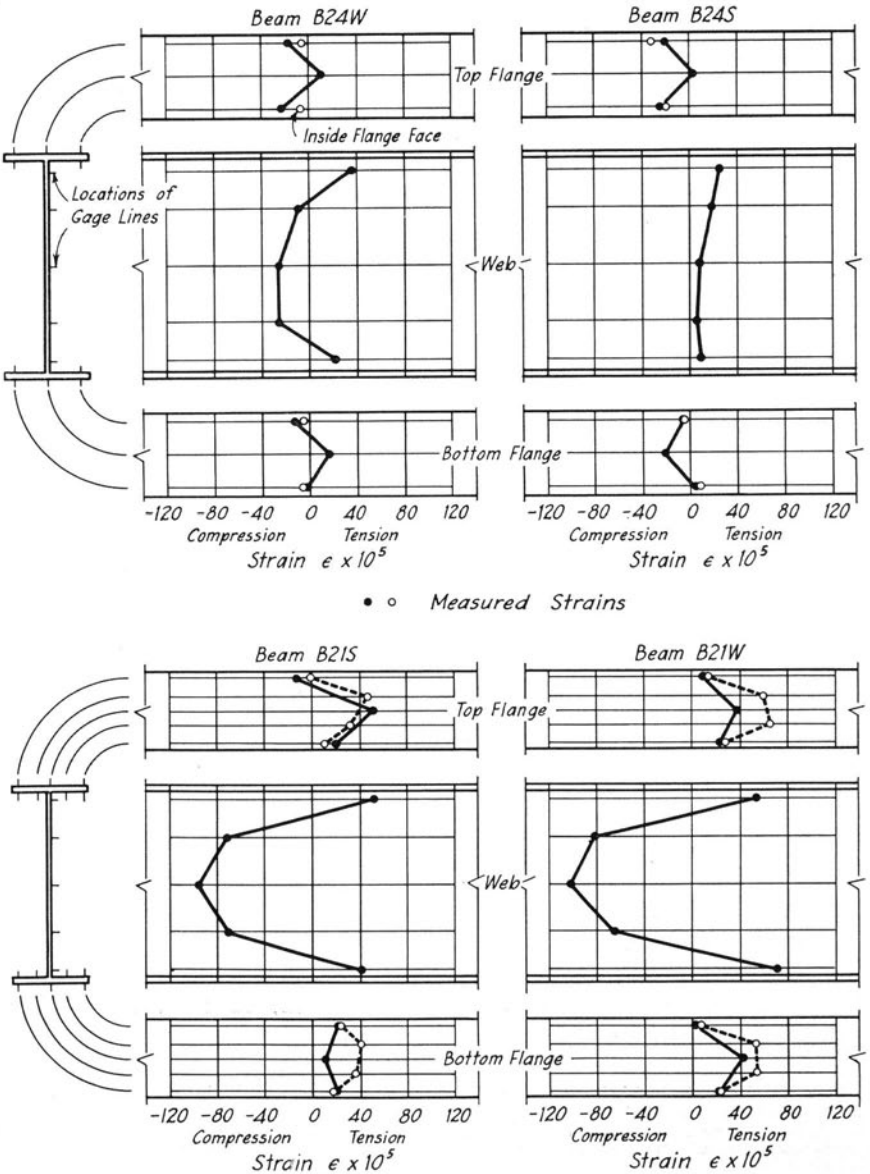

Fig. 39. Residual Strains in Rolled I-Beams

distribution curves are similar for all beams and also similar to the corresponding curves found in the tests of wide flange I-beams at Lehigh University.* The residual strains in the web of B24S are much smaller than in any other beam. The flatter distribution of residuals in this beam was probably caused by slight yielding of the bottom flange of the beam during testing, as three slip lines were found at the location of the residual strain gage lines.

The numerical values of the residual strains differ from one beam to another, and larger strains were measured in the smaller beams. It should be noted that at mid-depth of the 21-in. beams residual compressive stresses due to rolling were about 30,000 psi. The residual stresses in the flanges were much smaller, the average residual stress varying from a compression of about 3000 psi to a tension of about 9000 psi.

38. Behavior of Composite T-Beams Before Yielding of I-Beams

Since it is impractical to provide a continuous shear connection and since it is virtually impossible to provide shear connectors that prevent slip completely, some degree of incomplete interaction between the slab and the I-beam is an inherent characteristic of composite steel and concrete T-beams. This fact is brought out by the test data presented in the present section.

Slips. Of all measured quantities, slip between the slab and the beams is the most sensitive to the effects of incomplete interaction. That slip and consequent incomplete interaction were present in all four T-beams is illustrated conclusively in Figs. 40 and 41, in which the distribution of slip is shown for each beam. If the interaction had been complete no slip could have taken place between the beam and the slab. On the other hand, had there been no interaction, much larger slips would have occurred. For example, the theoretical end slip for B21W for no interaction is 0.173 in. when loaded at midspan with a load of 50,000 lb; the corresponding slip for this beam as tested is 0.013 in.

In Figs. 40 and 41 the distribution of slip along the beams is plotted at two values of load for each beam. Both measured and theoretical curves for incomplete interaction are shown.† The theoretical curves are in fair quantitative agreement with the measured values; however, since the theoretical curves are based on slips measured in all tests (Section 36), the quantitative agreement shows only that the slips must have been fairly consistent throughout the tests.

* W. W. Luxion and B. G. Johnston, "Plastic Behavior of Wide Flange Beams," The Welding Journal Research Supplement, November 1948, p. 543.

† The theoretical curves were computed on the basis of average stiffnesses of the shear connections. The average stiffnesses were determined from slips measured in several tests.

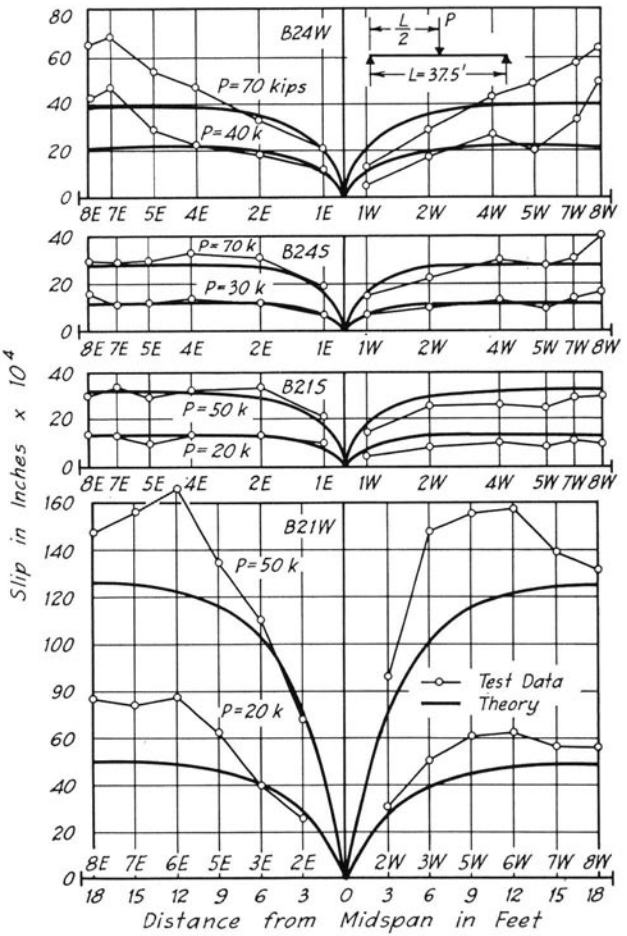

Fig. 40. Slip Distribution Curves, Concentrated Load at Midspan

When the slip distribution curves for the individual beams are compared at equal loads, comparatively large slips are observed for B21W. Slips for B24W are over 50 percent greater than those for B24S, whereas the difference between slips for B24S and B21S is of the same order of magnitude. Slips for B21W are three to five times as large as those for B21S. These observations are in very good agreement with values which could be expected on the basis of the spacing and the width of the shear connectors (Fig. 32).

Strains and Deflections. The most important question which may be asked in connection with the behavior of composite T-beams is: How

does the incomplete interaction affect the capacity and the deformations of this type of structure? The capacity of composite T-beams is discussed in Section 41; the strains and deflections of the beams are shown in Figs. 42–44 and in Tables 19 and 20.

In Fig. 42, strains measured on the bottom flange of the beam are compared with theoretical values for complete interaction and no interaction, and strains measured on the top of the slab are compared with the theoretical values for complete interaction. It can be seen that, with the exception of beam B21W, both the bottom flange and top slab strains

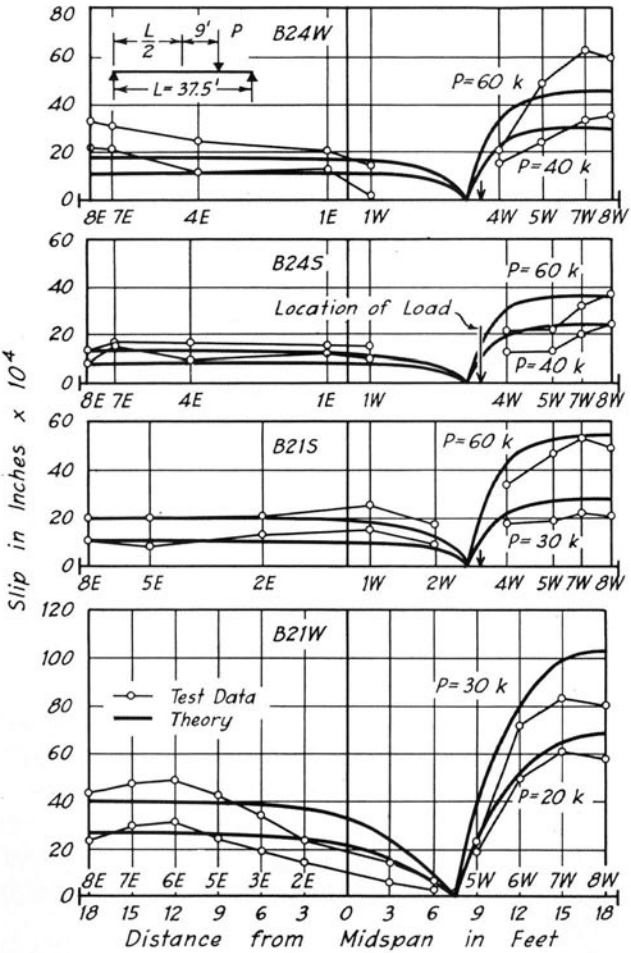

Fig. 41. Slip Distribution Curves, Concentrated Load at Quarter Point

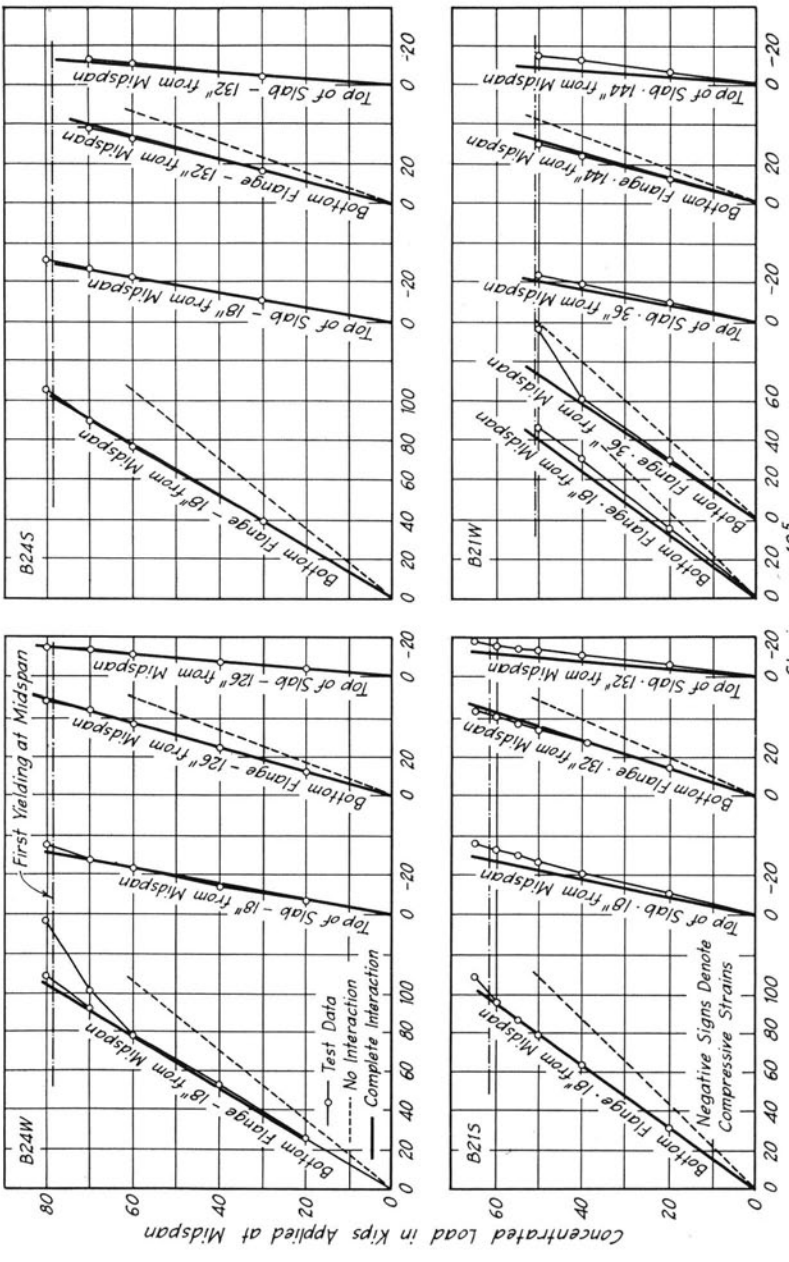

Fig. 42. Load-Strain Curves, Concentrated Load at Midspan

practically coincide with those for complete interaction. The measured values for B21W fall in between the theoretical lines, indicating that in this beam slip between the slab and the beam caused some increase of strains. Strains computed by the theory for incomplete interaction were in all cases in excellent agreement with the measured values; however, they are not included in Fig. 42 for reasons of simplicity.

In Fig. 43, deflections measured at midspan and near the quarter-points are compared with theoretical deflections for complete, incomplete, and no interaction. It can be seen that in all cases the measured

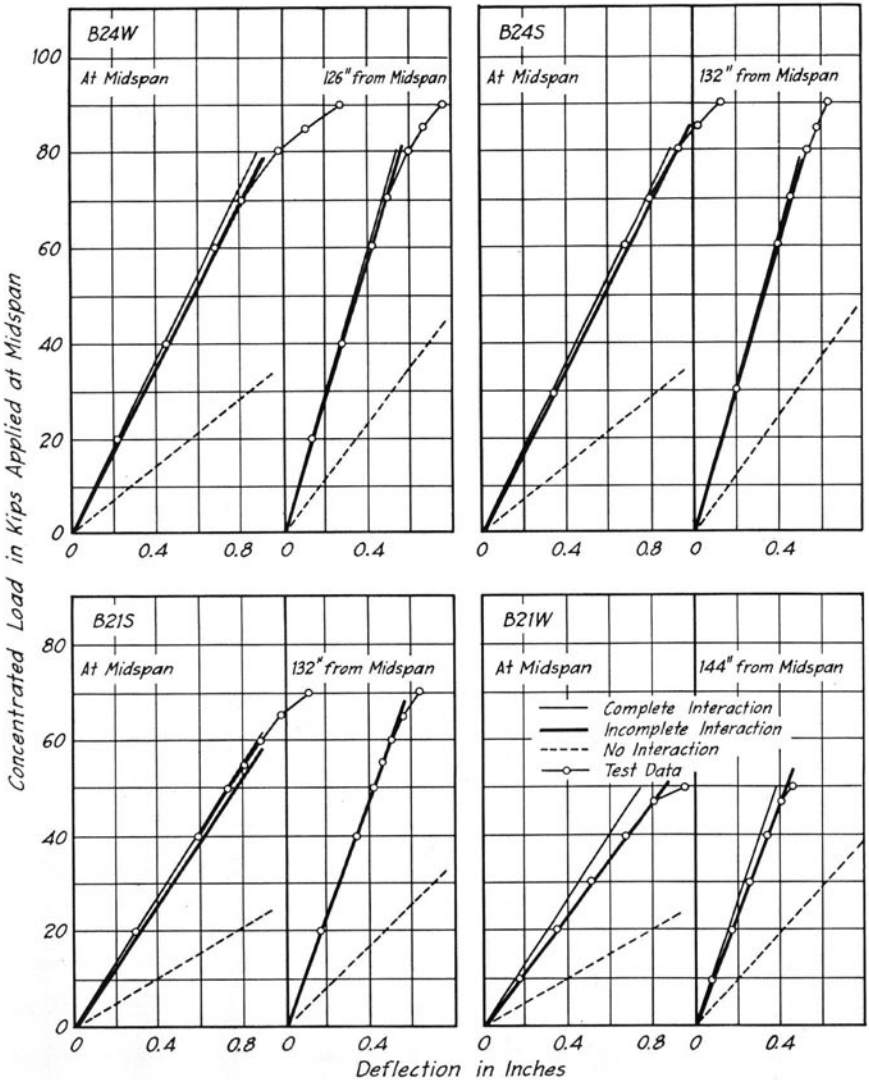

Fig. 43. Load-Deflection Curves, Concentrated Load at Midspan

deflections agree with those computed for incomplete interaction. Except at the quarter-point of B21S, measured deflections are always slightly larger than those computed for complete interaction. In all cases, the measured deflections were very much smaller than those computed for beams without any interaction.

Quantitative comparisons of measured and theoretical bottom flange strains at sections close to midspan and of deflections at midspan are given in Table 19. The theoretical values for complete interaction are taken as 100. It can be seen from this table that the relative measured values of both strains and deflections agree very well with the theory for incomplete interaction and that the decrease of interaction for the first three beams is entirely negligible. Even for beam B21W, built with an extremely weak shear connection, the theoretical increase of strains was only one seventh the theoretical increase for a beam without any interaction, and the corresponding increase of deflection was only one eleventh.

The effect of the decrease of interaction can be better observed for strains measured at the junction of the slab and the beam. This point is illustrated by the strain distribution curves plotted in Fig. 44. The test data and the theoretical values for both incomplete and complete interaction are included in this figure. The agreement between the test data and the theory for incomplete interaction is good.

Figure 44 as well as Fig. 43 and to some extent also Fig. 42 bring out one additional characteristic of the behavior of composite beams with incomplete interaction: the decrease of interaction is a somewhat localized effect. The decrease of interaction is always greater at locations which are close to the point of load application than at locations which are more remote from the load.

Strains Directly Under Load. In Fig. 42 and Table 19 the measured strains are compared with the theoretical values at locations some distance away from the section at which the load was applied to the beam. However, strains governing the design are those under the load. In Table 20 theoretical and test values of bottom flange strains are compared for locations directly under the load. It can be seen that the measured strains at this location are always smaller than those computed from the theory. Even when the effect of distribution of load over the area of the steel loading plate is considered, the difference is about 4 to 6 percent. These differences may be accounted for by the local distortions present under a concentrated load.

39. First Yielding of I-Beams

Local yielding as indicated by one of the strain gages or by observation of the first appearance of yield lines occurred at locations close to or at midspan. However, this yielding involved only individual yield

Table 19

Relative Values of Beam Strains and Deflections for Complete, Incomplete, and No Interaction

Concentrated load at midspan. Strains at section 18 in. from midspan. Deflections at midspan. Test data represent average values.

Beam	Relative Values in Percent Based on Complete Interaction							
	Bottom Flange Strains				Deflections			
	Theory for Complete Interaction	Theory for Incomplete Interaction	Test Data	Theory for No Interaction	Theory for Complete Interaction	Theory for Incomplete Interaction	Test Data	Theory for No Interaction
B24W	100	102	104	135	100	104	102	248
B24S	100	101	100	135	100	103	102	249
B21S	100	102	98	135	100	104	101	262
B21W	100	105	105	135	100	115	113	252

lines and did not seem to have any influence on the general behavior of the T-beams. General yielding occurred first on the bottom face of the bottom flange at midspan. The load at which first yielding occurred was determined from four load-strain curves for two mechanical and two electric strain gages located at midspan on the bottom of the beam. All these curves showed sharp increases at about the same load. The yield

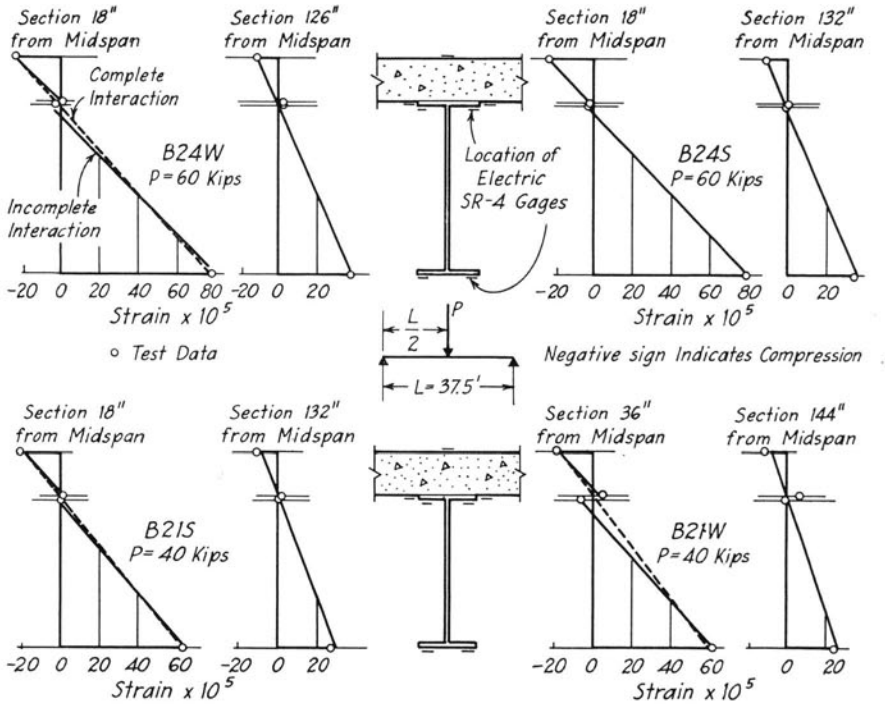

Fig. 44. Strain Distribution Curves, Concentrated Load at Midspan

loads so determined are listed in Table 21 and compared with theoretical values computed on the basis of yield strains determined from tests of tensile coupons.

With the exception of beam B21W all measured yield loads are higher than the theoretical ones. Part of the difference between the theory and tests must be attributed to the local load effects described in the preceding section, but these effects do not account for the whole difference. It is believed that the remaining difference was caused by the presence of residual strains.

Table 20

Ratios $\frac{\epsilon}{P}$ for Bottom Flange Strains at Midspan

Load at midspan. Test data represent average values.

Beam	$\frac{\epsilon \times 10^5}{P}$ in. 1/Kip			
	Test Data		Theory for Incomplete Interaction	
	1-in. SR-4 Gages	Berry Gage*	Concentrated Load	Load Uniformly Distributed over 14 in.
B24W	1.37	1.47	1.46	1.44
B24S	1.39	1.42	1.46	1.44
B21S	1.62	1.59	1.80	1.77
B21W	1.75	1.78	1.88	1.86

*5-in. gage was used in tests of B24W and B24S. 8-in. gage was used in tests of B21S and B21W.

The yield strains are analyzed in Table 22. With the exception of the dead-load strains for beams built without shoring, all strains included in this table are values measured at midspan. It seems likely that the difference between the total strains due to loading and the yield strains of the control coupons was caused by residual strains. As the gages at midspan were located about 1 in. from the edges of the bottom flange, the residual strains derived in Table 22 are in reasonable agreement with the residual strain measurements shown on Figs. 38 and 39.

In conclusion it must be emphasized that, partly because of the local effects of load but mainly because of the residual strains, the loads at which first yielding occurs are very uncertain and cannot be predicted with any satisfactory degree of accuracy.

The loads at first yielding expressed in terms of dead loads (DL) and live loads (LL) are listed in Table 23. The 24-in. deep beams yielded first at 3.35 LL (B24W) and at 3.30 LL (B24S); the 21-in. deep beams at 2.63 LL (B21S) and 1.99 LL (B21W). These values are compared and discussed in Section 45.

Table 21

Loads at First Yielding of Steel Beams

Concentrated load at midspan. Measured values represent load at which the load-strain curve for the bottom flange at midspan deviated from a straight line. Theoretical values computed for incomplete interaction and load distributed uniformly over 14 in. at midspan; yield point strain computed from Table 15.

Beam	Load P in Kips	
	Theoretical	Measured
B24W	64.6	79
B24S	69.5	78
B21S	56.6	62
B21W	47.9	47

Table 22

Bottom Flange Strains at First Yielding of Steel Beams

+ — tensile strain; − — compressive strain

Cause of Strain	Strain $\epsilon \times 10^5$			
	B24W	B24S	B21S	B21W
Dead load, computed strain	+22	....	....	+28
Dead load + Shoring, computed strain*	....	+22	+23	....
Concentrated load at Midspan, measured strain	+108	+108	+100	+82
	+130	+130	+123	+110
Tensile Coupon Yield Strain (from Table 15)	+115	+115	+119	+117
Derived Residual Strains	−15	−15	−4	+7

*Magnitude of shoring reaction taken from test data; see Section 45.

40. Behavior of Composite T-Beams After Yielding of I-Beams

Loading beyond first yielding demonstrated clearly the difference between beams B24W, B24S, and B21S on one hand and beam B21W on the other hand. While the shear connections of the first three beams were strong enough to retain a very high degree of interaction up to the ultimate load, all connectors of beam B21W yielded at the same load as the steel beam; this resulted in some loss of interaction as the loading continued.

Behavior of Typical Beams. In each of beams B24W, B24S and B21S, yielding at midspan spread almost immediately through the full thickness of the bottom flange after the yield load had been reached. As loading continued, yielding spread both toward the support and toward the upper flange so that the yield lines formed approximately an isosceles triangle with its peak at midspan. As yielding approached mid-depth of the beam a major portion of the deflection was caused by rotations at

Table 23

Capacities of Beams in Terms of Dead and Live Loads

1 LL = 23,600 lb at midspan

Beam	Bottom Flange Stress in psi at 1 DL + 1 LL		Load at First Yielding	Load at Deflection $\frac{L}{200}$ = 2.25 in.	Ultimate Load Capacity
	Design Data	Test Data			
B24W	16 850	16 900	1 DL + 3.35 LL	1 DL + 4.35 LL	1 DL + 5.20 LL†
B24S*	.....	16 700	1 DL + 3.30 LL	1 DL + 4.44 LL	1 DL + 5.40 LL‡
B21S*	17 950	18 000	1 DL + 2.63 LL	1 DL + 3.50 LL	1 DL + 4.32 LL
B21W	.....	20 200	1 DL + 1.99 LL	1 DL + 2.92 LL	1 DL + 3.35 LL

*Dead load includes a part of shrinkage stress.

†At maximum test load, 1 DL + 4.70 LL, beam did not fail; ultimate capacity estimated on basis of Fig. 47 as 120 kips.

‡At maximum test load, 1 DL + 4.87 LL, beam did not fail; ultimate capacity estimated on basis of Fig. 47 as 130 kips.

midspan; a semi-plastic hinge formed at that section. The deflection line of the beam changed from a curve with continuously changing curvature to a curve consisting of two slightly curved portions interconnected by a short sharp curve at midspan.

Owing to the sharp change of curvature at midspan the adjacent shear connectors were subjected to large deformational loads, and yielding at the central connectors was observed before the maximum test load was reached. The yielding of connectors was limited to a short distance on both sides of the load. As the loading continued and yielding in the beam spread toward the supports, yielding of the shear connectors spread slowly in the same direction, but in none of the three beams did it ever extend farther than to the connectors at about the quarter-points. Thus the increased slip remained a local phenomenon restricted to the central portion of the T-beam. This point is illustrated by the slip distribution curves in Fig. 45.

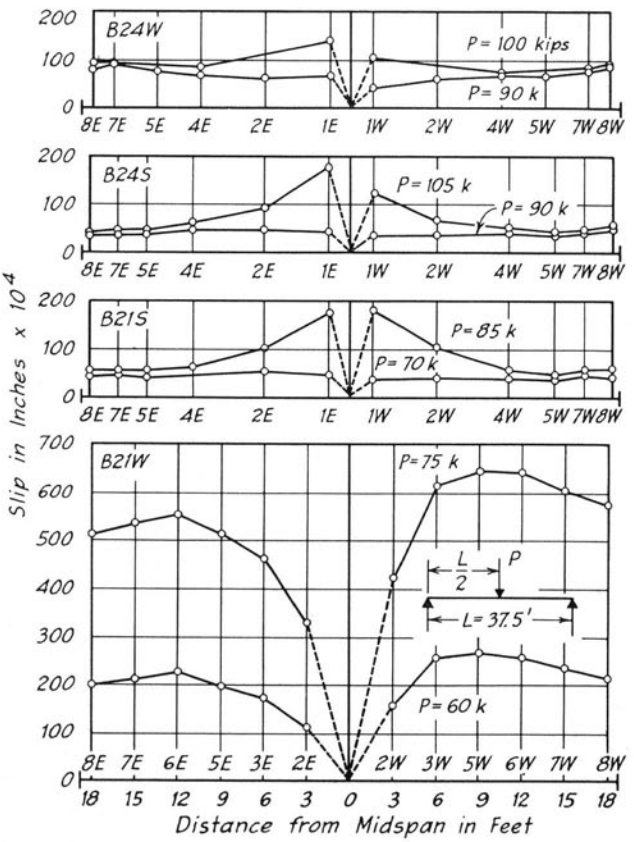

Fig. 45. Slip Distribution Curves in Tests Beyond First Yielding

That the moderate yielding of a few shear connectors did not impair the interaction to any appreciable degree is shown by the strain distribution curves in Fig. 46, plotted for all three beams at a section 18 in. from midspan at loads about half-way between first yielding and the ultimate. Even though the shear connectors at these sections began to yield at much lower loads, the decrease of interaction was small.

It can also be seen from the load-strain curves for the bottom flange at midspan plotted in Fig. 46 that a fair degree of interaction must have been present throughout the tests of the T-beams. If the interaction had been lost or decreased appreciably, the load-strain curves would have flattened out in a manner similar to that indicated by the dotted lines for beams without interaction. For all three beams a steady increase of load with strain was observed.

The increase of load with plastic strains was accompanied by large deflections. In Fig. 47 load-deflection curves are plotted for each beam at midspan and at quarter-points. The full range of deflections up to the maximum load applied is shown. It should be noted that very large deflections on the order of several inches were observed on each beam and especially on B21S. It also should be noted that the deflection curves never flattened out completely.

The load-strain curves for gages located on the top flange and on the bottom face of the slab, shown in Fig. 46, indicate that the neutral axis of the section shifted toward the top of the slab as the loading continued beyond first yielding. First cracking of the bottom face of the slab was detected after the second or third increment of load beyond yielding. All tensile cracks were perpendicular to the longitudinal axis of the beam and were grouped around midspan at a fairly regular spacing of about 6 in. With further increase of load more cracks appeared farther away from midspan and the existing cracks penetrated deeper into the slab.

Behavior of Beam with Weak Shear Connection. Beam B21W was built with a connection designed to yield simultaneously with the beam. The test of this beam showed that this simultaneous yielding of the shear connectors and the beam had a profound influence on the behavior of the beam when stressed beyond first yielding.

The same increment which caused first yielding of the steel beam also caused yielding in all shear connectors. Thereafter a rapid increase in both slip and shear connector strains was observed as the loading continued. The distribution of slip after yielding, shown in the bottom part of Fig. 45, retained about the same shape as before yielding (Fig. 40). In beam B21W yielding spread faster in the direction of the beam axis than in the other beams, and much smaller concentration of rotations at midspan took place. A visible sharp break of curvature at midspan could be observed only at loads approaching the ultimate.

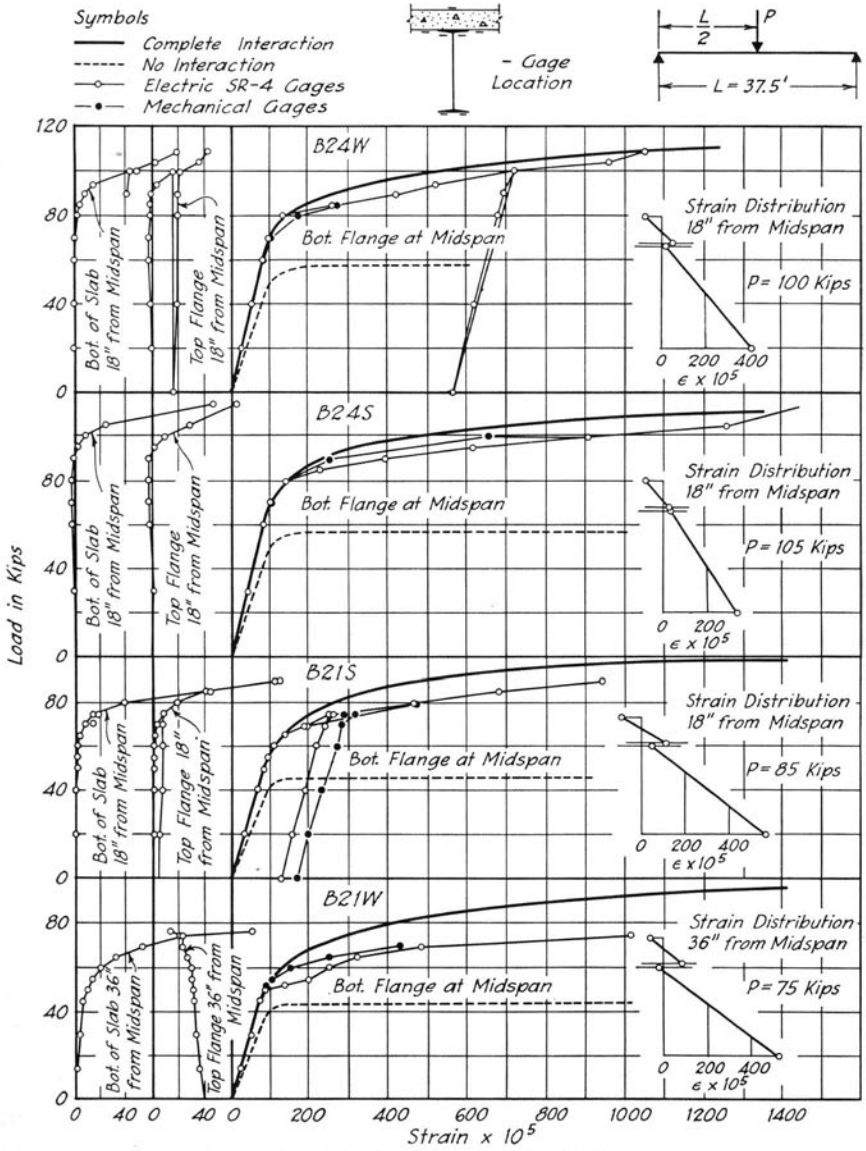

Fig. 46. Strains in Tests Beyond First Yielding

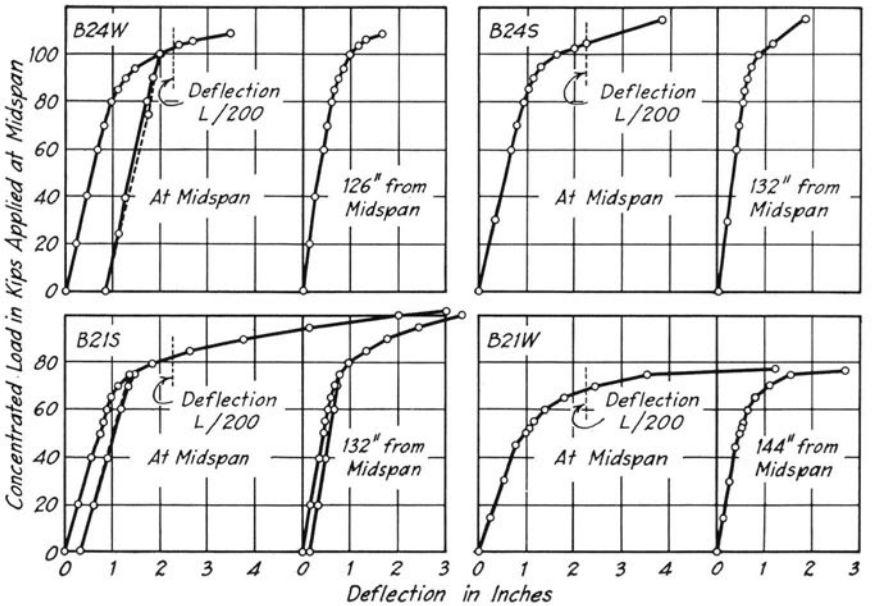

Fig. 47. Load-Deflection Curves in Tests Beyond First Yielding

The load-strain and strain distribution curves for B21W plotted in Fig. 46 show a fairly marked decrease of interaction after the yield load was exceeded. Strains measured on the bottom face of the top flange showed compression throughout the tests, while the bottom slab fibers were in tension. The load-strain curves for the bottom flange at midspan flattened out at a load of 75 kips. At that load the yield lines extended to a height of about 8 in. from the bottom of the beam.

The deflections, shown in Fig. 47, increased in beam B21W at a markedly faster rate than in B21S and the load-deflection curves flattened out at a load of 75 kips.

Test Data vs. Theory. In Fig. 46 bottom flange strains measured at midspan are compared with the theoretical curves for complete and no interaction. The assumptions and method used for the computation of theoretical strains are given in Appendix A. Two test curves are included for each beam, one obtained from mechanical strain gages, the other from electric gages. The test curves are averages of two gage readings.

After yielding had taken place, the measured load-strain curves always lay below the theoretical curves for complete interaction. The

difference might have been caused by one or more of the following factors: (1) the theoretical analysis did not include the effects of a decrease in interaction, (2) residual stresses were neglected in the analysis, and (3) while yielding in a mild steel beam progresses irregularly in form of wedges, the theoretical analysis was based on the assumption of a uniform spread of yielding.

It is obvious that a decrease of the degree of interaction would decrease the magnitude of the load corresponding to a given strain. The question remains whether the decrease of interaction in the beams tested was large enough to account for the differences between the theory for complete interaction and the test data. It seems reasonable to expect that if the decrease of interaction were large enough to lower the load-strain curves appreciably, the difference between the theory and the test data would increase rather than decrease with the load. While this is the case for B21W, a precisely opposite tendency may be observed for the first three beams. Furthermore, the strain distribution curves and the ultimate capacities indicate that the decrease of interaction was small.

Residual stresses due to rolling and shrinkage were neglected in the theoretical analysis, and a continuous shoring instead of a single intermediate support was assumed. Those three assumptions do not influence the ultimate capacity and only the third one would have a small influence on the elastic stresses. Hence the theoretical elastic strains and the ultimate capacities for beams with a high degree of composite action are in good agreement with the test results. On the other hand, the load-strain curves beyond first yielding are influenced by all three types of stresses.

Studies of the effects of the differences in shoring and of shrinkage stresses on the load-strain curves indicated that both of those effects are negligible. On the other hand, the residual stresses due to rolling were large enough to account for a substantial part of the discrepancy between the theory and the test data.

The residual stresses due to rolling cannot have any effect on the load-strain curves once the beam has yielded throughout the full depth of the I-beam. Since the theoretical curves lay above the measured curves even at loads at which the I-beam had undoubtedly yielded through its full depth, it is very probable that the discrepancy between the theory and the test results was caused by the incorrect assumption regarding the manner in which yielding spreads through the beam. This conclusion is supported also by the evidence obtained from the tests of wide-flange beams at Lehigh University.*

* W. W. Luxion and B. G. Johnston, "Plastic Behavior of Wide Flange Beams," The Welding Journal Research Supplement, November 1948, pp. 538–54.

In Fig. 48 two theoretical load-deflection curves are plotted for beam B21S. As can be expected, the curve based on theoretical strains (full line) does not agree with the test data, whereas the agreement for the second curve, based on measured strains (dotted line), is good. The theoretical deflections were computed as outlined in Appendix A.

It may be stated in summary that the differences between the theoretical load-strain curves for complete interaction and the test data were caused primarily by the combined effects of residual rolling stresses and

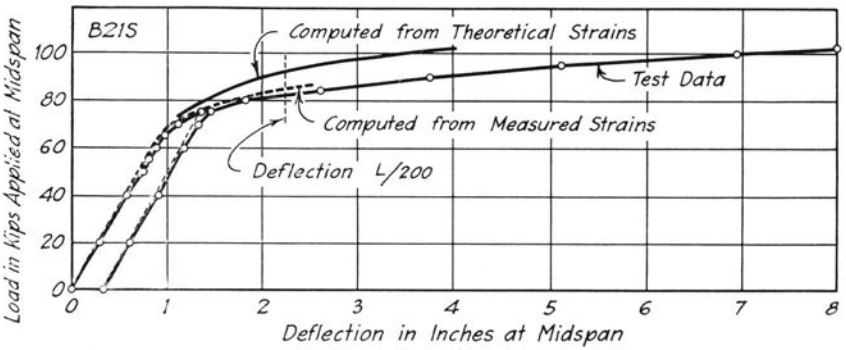

Fig. 48. Computed and Measured Load-Deflection Curves for Beam B21S

of inaccurate assumptions regarding the mechanism of yielding. It is believed that the degree of interaction was high enough to insure practically complete composite action throughout the tests. An exception to this was beam B21W, in which a detrimental decrease of interaction between the slab and the beam was observed. However, even this beam, built with a very weak shear connection, had appreciably better load-strain characteristics than those which were indicated by the theory for beams without interaction.

41. Ultimate Loads of T-Beams

Behavior at Failure. In all capacity tests load was applied at midspan. Only tests of beams B21S and B21W were carried up to the ultimate load. Tests of beams B24W and B24S were stopped at somewhat lower loads because the capacity of the loading frame had been reached and danger of its failure was imminent.

The maximum load applied at midspan of beam B24W was 111 kips and for B24S was 115 kips; final failure was not reached. The shapes of the load-deflection curves in Fig. 47 seems to indicate that the ultimate load probably would not have exceeded 120 kips for B24W and 130 kips

for B24S. The behavior at the maximum load was quite similar for both beams. Extensive yielding was observed in the steel beams. The bottom flange yielding extended along about 9 ft of the middle portion of the beam, and at midspan yielding extended up to the top flange. Yielding was not observed in the upper flanges of either of the two beams; maximum strains measured in those flanges were about 100×10^{-5} at section 18 in. away from midspan. It is believed that continued loading would have led eventually to yielding of the upper flanges. At the maximum load the slabs of both beams were cracked extensively over a distance of about 5 ft at midspan. It could be seen on the slab edges that the cracks penetrated to about half the depth of the slab. Yielding did not take place in either of the end connectors.

The ultimate load for beam B21S was 102 kips. At this load the concrete slab failed by crushing of the concrete adjacent to the loading plate. The crack is shown in Fig. 49. At this load the total deflection at midspan was 8 in. The deflected shape of the beam after the test to failure is shown in Fig. 50. At the time of failure yielding was very extensive. It penetrated through the full depth of the beam not only at midspan but also at sections 18 in. away from midspan and extended over a 12-ft

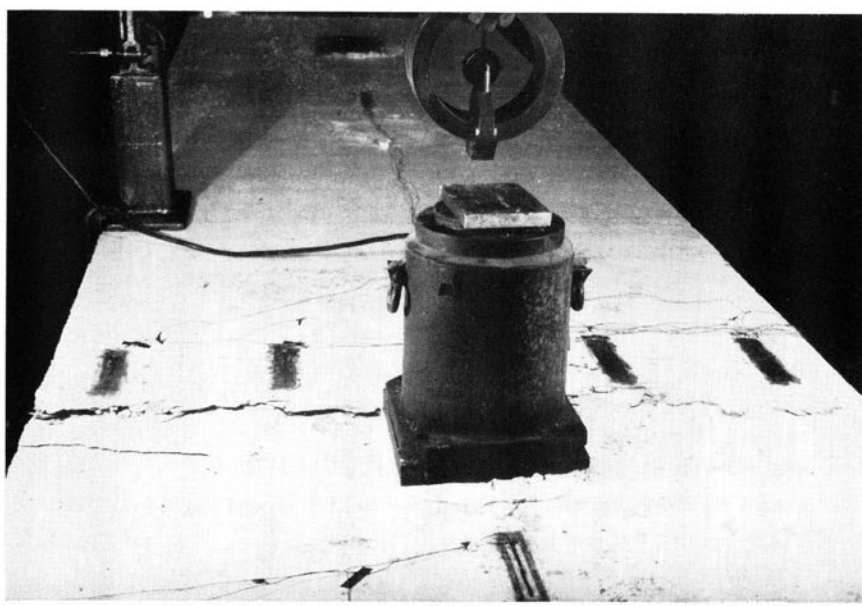

Fig. 49. Compressive Crack on Slab of Beam B21S

length of the bottom flange. The cracking of the slab extended about 3.5 ft on each side of midspan and penetrated about 4 in. into the slab. Yielding was not reached in any of the end connectors. After crushing of the slab, load dropped off.

Beam B21W failed at an ultimate load of 79 kips by fracture of the welds of the longitudinal tensile reinforcement in the slab. However, the load-deflection curve was practically horizontal at this load (Fig. 47), so that it is certain that the ultimate load could not have exceeded 80 kips

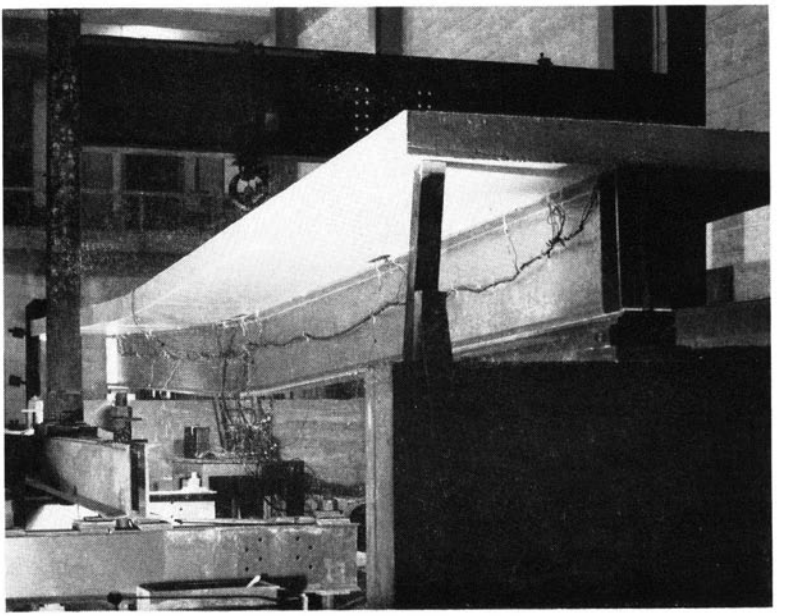

Fig. 50. Beam B21S After Failure

had the beam failed by crushing of the slab. Even though the yielding of the bottom flange spread over a distance of 20 ft, it penetrated only just above mid-depth. The upper flange was in compression throughout the test. Cracking of the slab was also quite extensive; cracks were observed over a distance of 15 ft and to a depth of about 4 in. In all shear connectors very extensive yielding was observed. After the ultimate load had been reached and the load dropped off, loading of beam B21W was continued. At first, compression failure took place on top of the slab in the same way as on B21S, and at a deflection of about 10 in. several

connectors broke off on the west half of the beam. It was found after the removal of the slab that all but one connector on the west half of the beam had broken. Extensive honeycombing was found around the unbroken connector. All connectors which failed were broken off through the web at the junction with the welded flange. At the end of testing the beam was still able to sustain a load of 48.4 kips.

Measured vs. Theoretical Ultimate Loads. The ultimate loads for all four beams are listed in Table 24, in which measured values and theoretical values for complete and no interaction are given. It can be seen that the test data are much closer to the values for complete interaction than for no interaction. It can also be seen from this table that for the first three beams the actual ultimate loads are about twice as large as those for no interaction.

Table 24
Ultimate Loads on T-Beams

Beam	Ultimate Load at Midspan in Kips				
	Theory for Complete Interaction*				
	Based on Ultimate Concrete Strain 380 × 10^{-6} Strain Hardening		Rectangular Stress Blocks	Test Data	Theory for no Interaction
	Neglected	Accounted For			
(1)	(2)	(3)	(4)	(5)	(6)
B24W	116.7	.....	117.4	111†	58.7
B24S	114.9	.....	115.2	115†	57.6
B21S	100.6	106.8	101.4	102	46.3
B21W	96.8	.....	97.1	79	45.0

*For assumptions see Appendix A.
†Maximum test load; test discontinued before failure occurred.

Theoretical ultimate loads computed as outlined in Appendix A are listed in column 2 of Table 24. Computation of ultimate loads may be simplified if a rectangular stress block is assumed for the concrete at failure and if the compressive reinforcement in the slab is neglected. Ultimate loads computed on this basis are shown in column 4. They differ from the more accurate values by only a fraction of 1 percent.

A strict comparison may be made between the tests and the theory for B21S only. This T-beam failed by crushing of the concrete slab at a load of 102 kips; the theoretical ultimate load is 101 kips. It must be mentioned, however, that at the ultimate load the bottom flange strains were of the order of 0.05 in. per in., which is large enough to cause an increase of the load-carrying capacity due to strain hardening of the steel.

When this effect is included in the theory, the computed ultimate load for B21S is 107 kips, or 5 percent greater than the measured value.*

It has been stated before that the maximum loads applied to beams B24W and B24S were not the ultimate loads. It was estimated that the ultimate loads for these two beams would not have exceeded 120 and 130 kips respectively. The corresponding calculated loads are 117 and 115 kips, without considering the effects of strain hardening. Hence it may be concluded that for beams B24W, B24S and B21S the ultimate loads were, for all practical purposes, equal to those computed on the basis of complete interaction.

The ultimate capacity of beam B21W was 79 kips, but the computations neglecting strain hardening show for complete interaction 97 kips, a difference of 23 percent. It is obvious from the description of the behavior of this beam that the reason for the lower measured ultimate load was the imperfect interaction between the slab and the beam. It should be noted, however, that the corresponding ultimate load for beams without any interaction would be only 45 kips.

Ultimate Loads vs. Design and Yield Loads. The beneficial effect of a good shear connection is more forcefully demonstrated if the ultimate loads of the T-beams are expressed in terms of dead and live loads. This is done in the last column of Table 23. It required 4.3 LL, in addition to the dead load, to break the slab of beam B21S, and it is estimated that for the 24-in. beams more than 5 LL would have been needed to cause failure. A similar comparison for B21W shows that this beam carried only 3.3 LL. It is evident that a good shear connection insures a considerable increase of the ultimate capacity of composite T-beams.

The loads at first yielding are also included in Table 23. On the average it took 1.6 times as many live loads to cause failure as to cause first yielding. The reserve strength between yielding and ultimate loads for beams B24W, B24S and B21S was on the order of 40 percent of the ultimate load.

It was shown previously that the ultimate loads were reached only after deflections of the order of several inches had occurred. The load-deflection curves also showed that large portions of the load capacities were exhausted before the extreme deflections were observed. This point is brought out in Table 23, in which the load capacities at midspan

* Other investigators have also found a good agreement between the computed and measured ultimate loads for composite T-beams with strong shear connection. See, for instance, reference 29, pp. 15–16.

deflections equal to $\frac{1}{200}$ of the span length are given in terms of dead and live loads. At this deflection beams B24W and B24S carried 4.4 LL and beam B21S 3.5 LL. These values represent an average increase of 32 percent over the yield loads, an increase that corresponds to more than 50 percent of the entire reserve strength which the beams possessed at the time of first yielding.

Table 25

Properties of Shear Connections

Values $1/C$ calculated from measured slips by method given in Univ. of Ill. Exp. Sta. Bul. 396, Section 54.

Beam	$\frac{1}{C}$	$\frac{k}{s}$	Connector Spacing s		Connector Modulus k		Equivalent Spacing of Connectors,* in.
		10^6 lb/in.^{2}	Actual, in.	Ave., in.	For $s_{av.}$, 10^6 lb/in.	For $s_{min.}$, 10^6 lb/in.	
B24W	39	0.374	18	18	6.73	6.73	18
B24S	54	0.513	12, 15, 18	14.6	7.49	6.15	13.1
B21S	44	0.366	12, 15, 18	14.6	5.35	4.29	13.4
B21W	11	0.0907	36	36	3.28	3.28	36

*Based on $k = 6.73 \times 10^6$ lb/in. per 6-in. width for B24W and B24S and on $k = 4.92 \times 10^6$ lb/in. per 6-in. width for B21S and B21W. Modulus k considered proportional to the connector width.

42. Shear Connection

It has been pointed out in the preceding sections that beams B24W, B24S and B21S exhibited a very high degree of interaction throughout the tests and that their ultimate loads were practically equal to those for beams with complete interaction. The degree of interaction in beam B21W was lower than that of the other three beams and its ultimate load was affected noticeably by the lack of interaction between the steel beam and the concrete slab. A quantitative explanation of the reasons for this phenomenon is given in this section.

Properties and Behavior of Shear Connections. The elastic properties of the connections for the beams tested and the spacings of the individual connectors are summarized in Table 25. The elastic properties were computed from measured slips by a method based on Newmark's analysis of composite beams with incomplete interaction.* In this table the parameter $1/C$ is a quantity which furnishes a convenient measure of the degree of interaction. It may be expressed as follows:

$$\frac{1}{C} = \frac{I}{\frac{1}{n} I_s + I_b} \frac{1}{E_b} \frac{z}{\bar{y}_s} \frac{L^2}{A_s} \frac{k}{s}$$

* Reference 112, pp. 132–33.

in which

I, I_s, I_b = moments of inertia of the composite, slab, and I-beam section, respectively, in.^{4}

$n = \frac{E_b}{E_s}$

E_s, E_b = moduli of elasticity of the concrete in the slab and the steel in the beam, respectively, lb/in.^{2}

z = distance between centroidal axes of the slab and the beam, in.

$\bar{y}_s$ = distance between the centroidal axis of the slab area and the neutral axis of the composite section, in.

A_s = area of the slab, in.^{2}

L = span length of the beam, in.

k = modulus of connector equal to the ratio of the load on connector to the corresponding slip, lb/in.

s = spacing of connectors, in.

It has been shown in the appendix of Bulletin 396 * that the degree of interaction increases with increasing values of $1/C$. Thus it can be seen from the formula given above that the degree of interaction is directly proportional to the square of the span length and to the modulus of connectors and is inversely proportional to the spacing of the connectors and the slab area. Or, for shorter spans and heavier slabs, stronger and more closely spaced shear connectors are needed if the degree of interaction is to be kept constant.

Both the theoretical studies of variations in the degree of interaction with $1/C$ and the results of the small-scale T-beam tests indicated that beams with $1/C > 20$ will behave as beams with complete interaction throughout the elastic range of stresses. The small-scale tests indicated also that such beams probably will retain the high degree of interaction up to the ultimate load. It can be seen from Table 25 that beams B24W, B24S and B21S had $1/C$ values in the range of 39–54, while the beam B21W $1/C$ was equal to 11. Thus the limiting value of $1/C = 20$ is substantially confirmed by the test results for full-scale T-beams.

It was shown in the discussion of the behavior of composite T-beams stressed beyond yielding that in beams with a strong shear connection yielding and therefore also large slips occur only in connectors located close to the load. On the other hand, in beams with a weak shear connection yielding occurs in all connectors. This behavior is illustrated clearly in Figs. 51 and 52. In Fig. 51 maximum strain for several shear connectors is plotted against the load on the beam for each T-beam.

* Reference 112, p. 122, Fig. 49.

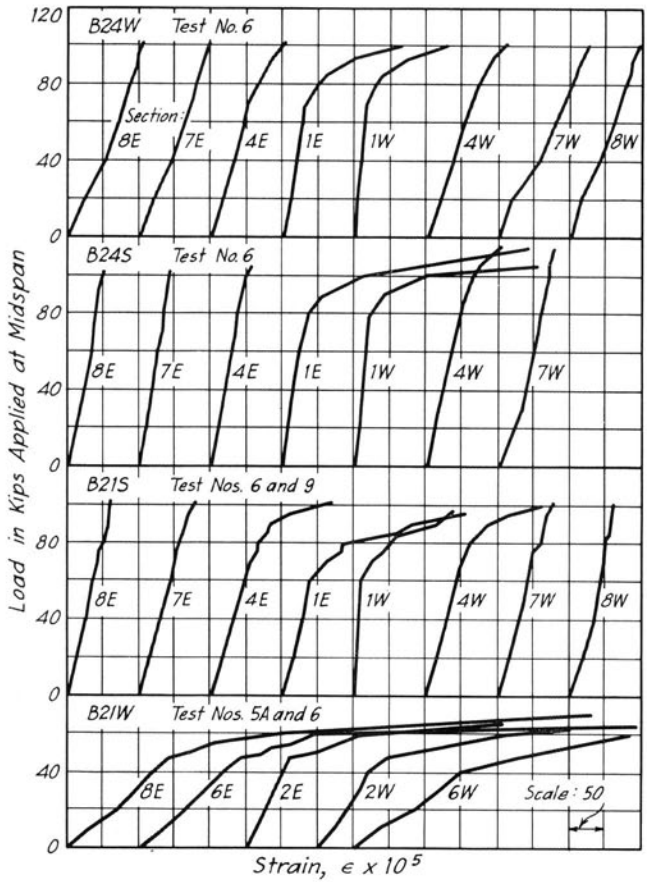

Fig. 51. Maximum Strains in Shear Connectors of Composite Beams

Slips plotted in the same way for the same connectors are shown in Fig. 52. Only the results of either one or two tests are included in these figures, so that the effects of previous loadings and of dead load are omitted. Nevertheless, the curves give a fair idea of the magnitudes of strains and slips and illustrate the point in question: for beams B24W, B24S and B21S a sharp increase of strains and slips after yielding can be observed only for connectors at 1E and 1W—that is, only for connectors located immediately next to the load. On the other hand, load-strain and load-slip curves for all connectors of beam B21W show a very rapid increase of both the maximum strains and slips after the beam has yielded.

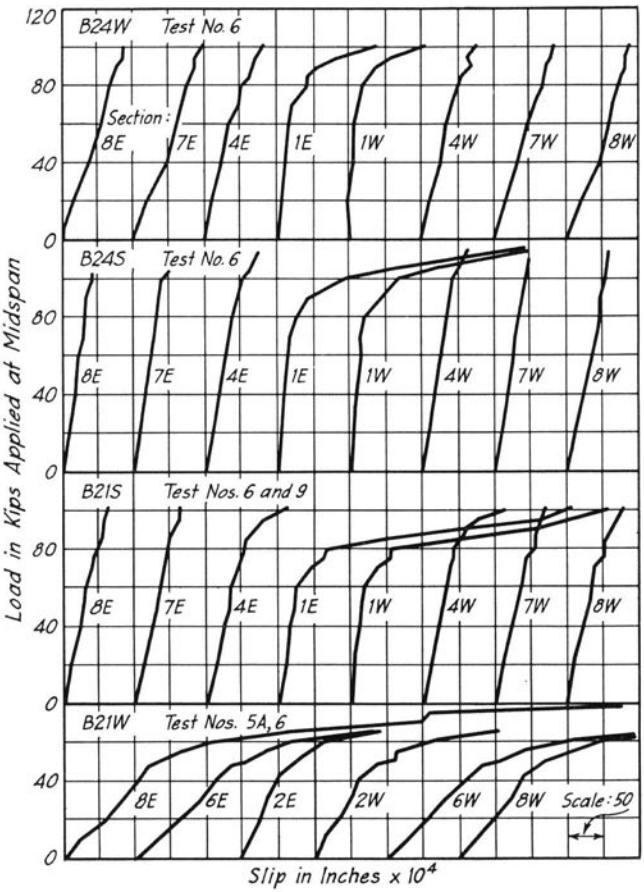

Fig. 52. Slip at Various Sections of Composite Beams

Large strains and slips at locations close to the load are caused by large rotations taking place at the section of maximum beam moment after yielding has occurred. Thus it may be said that the shear connectors are subject to deformational stresses, which inevitably cause yielding of connectors. However, it was brought out in the tests that this yielding is confined to the connectors located close to the section of the maximum moment and that it is unimportant from the standpoint of the load capacity of beams. So long as the end connectors do not yield, a large decrease of interaction cannot occur.

Effect of Manner of Distributing Connectors. The curves plotted in Figs. 51 and 52 and the observation that yielding in the connectors on

beams B24W, B24S and B21S was caused by localized deformational stresses raise the question whether the manner of distributing the connectors along the beam affects the stiffness and capacity of the connection. The effects of the manner of distributing the connectors on the connection stiffness were studied on the basis of elastic properties. The results of these studies are presented in Table 25. If the connectors were equally effective in comparable beams, the moduli of the individual connectors of equal size based on an average spacing would have been the same, provided that the spacing of shear connectors was the only variable. A comparison of beams B24W and B24S shows that the equivalent spacing based on equal values of k is 13.1 in. for B24S as compared to the average spacing of 14.6. In the same way the equivalent spacing for beam B21S based on a k value taken from B21W is 13.4 as compared to the average spacing of 14.6 in. These differences between the equivalent and average spacing are consistent. Whether they were caused by the differences in the manner of distributing the connectors or whether they were due simply to the approximations involved in applying the theory used for these computations, is not known. However, the differences were small and it seems probable that the distribution of connectors had no appreciable effect on the connection stiffness.

How the manner of distributing connectors along the beam affects the capacity of the connection cannot be determined on the basis of the data available, but it is certain that all three beams, beam B24W with evenly distributed connectors and beams B24S and B21S with connectors spaced at distances decreasing from midspan toward the supports, retained practically complete interaction up to the ultimate load.

The foregoing discussions lead to the belief that small variations in spacing the connectors, such as those encountered in the beams tested, have no appreciable influence on either the stiffness or the capacity of the shear connection.

Effect of Bond. During the construction of beam B21W no attempt was made to prevent bond between the top surface of the I-beam and the slab. The results of the first test made with this beam revealed the presence of bond. Only after eleven repetitions of a load of 40 kips was the bond broken. After breaking the bond another test was made similar in all respects to the first one. Some of the results from these two tests are presented in Fig. 53.

Load-slip and load-strain curves for the connector located at the east end of the beam, load-deflection curves at midspan of the beam, and strain distribution curves for a section 36 in. from midspan are shown in Fig. 53. All these data show that bond is a very effective shear connection. It should not be forgotten, however, that large deformational

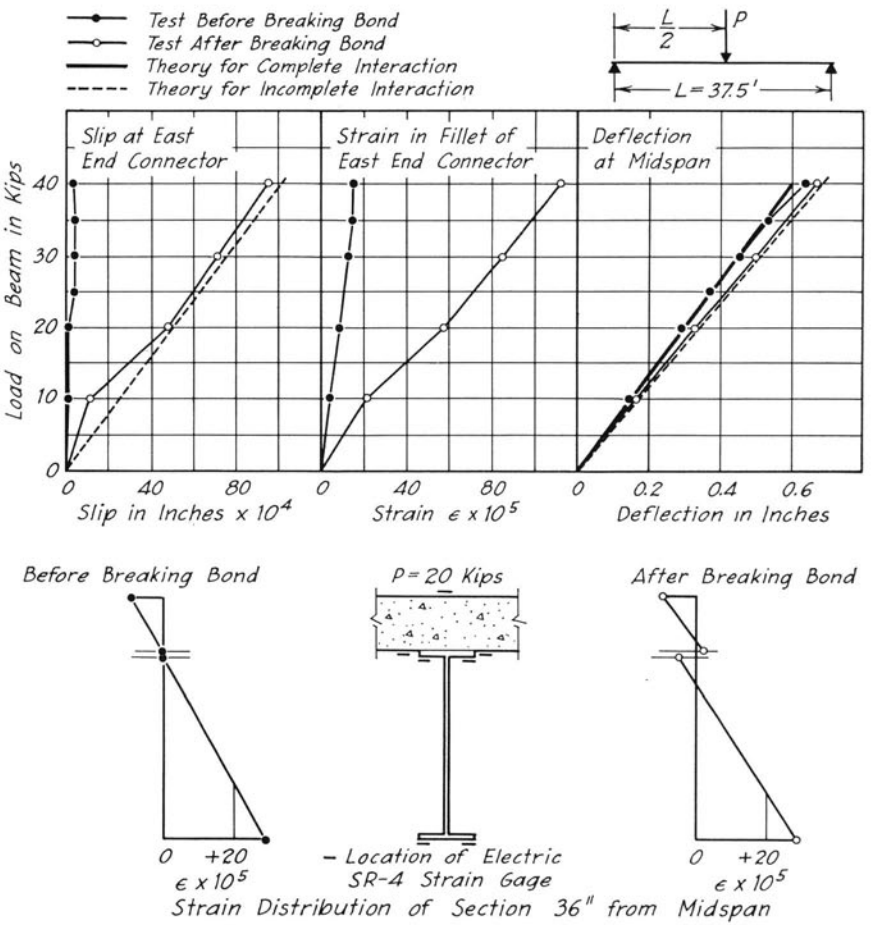

Fig. 53. Effect of Bond on Degree of Interaction

stresses at high loads cannot possibly be resisted by bond. Therefore bond cannot insure complete interaction up to the ultimate load. Furthermore, shrinkage and warping of the slab as well as dynamic loading may destroy the bond even at working loads.

43. Distribution of Strain Across Concrete Slab

It was assumed in all theoretical calculations that strain distribution was uniform across the full width of the slab. This assumption was checked experimentally in the tests of beams B24S and B21S.

In both tests five strain gages were placed on the top of the slab at a section 18 in. away from midspan. The results of these tests are shown in Fig. 54. Although the measured distribution is not entirely uniform,

the differences between the individual gage readings are small. The strains show no consistent decrease toward the edges of the slab. The maximum differences among the individual readings were observed at loads approaching failure. The maximum difference from the average was 15 percent for B24S and 8 percent for B21S.

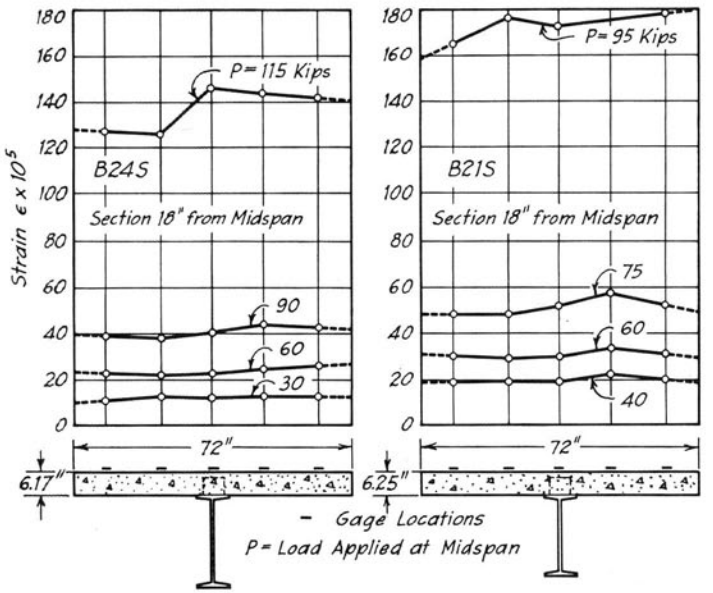

Fig. 54. Strain Distribution Across Slab of Composite T-Beams

Whether the full width of the slab of a composite T-beam is entirely effective in resisting moment depends on the ratios of slab width to span length and slab width to slab thickness. The width of the slabs on B24S and B21S was approximately one-sixth of the span length and was about 12 times the slab thickness.

44. Vertical Separation of Slab from I-Beam

One advantage of a flexible channel connector is that the free flange of this connector anchors the slab to the beam. The tendency toward vertical separation of the slab is undoubtedly present in a composite beam subject to dynamic loading or warping the slab. It was desired, however, to find out experimentally how serious such a tendency is when the beam is loaded with a static load.

Beam B21W was especially suitable for the study of this problem because its connectors were spaced at 36 in. The vertical separation or uplift was measured at four locations—on each side of the beam at points

7.5 ft away from midspan (Fig. 36). At each location the dial indicators were thus midway between two connectors. Results of these measurements were averaged; they are presented in Fig. 55. It can be seen from this figure that the separation was about 0.003 in. before yield loads were reached, and increased rapidly as the load approached the ultimate value. At failure the separation was 0.042 in.

The tendency for separation was measured also by special strain gages on shear connectors at Sections 2E and 2W on beam B21W (Fig. 36). On each connector, two electric gages were cemented to the front face of the channel directly opposite the gages on the back face as indicated in Fig. 55. In this figure load-strain curves are shown for each pair of opposing gages. In addition, the difference between the readings is plotted for each pair (heavy lines). With one exception, the difference was always a tensile strain. On the basis of the axial strains determined from these tests it may be estimated that the separation of the slab from the beam at locations close to the connectors was probably less than 0.01 in. even at failure.

Thus the test data show that the tendency of the slab to lift from the beam was definitely present in the static tests of the beam B21W, and also that the free flange satisfactorily performed its function as an anchorage. It can be observed also that even though the separation at

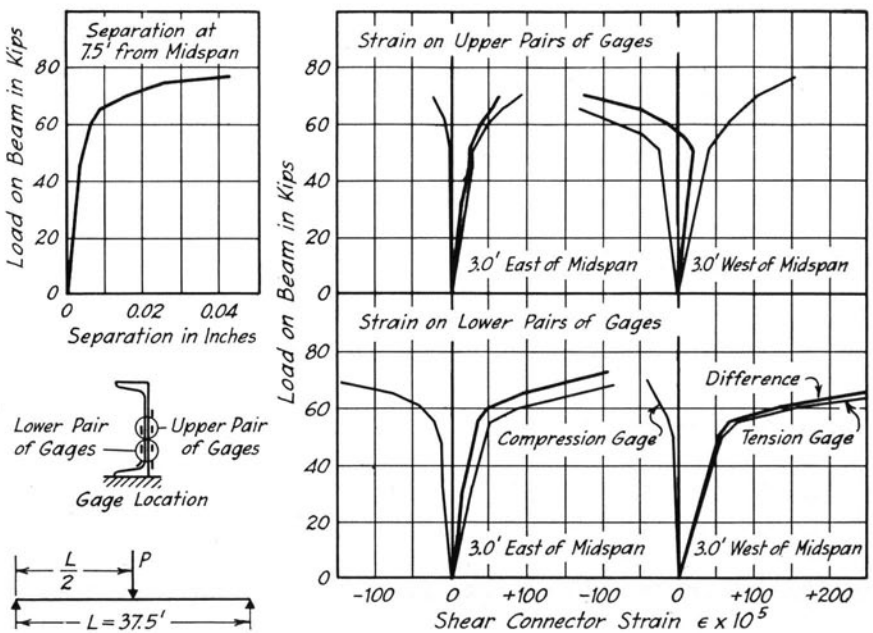

Fig. 55. Vertical Separation of Slab from Steel Beam, Beam B21W

locations between two connectors was probably not large enough to have any detrimental effect on the behavior of the T-beams, it might allow moisture to enter under the slab and thus result in corrosion of the upper flange.

45. Effect of Shoring on Behavior of Composite T-Beams

The load-deformation characteristics of a composite T-beam are influenced by the manner of its construction. A composite beam in which the steel beams are temporarily supported by shoring during casting and hardening of the slab will carry both dead and live load by the full composite section. On the other hand, if no shoring is used the dead load is carried by the steel beam alone. Since one of the objects of the T-beam tests was to investigate this effect of shoring, in two of the four specimens the I-beams were supported at or close to midspan while the slab was cast and cured. Unfortunately, the beams tested were not very suitable for the investigation of the effect of shoring; since they were rather short, the effects of shoring were not as pronounced as they would be for longer beams with greater dead load.

Removal of Temporary Supports. Beam B24S was supported with a nondeflecting support at midspan, and beam B21S was propped with an elastic ring dynamometer placed 18 in. from midspan. Since the dynamometer was flexible, it was adjusted daily during the curing period to keep the support at a constant elevation. The dynamometer readings on B21S indicated a steady increase of the shoring load with time due to shrinkage of the slab. In 19 days the increase was 3600 lb. It was feared that a further increase of the load might cause cracking of the slab, and the shoring load was therefore decreased by 800 lb at that time.

Several weeks after casting the slab the temporary supports were removed. A set of strain, deflection, and slip readings was taken before and after removal of the load. In order to obtain checks on the readings, the shoring load for beam B21S was removed in three increments and readings were taken after each increment. The strain and deflection readings on both beams were fairly consistent and in reasonable agreement with values computed on the basis of incomplete interaction. Although the slip readings and shear connector strain readings were small, they were consistent and indicated that bond did not exist between the slab and the beam. The maximum slip measured was 0.0004 in. for B24S and 0.0018 in. for B21S. The maximum shear connector strain was 8×10^{-5} for B24S and 12×10^{-5} for B21S.

At the time of construction, beam B24S was shored with a reaction of 15,000 lb. From the strain and deflection readings made at the time

of shore removal a reaction of 17,800–19,000 lb with an average value of 18,800 lb was computed. The difference between the original jacked-in reaction and the final computed reaction was due to two factors—shrinkage of the slab, and changes due to the removal of the forms corresponding to a reaction of 1400 lb. Thus the change in the shoring reaction due to shrinkage must have been about 5200 lb.

On B21S the jacked-in reaction was 14,800 lb, of which about 1400 lb was contributed by the weight of the forms. Thus the net shoring reaction after removal of the forms was 13,400 lb. After the slab had hardened, the jacked-in load was first lowered by 800 lb and two days later removed entirely. Just before its complete removal the reaction was 16,200 lb. These readings of the dynamometer were consistent with both the deflections and the strains on the bottom flange of the beam. Thus the difference between the original and final reaction attributed to the shrinkage of the slab was 3600 lb.

Effects of Shoring. Load-strain curves for the bottom flange strains at midspan with the load at midspan are shown for B24W, B24S and B21S in Fig. 56. Theoretical curves computed on the basis of complete interaction are plotted in the upper figure; the test curves are plotted in the lower figure. Only live load is included. Strains corresponding to zero load are actually dead load strains.

Curves for B24W and B21S are of primarly interest. Both of these beams were designed in accordance with the 1944 AASHO specifications,* B24W without temporary supports and B21S with them. It can be seen from the computed curves that the governing strains are about equal at the design load but that above this point the load corresponding to an equal strain is always higher for beam B24W. Both the computed yield and ultimate loads for B24W are 16 percent higher than for B21S. Beam B24S, also included in Fig. 56, was a variation of beam B24W in that it had the same dimensions but was built with temporary supports. Thus the effect of shoring alone can be studied by comparing beams B24W and B24S. Theoretically the governing strain at the design load was 10 percent lower for B24S than for B24W, the yield load 5.5 percent higher. The theoretical ultimate load for B24S was somewhat lower because of the lower yield strength of steel; however, if the yield strengths had been equal, the theoretical capacities would have been practically the same for both beams.

The test data are shown in the lower part of Fig. 56. They are in good qualitative agreement with the computed curves except that the relative

* "Standard Specifications for Highway Bridges," American Association of State Highway Officials, Washington, D. C., 1944, p. 195, Article 3.9.3.

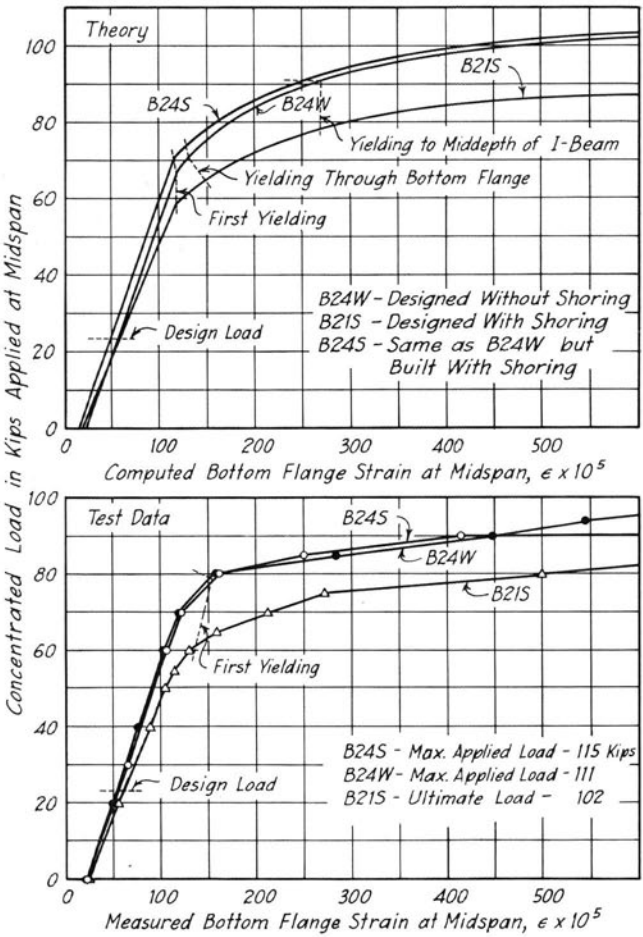

Fig. 56. Effect of Shoring on Load-Strain Curves

weakness of beam B21S is somewhat more pronounced at loads below yielding and the curves for B24W and B24S are almost identical.*

The results of quantitative studies of the effect of shoring are given in Table 23. In this table loads at first yielding, at a deflection of L/200, and at failure are given in terms of dead and live loads. In addition measured bottom flange stresses at 1 DL + 1 LL are compared with the computed stresses for the beams B24W and B21S, which represent actual

* The dead-load stresses for B24W and B24S also were practically equal—Table 22.

designs. Comparison at a deflection of L/200 is included because failure of beams B24W and B24S was not reached in the tests, and the failure loads in Table 23 were estimated.

There was practically no difference between the computed and measured stresses at 1 DL + 1 LL for B24W and B21S. At the same time the factor of safety against yielding, against a deflection of L/200, or against the ultimate capacity was consistently lower for B21S. At first yielding, beam B24W carried 3.35 LL whereas B21S carried only 2.63 LL; that is, the factor of safety against yielding was 27 per cent lower for B21S than for B24W. Even though the difference was caused in part by the differences in residual stresses, it is clear that the primary cause of the lower factor of safety for B21S was the manner in which advantage was taken of the shoring in the design. At a deflection of L/200 the factor of safety for B21S was 20 per cent lower than for B24W and at the ultimate 17 percent lower, when based on live load only. On the other hand, when beam B24W is compared with the beam B24S, no significant difference can be found between their load-carrying capacities at any stage.

It may be stated in conclusion that shoring compared with not shoring beams of the same size had no effect on the capacity of the beams tested, whether based on yielding, on a certain limiting deflection, or on the ultimate load.

46. Comparison of Behavior of Connectors in T-Beam and Push-Out Tests

A study of the behavior of flexible channel shear connectors was one of the purposes of the T-beam tests. The previous tests of small-scale T-beams and push-out specimens indicated that the behavior of a channel shear connector in a push-out specimen is very similar to that of a connector in a T-beam. Therefore, in planning the series of full-scale specimens the push-out tests were included for the purpose of investigating the large number of variables which may influence the design of channel connectors, while the T-beams were built with only one of the types of channel connectors included in the push-out tests. Thus an opportunity for comparing the behavior of this type of connector in the two kinds of tests was afforded.

Load-Slip and Load-Strain Curves for Channel Connectors. The load-slip and load-strain curves for the end connectors on the T-beams are compared with similar curves for connectors in push-out specimens in Figs. 57–59. The load transmitted by the end connectors in T-beams could be determined with good accuracy because of the high degree of interaction at their locations. The ratios of the load on an end connector

Table 26

Ratios of Load per Connector, Q, to Load on Beam, P, for End Connectors on Composite T-Beams

All ratios are given for connectors located at Sections 8. Computed on the basis of incomplete interaction.

Beam	Ratios Q/P For Concentrated Load P Applied at Midspan	9 ft from Midspan	15 ft from Midspan
B24W	0.372	0.545	0.557
B24S	0.248	0.366	0.394
B21S	0.277	0.407	0.427
B21W	0.824	1.112	.....

to the load on the beam, used in connection with Figs. 57–59, are given in Table 26. From the push-out tests, specimen 4C3C9 was selected on the basis of type, size, and concrete strength as being comparable with the connectors in the T-beams. Test data for specimen 4C3W2 were also compared with those for the connectors of beam B21W; in this choice similarity in size and type of connector was the decisive factor.

In Figs. 57–59 complete load histories are given for the beam connectors. Live as well as dead (shoring) loads and residual deformations are included. For the push-out connectors, only the virgin curves—that is, the curves connecting points representing first loading for each particular load—are shown.

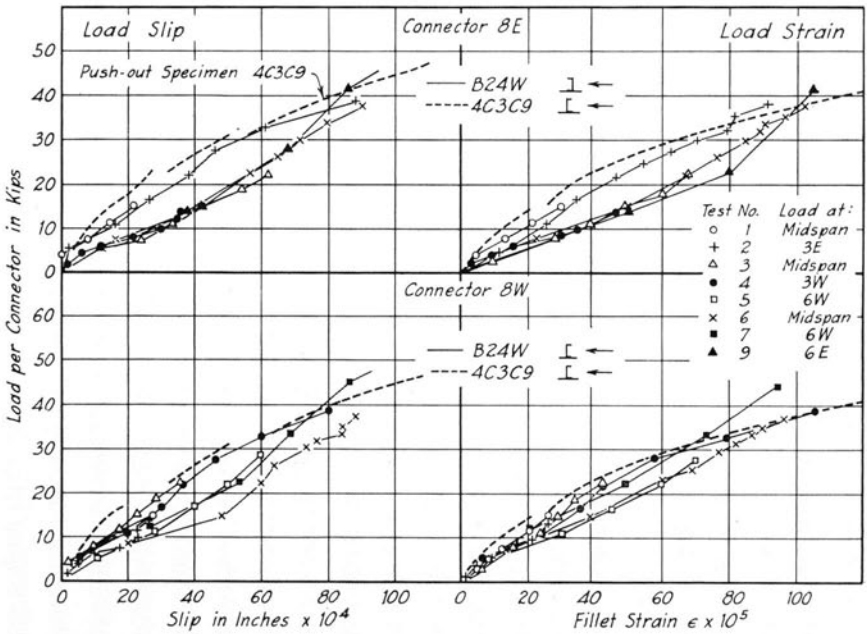

Fig. 57. Load-Slip and Load-Strain Curves for End Connectors of Beam B24W

In Fig. 57 load-slip and load-strain curves are plotted for connectors 8E and 8W of B24W. The pattern of the curves for both beam connectors is fairly regular; the virgin curve for T-beam connectors follows closely the shape and magnitude of the corresponding curve from the push-out test (dotted line); the other curves follow a trend somewhat similar to that shown in Figs. 23 and 24 for the reloading curves of the intermittently loaded push-out specimens. It may be noted, however, that residual slips and strains were measured in the push-out tests even after small preloading, whereas no residuals, or very few, were observed in the T-beam tests. Kinetic friction between the beam and the slab due to the characteristics of the type of specimen was given as a reason for the residuals in the push-out tests; there is no reason to believe that similar kinetic friction should exist between the beam and the slab at the ends of the T-beams.

The fairly regular pattern of the load-slip and load-strain curves for connectors at 8E and 8W is violated only by curves for very high loads applied at section 6E or 6W near the end of the beam at which the connector was located. The degree of interaction must have been comparatively low at these locations and the loads transmitted by the connectors smaller than indicated by the ratios in Table 26. The same phenomenon was observed on beams B24S and B21S (Fig. 58).

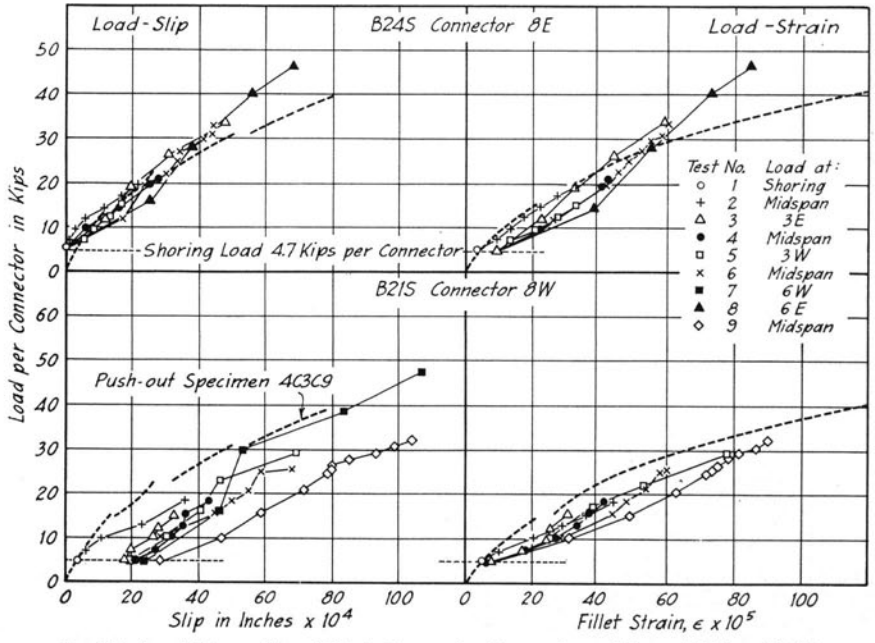

Fig. 58. Load-Slip and Load-Strain Curves for Connectors of Beams B24S and B21S

The curves in Fig. 57 also bring out the point that the orientation of a channel connector with respect to the direction of load does not influence significantly the behavior of the connector. All connectors in the T-beams faced in the same direction, so that the load was applied to the back side of connector 8E but to the front side of connector 8W. The load-slip and load-strain curves for these connectors do not differ significantly either in shape or in magnitude.

In Fig. 58 load-slip and load-strain curves are plotted for connector 8E on B24S and for connector 8W on B21S. For both specimens load on the connectors due to the removal of the shore (dead load) is included. Curves for the T-beam specimens are compared with the corresponding virgin curves for push-out specimen 4C3C9. The envelope curves for shear connectors tested in the two types of specimens compare favorably.

Two major irregularities may be observed in Fig. 58. In the test of beam B24S no slips due to dead load were found at connector 8E. As the zero reading remained unchanged even after several successive loadings, it seems most probable that the zero reading for slip before removal of the shore must have been erroneous. The second marked irregularity is the large spread of the load-slip curves for the individual tests of

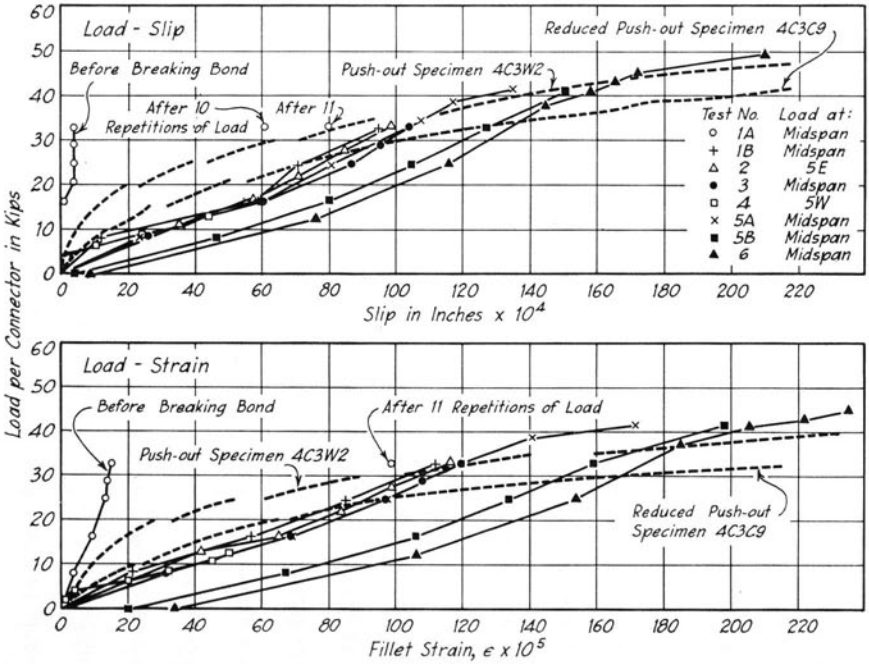

Fig. 59. Load-Slip and Load-Strain Curves for Connector at Section 8E on Beam B21W

connector 8W on B21S. Comparatively large residual slips and somewhat smaller residual strains were observed on all connectors after each test of this beam. As a similar phenomenon was not observed in any other beam, it is possible that the residuals resulted from an unsatisfactory compaction of concrete around the connectors during casting of the slab.

When the curves in Figs. 57 and 58 are compared it may be noted that the differences between the virgin curves and the curves for successive loadings are smaller in B24S than in B24W. This apparent discrepancy is attributed to two factors. First, the maximum load of the virgin curves was about 15 percent higher for B24W than for B24S. Second, the load on shear connectors in B24W was always fully released, while the connectors on B24S were loaded permanently by the dead load.

The load-slip and load-strain curves for connector 8E on beam B21W are shown in Fig. 59. This connector differed from those discussed above in that the first load applied to it was large enough to cause a slip of about 0.0100 in. and a maximum strain of about 120×10^{-5}. Hence, up to these values of slip and strain the virgin load-slip and load-strain curves are unknown. Furthermore, both very large slips and strains substantially in excess of the yield strain were measured on this connector.

The test results for B21W are compared with those for push-out specimens 4C3W2 and for 4C3C9. For this comparison slips and strains for 4C3C9 were multiplied by $\frac{2}{3}$, the ratio of the widths of the respective connectors. The comparison is satisfactory at high loads. Although the virgin curve for the beam connector is unknown for low loads, the trend shown by the data available indicates that the comparison would probably have been satisfactory if the full virgin curves had been available.

The curves in Fig. 59 show that large residual slips and strains take place only after yielding has taken place in the shear connectors.

Strain Distribution Curves for Channel Connectors. In Fig. 60 strain distribution curves for two end connectors on each beam are presented, and compared with similar curves obtained from push-out tests. For beams B24S and B21S curves for connectors 7W instead of 8W are plotted because some of the gages on the latter connectors ceased to work during testing.

In general, the agreement for all curves is good. It is obvious from these curves that the behavior of the channel web was about the same irrespective of whether the connector was tested in a T-beam or in a push-out specimen. Furthermore, there was little difference for loads applied on the front and back sides of the channel.

The agreement between the curves plotted in Fig. 60 is satisfactory qualitatively as well as quantitatively. An exception to this agreement

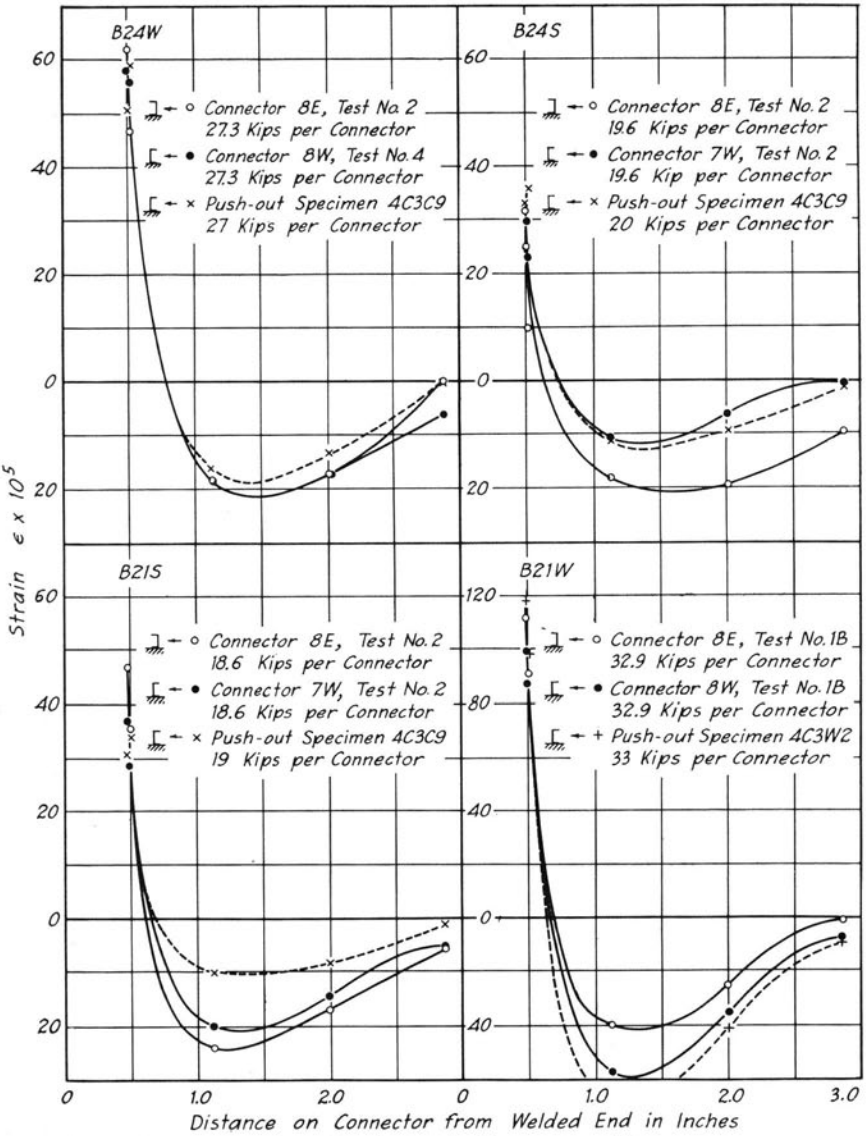

Fig. 60. Strain Distribution for Connectors on T-Beams

was the curves for the connectors on beam B21S. A similar discrepancy was observed for the load-slip curves of the connectors on beam B21S, and it was suggested that an unsatisfactory compaction of the concrete around the connectors during casting the slab might have been the cause. Obviously, if the stiff flange could move without transmitting much of the load, an increased portion of the load would be carried by the web.

Load on Channel Connectors. The loads carried by the end connectors at various significant stages of loading are listed in Table 27, in which all loads are stated in pounds per inch width of connector. The loads corresponding to one design load, to first yielding of the I-beam, and to the maximum test load are given.

The loads in columns 2 and 3 were computed for one design load of 23,600 lb. The shear connectors were designed for the load placed at midspan. The corresponding values, computed on the basis of Table 26,

Table 27

Load per Unit Width of End Connectors on Composite T-Beams at One Design Load, At First Yielding of Beams and at Maximum Test Load

All loads are given for the most stressed connectors. All loads are computed with data from Tables 18, 21, 24, and 26 on the assumption of proportionality between load and width of connector. Loads for beams B24S and B21S include loads due to shore removal.

Beam	Load per Unit Width of Connectors in lb/in.			
	At One Design Load*		At First Yielding of Beam	At Maximum Test Load
	At Midspan	Near End		
(1)	(2)	(3)	(4)	(5)
B24W	1460	2910	4890	6880
B24S	1760	2730	4000	5530
B21S	1870	2740	3650	5490
B21W	4860	9780	9680	....

*Connectors were designed for a load of 23,600 lb at midspan. Corresponding values are listed in column (2). The end connectors will be stressed most when the load is applied close to one support. For such a case the vertical shear corresponding to one design load is approximately 23,600 lb. Values listed in column (3) are computed for this case.

are given in column 2. In column 3 are listed the largest loads on the end connectors which can be caused by one design load. These loads were computed on the basis of complete interaction (Table 18) for a vertical shear of 23,600 lb. The loads listed in columns 4 and 5 were computed from the measured yield and maximum loads (Tables 21 and 24 respectively) and from the ratios of the load per connector to the load at midspan of the beam (Table 26).

None of the end connectors to which the loads listed in Table 27 apply was stressed to yielding except those on beam B21W. These connectors yielded approximately at the same load as the beam. Hence the load of 9680 lb represents the yield load per inch width of the channel connectors used in the tests of T-beams. Since the connectors for all beams were made from the same type of channel and the concrete was about the same quality, the factors of safety against yielding of connectors may be computed on the basis of this load. If one design load is placed at the end of the beam, the factor of safety against yielding of the end connectors on beam B24W is 3.33 and on B21S, 3.53 or 4.55 depending

on whether the total load or the live load only is considered. These factors of safety seem to be fairly high. It should be remembered, however, that if it is desirable to retain a high degree of interaction up to the ultimate load, yielding should not occur in the connector before ultimate flexural failure of the T-beam. The factor of safety against yielding of end connectors at the ultimate was 1.76 for B21S if based on total load, and 1.89 if based on live load only. Even this factor of safety seems rather high. On the other hand, the same factor of safety for B24W was somewhat less than 1.4, a reasonable value which is high enough to guarantee good interaction up to the ultimate failure.

Applicability of Theoretical Analysis to Channel Shear Connectors. The discussion in the preceding section leads to the conclusion that channel shear connectors in a T-beam and in a push-out specimen behave in the same manner for all practical purposes. Consequently the analysis and simplified formulas for channel shear connectors derived in Chapter II on the basis of the push-out tests should be applicable to the connectors in a T-beam as well.

Slips, maximum strains, and pressure on the surrounding concrete computed from the theory (Section 26) and the simplified formulas (Section 27) are compared in Table 28 with measured slips and strains. For each beam, comparison was made at two loads—at the design load (Table 27, column 3) and at a higher load. For beam B21W test data for one design load were missing; hence the comparison at one design load is omitted. It can be seen from the ratios of computed to measured slips (columns 6 and 7) and strains (columns 11 and 12) that the more exact theory gives values of both slip and strain which are too small while the simplified formulas give good values of strains and somewhat small values of slip. In all, the theory and even more so the simplified formulas give a fair approximation of the actual values.

It may be noted in Table 28 that the maximum pressure on the concrete at one design load was 0.96 to 1.19 times the compressive strength of the concrete (Table 14) if computed by the more exact theory, and 0.85 to 1.05 if computed from the simplified formula.

Welds on Channel Connectors. Connectors on all four beams were connected to the top flange of the I-beams by means of $\frac{3}{16}$-in. continuous welds on the front and back sides of each channel. The load-slip data and the examinations of the specimens after the test to failure revealed that welds remained intact on all connectors. The maximum loads applied to the end connectors of beams B24W, B24S and B21S may be computed from Table 27 and the approximate maximum load on the end connectors of beam B21W may be computed from data given in Tables 24 and 26:

Table 28
End Shear Connectors; Comparison of Theory with Results of T-Beam Tests

Specimen	Load on Connector	Slip					Maximum Strain					Maximum Pressure on Concrete	
		Theory*	Simplified Formula†	Test Data	Ratio (3)/(5)	Ratio (4)/(5)	Theory*	Simplified Formula†	Test Data	Ratio (8)/(10)	Ratio (9)/(10)	Theory*	Simplified Formula†
(1)	lb (2)	10^{-4} in. (3)	10^{-4} in. (4)	10^{-4} in. (5)	(6)	(7)	10^{-5} (8)	10^{-5} (9)	10^{-5} (10)	(11)	(12)	psi (13)	psi (14)
B24W	17 000¶	14	17	28	0.50	0.61	21	34	35	0.60	0.97	6 530	5 800
	38 200	60	66	83	0.72	0.80	91	108	99	0.92	1.09	13 110	12 660
B24S‡	16 400¶	13	15	16	0.81	0.94	20	31	26	0.77	1.19	6 120	5 430
	34 000	47	53	48	0.98	1.10	74	89	60	1.23	1.48	11 790	11 260
B21S‡	16 500¶	12	12	...	...	...	18	30	32	0.56	0.94	6 190	5 470
	28 700	32	35	67	0.48	0.52	50	67	80	0.63	0.84	10 280	9 510
B21W	38 700	128	140	111	1.15	1.26	152	210	141	1.08	1.49	19 540	19 230

*Equations 8, 20, and 23, Section 26.
†Equations 26, 25, and 24, Section 27.
‡Effect of dead load included.
¶Design load for end shear connectors (Table 27, column 3).

Specimen	Maximum Load on End Connectors, kips
B24W	41.3
B24S	33.2
B21S	32.9
B21W	65.1

The welds on connectors of the first three beams were identical with those on the connectors of push-out specimen 4C3C11, and the welds on connectors of Beam B21W were identical with those on the connectors of push-out specimen 4C3W2. The welds on push-out specimens 4C3C11 and 4C3W2 failed at loads of 118.2 and 81.9 kips per connector respectively. The factors of safety against failure of welds at the maximum load were 2.86, 3.56, 3.60, and 1.25 for beams B24W, B24S, B21S, and B21W respectively.

At 1 DL + 1 LL the factors of safety against the weld failure were 6.8, 7.3, 7.2, and 2.1 for beams B24W, B24S, B21S, and B21W respectively.* Had the welds been designed according to the current specifications for welded highway bridges† the factor of safety against failure of the welds would have been about 6.

C. DISCUSSION OF TEST RESULTS

47. Behavior of Composite Steel and Concrete T-Beams

Four composite steel and concrete T-beams with a span length of 37.5 ft were tested for the purpose of determining the behavior of composite beams and also their shear connections. The results of the small-scale tests‡ indicated that incomplete interaction between the beam and the slab is an inherent characteristic of this type of beam—a finding confirmed by the tests reported in this bulletin. However, these tests proved also that a very high degree of interaction may be achieved and retained up to the ultimate load if the shear connection is designed properly. If this is the case, then the behavior of a composite steel and concrete T-beam differs very little from that which would be expected if complete interaction were present.

In three of the four beams tested the shear connection retained a very high degree of interaction up to the maximum load applied. Up to first yielding of the steel I-beams deflections and strains in these beams were proportional to the load and their magnitudes were almost identical with

* Computed from the data in column 3 of Table 27.

† "Standard Specifications for Welded Highway and Railway Bridges," Fourth Edition, American Welding Society, p. 10, Article 209c.

‡ Reference 112, pp. 63-71, Section 25.

those computed for complete interaction. First yielding occurred in the bottom flange of the steel I-beams under the load. As the loading continued, yielding spread toward the supports and penetrated high into the webs of the beams. Deflections and strains increased at an increasing rate and there was a visible concentration of rotations at the section directly under the load. Before the ultimate load was reached, yielding penetrated throughout the full depth of the I-beams and tensile cracks pentrated deep into the concrete slab. The ultimate load was reached only in one beam; at this load the slab failed by crushing of concrete. The ultimate load was in good agreement with the value computed for complete interaction.

The fourth beam was built with a relatively weak shear connection. In this beam the shear connectors started yielding at the same load as the beam. Before first yielding occurred, deflections of this beam were 15 percent and strains 5 percent larger than those computed on the basis of complete interaction. After yielding began, both deflections and strains increased rapidly. Yielding spread toward the supports, and in the vertical direction at midspan yielding extended to about mid-depth of the I-beam. The top flange of the I-beam remained in compression throughout the test. Failure of this beam was caused by breaking of welds of reinforcing bars, which was followed by crushing of the concrete of the slab. At the time of failure appreciable slip had taken place between the beam and the slab, and as a result of this slip the ultimate load on beam B21W was about half way between that computed for complete and no interactions.

A composite T-beam is a tough structure. It has high reserve strength after the first yielding occurs, and the ultimate load is reached only after large deflections have taken place. In the beams tested, the capacity beyond first yielding of the steel beam was of the order of 40 percent of the ultimate load, while a similar reserve strength for identical beams but without interaction between the beam and the slab was estimated at about 10 per cent. In the beam tested to destruction, deflection corresponding to the ultimate load was equal to $\frac{1}{56}$ of the span length, but a large part of the reserve strength was exhausted at much smaller deflections. Over 50 percent of the total reserve strength was needed to reach a deflection of $\frac{1}{200}$ of the span length.

The width of the slabs of the four T-beams tested was approximately equal to one-sixth of the span length and was about 12 times the thickness of the slab. Measurements made on two beams showed that under these conditions the distribution of strain across the full width of the slabs was essentially uniform.

The data for one beam proved that the slab of a composite T-beam has a tendency to separate from the steel beam in the vertical direction The separation was small at locations close to the shear connectors because all connectors used in these tests provided an effective anchorage for the slab: on the other hand, in the beam with connectors spaced at distances equal to six times the slab thickness, fairly large separation was measured at locations between two adjacent connectors.

48. Load-Carrying Capacity of Composite T-Beams

The load-carrying capacities of the four T-beams were evaluated in terms of dead and live loads* at first yielding, at a deflection of L/200, and at the ultimate load (Table 23). The capacities of beams B24W and B24S were practically identical; yielding occurred at 3.3 LL, deflection of L/200 was reached at 4.4 LL, and the ultimate capacity was 5.3 LL. The corresponding capacities of beam B21S were 2.6 LL, 3.5 LL, and 4.3 LL. This beam carried approximately 20 percent less live load because of the smaller cross-section of the I-beam.

Beam B21W carried 2.0 LL, 2.9 LL, and 3.3 LL. With the exception of the shear connection this beam was identical with beam B21S. Thus the 24-percent decrease of the live-load capacity must have been caused by the lower stiffness of the shear connection.

The yield loads determined experimentally were larger than the computed values (Table 21). The difference was caused primarily by the presence of residual stresses due to rolling the steel beams and due to shrinkage of the slabs.

For B21S the measured ultimate load and the ultimate load computed for complete interaction differed by only about 1 percent (Table 24). The ultimate loads computed for beams B24W and B24S and the maximum loads reached in the tests also indicated a good agreement between the theory and the tests. The ultimate load for B21W was 27 percent lower than that computed for complete interaction.

49. Behavior of Shear Connection of Composite T-Beams

In all four beams the slabs were connected to the beams by means of flexible channel connectors. This type of connector not only provides for the transfer of horizontal shear but also anchors the slab to the beam in the vertical direction.

In three of the four beams the shear connection was strong enough to provide practically full interaction up to the maximum load. In all

* The procedure used for computing the live load is described in Section 31.

three beams shear connectors located close to the load yielded after large inelastic deflections had been observed on the beam, but this yielding was restricted to shear connectors in the middle half of the beams. The remaining connectors located closer to the supports did not yield. This phenomenon can be explained as follows. At loads exceeding yielding a semi-plastic hinge is formed in the portion of the beams directly under or close to the load, and large rotations take place at this section. The concrete slab resists large rotations at this section and therefore tends to deform the adjacent connectors. These connectors are then subject not only to the horizontal shear but also to large deformational stresses. As soon as the connectors located closest to the section of the semi-plastic hinge begin to yield, both an increasing portion of the horizontal shear and some deformational stresses are transferred to the next pair of connectors, and in this way yielding spreads slowly from the location of the load toward the supports. The test results indicated that if the load on shear connectors is computed on the basis of horizontal shear corresponding to the ultimate load, and if the factor of safety against yielding of the connectors is 1.4 or larger, the yielding will ordinarily not spread all the way to the supports.

One of the beams was designed for simultaneous yielding of the beam and the connectors. Tests demonstrated that in this beam all connectors began to yield as soon as the yield load of the steel beam was reached. This general yielding of shear connectors caused a noticeable decrease in the degree of interaction between the beam and the slab and a large decrease in the ultimate load capacity of the beam.

Elastic analysis of composite beams with incomplete interaction shows that the degree of interaction may be expressed by a value denoted as $1/C$ and defined in Section 42. Tests of composite T-beams indicated that a satisfactory degree of interaction will be retained up to destruction when the properties of the connection are such that $1/C$ is greater than 20. However, caution should be exercised in applying this limit, since it has been derived from an elastic analysis and confirmed by only a relatively small number of tests.

In two of the four beams the connector spacing decreased from midspan toward the supports. Comparison of the behavior of these beams with those in which the spacing was uniform indicated no substantial differences in the behavior of either the beams or the connections.

50. Effectiveness of Bond as Shear Connection

In three of the beams tested, provision was made during construction to prevent bond between the slab and the steel beam. This was done in

order to make sure that all horizontal shear would be transmitted through the shear connectors. In one beam, however, no attempt was made to prevent natural bond, so that it was possible to determine the effectiveness of bond in transmitting horizontal shear.

As long as it was present, bond proved to be a very effective shear connection. Practically no slip could be measured between the slab and the beam before the bond was broken. One application of load equal to 1.7 LL, corresponding to a shearing stress of 112 psi, did not break the bond. However, the bond broke after the same load was applied 11 times. Furthermore, if the static load had been increased instead of repeated, at loads approaching ultimate large deformational bond stresses would have occurred between the slab and the I-beam; it is believed that such bond stresses would have caused bond failure. Hence it may be concluded that even though bond is a very good shear connection, it may be an unreliable one.

51. Shoring of Composite T-Beams

Two composite T-beams were built with temporary supports which were removed only after the concrete of the slabs had hardened. Because of a relatively short span and consequent small dead load these beams were not entirely suitable for demonstrating the effects of shoring.

Except for the slip and the shear connector strain readings, the tests showed no difference in the behavior of two identical beams, one built without and the other with a temporary support. Theoretical studies indicate that the load-carrying capacity based on the first yielding of the beams is somewhat higher for beams built with shores, the difference depending on the ratio of live to dead load. The ultimate capacity, however, is practically independent of shoring.

The current specifications for highway bridges permit consideration of the effect of temporary shoring.* In the design of beams built with temporary supports both dead and live load is considered to be resisted by the full composite section, while in beams which are unsupported during casting and curing of the slab, dead load is assigned to the beams only. If the ratio of live to dead load at working stresses is low, design for working stresses allows the use of a steel beam of smaller size if advantage is taken of shoring. Both the tests and the theoretical studies have shown, however, that a beam designed in this way carried less load at first yielding and had lower ultimate capacity than a corresponding beam designed without shoring. It is obvious, then, that a composite

* "Standard Specifications for Highway Bridges," American Association of State Highway Officials, Washington, D. C., 1944, p. 195, Article 3.9.3.

T-beam designed for 1 DL + 1 LL have lower factors of safety both against first yielding and ultimate failure if advantage is taken of shoring in accordance with the current specifications for highway bridges.

If instead of designing for working stresses, a composite T-beam is designed on the basis of its ultimate flexural capacity, the shoring has no influence on the size of the beam. The ultimate capacity of such a beam depends only on the type, location and magnitude of the load acting on the beam at the time of failure; these conditions are similar for both the shored and unshored beams.

A design based on an equal factor of safety against the first yielding would be intermediate between the designs based on working stresses and on ultimate capacities. If designed on the basis of the load at first yielding, a beam of smaller moment of inertia is required for a shored than for an unshored T-beam. However, this difference is small, because the ratio of live to dead load at first yielding is usually large.

The tests have also shown that if a temporary support is kept at a constant elevation during curing of the slab, the shoring reaction will increase due to shrinkage. If only one or few supports are used, the possibility of tensile cracking in the slab above the support should be considered. In the tests reported in this bulletin only one support at midspan was used. The increase of the shoring reaction due to shrinkage was about 30 percent.

52. Channel Shear Connectors for Composite T-Beams

By far the most important conclusion regarding channel shear connectors gained from the tests of composite T-beams is that the behavior of a channel connector in a composite T-beam is essentially the same as the behavior of similar connector in a push-out specimen. This conclusion permits the application of the results of extensive tests of push-out specimens to the connectors in composite T-beams. The results of the push-out test data have been discussed in Sections 16–23.

With the aid of results from the full-scale push-out tests a semi-empirical analysis has been developed for the flexible channel shear connectors. This theory was compared with the results of the T-beam tests in Section 46 and a satisfactory agreement was found.

From beams in which a high degree of interaction was retained up to the ultimate load, the load on shear connectors located at some distance away from the load acting on the beam was practically equal to the product of horizontal shear and connector spacing, the horizontal shear being computed on the basis of complete interaction. The load on connectors located close to the load acting on the beam and the load on

all connectors of the beam with a relatively weak shear connection was lower than that computed on the assumption of complete interaction. Comparisons of the T-beam and push-out test data indicated that in this latter case the loads on shear connectors may be computed fairly accurately from the theory for composite T-beams with incomplete interaction. Both procedures—those based on complete interaction and those based on incomplete interaction—were found to be applicable only up to loads which caused yielding of the shear connector in question but were independent of the yielding of the steel beams.

The tests of T-beams confirmed the finding of the push-out tests that the direction of loading—application of the load to the front face or to the back face of the channel—had no significant effect on the static behavior of a channel shear connector.

The upper flange of the channel shear connectors proved effective in preventing a vertical separation of the slab from the steel beam.

The welded connections of shear connectors were sufficiently strong so that welds remained undamaged even after the test to failure. For beams with an adequate shear connection the factors of safety against failure of welds were about seven at one design load.

IV. SUMMARY OF RESULTS

Four composite steel and concrete T-beams with channel shear connectors were tested on simple spans of 37.5 ft by applying single concentrated loads at the center line and at other points. In the main these beams were designed according to the AASHO Specifications for H-20 loading. Individual channel shear connectors were investigated with the aid of 43 push-out tests (Figs. 1 and 2, Table 1).

The description of specimens, their manufacture and testing, and the test results have been presented in detail in this bulletin. The results of the push-out tests have been discussed in Chapter IIC and the results of the T-beam tests presented in Chapter IIIC. The more important test results are as follows.

(1) A composite concrete and steel T-beam is a very tough structure, far superior to a similar beam without connection between the slab and the beam. When an adequate shear connection is provided, the load causing first yielding is increased and the corresponding deflections are decreased considerably. A composite T-beam has high reserve strength after first yielding, and the ultimate load is reached only after large deflections have taken place.

(2) An inherent characteristic of composite steel and concrete T-beams is that some slip between the slab and the I-beam is inevitable. However, if the connection is designed properly, the slip is so small that for all practical purposes the beam may be considered as one with complete interaction.

(3) In all four beams the initial failure was caused by tension stress exceeding the elastic limit in the bottom flange of the I-beam. Yielding caused excessive deformations in the vicinity of the load, resulting in final failure by compressive crushing of the concrete slab (Sections 39, 40, and 41).

(4) The ultimate load-carrying capacities of beams with an adequate shear connection were practically equal to those computed for complete interaction (Section 41). In a beam in which the shear connection was purposely made weak, the ultimate capacity was definitely decreased. This decrease is best shown in terms of the live-load safety factors (Table 23).

(5) The strain distribution across the width of the top of the slab was approximately uniform. Maximum difference over the width was 15 percent (Section 43).

(6) Two beams were built with shoring at midspan. For beams of identical dimensions shoring had practically no effect on either the behavior or the capacity of the beams (Section 45).

(7) The natural bond between the I-beam and the slab is very effective in transmitting horizontal shear, but is unreliable because it may be broken long before the ultimate load is reached (Section 42).

(8) Channel shear connectors welded to the top flange of the I-beams proved to be a reliable shear connection. An individual channel shear connector acts like a dowel (Sections 14 and 46). The T-beam tests indicated that even though the connectors near the load may yield, a shear connection composed of channel shear connectors is adequate if the end connectors do not yield at the ultimate flexural load (Section 42).

(9) The deformations and stresses in a channel connector may be computed with satisfactory accuracy from semi-empirical formulas derived in Sections 26 and 27.

(10) Maximum stress in a channel connector occurred at the lower fillet of the channel (Fig. 2). Maximum pressure on the concrete behind the connector occurred at the channel flange welded to the beam.

(11) At high loads the maximum pressure on the concrete behind a shear connector greatly exceeded the cylinder strength of the concrete, but no concrete failures due to compression were recorded; push-out specimens with concrete fillets were an exception to this result (Section 15).

(12) The flange thickness, web thickness, and width affected the behavior of a channel connector. Within the range of variables included in these tests the effect of the height of channel was negligible. The effect of the width was approximately linear. The effect of web thickness was definitely present, but was considerably smaller than the effect of the thickness of the connecting flange (Section 12). The behavior of a channel connector was also affected by changes in the strength of concrete.

(13) The orientation of a channel shear connector (that is, whether the load comes on the face or back of the channel) did not affect its behavior (Sections 13 and 46).

(14) The tests proved that a tendency toward separation of the slab from the beam in the vertical direction was present. This separation was checked effectively by the channel shear connectors except in the beam with connector spacing equal to six times the slab thickness (Section 44). Maximum spacing in the remaining beams was equal to three times the slab thickness.

(15) Both uniform and variable spacing of channel shear connectors was used, but no effect on the ultimate load-carrying capacity of the T-beams could be detected (Section 42).

(16) The welds connecting the channel connectors to the I-beams were found satisfactory in all tests. For the three T-beams with an adequate shear connection the factor of safety against failure of welds was about seven under static loads (Section 46).

(17) The lightest rolled steel channels are probably the most economical to use. Bulb angles may also be indicated as good connectors, although no tests were made on them (Section 21).

APPENDIX A: DEFORMATIONS OF COMPOSITE BEAMS STRESSED BEYOND ELASTIC LIMIT

53. Inelastic Strains in Composite Beams with Complete Interaction

The theoretical strains for composite beams with complete interaction stressed beyond the elastic limit were computed for the following assumptions.

(a) The stress-strain relations for steel members, the I-beams and the reinforcing bars, are trapezoidal, the initial part having a slope equal to the measured modulus of elasticity and the stress ordinate of the horizontal part being equal to the measured yield point stress (for numerical values see Table 15). The stress-strain curves in tension and compression are assumed to be equal.

(b) The stress-strain relation for concrete in compression is trapezoidal, the initial part having a slope equal to the average measured initial modulus of elasticity and the stress ordinate of the horizontal portion being equal to the average measured compressive cylinder strength (for numerical values see Table 14).

(c) Concrete does not resist tension.

(d) The distribution of strains across any section is linear.

(e) Failure occurs when the compressive strain in the extreme fibers of the slab reaches a value of 380×10^{-5}.* The failure load corresponds to the maximum load.

(f) The slab and the I-beam are rigidly interconnected, so that no slip can take place between these two elements.

From assumptions (a)–(f) and from the conditions of equilibrium, strain may be computed at any desired point on the beam at any load.

54. Inelastic Strains in Composite Beams with No Interaction

Assumptions (a)–(d) listed in Section 53 are identical for a beam either with or without interaction. In addition to these four assumptions, for the beams without interaction between the concrete slab and the steel I-beam it was assumed that:

* This value of maximum concrete strain is based on the works of R. Chambaud and E. Hognestad:

R. Chambaud, "Etude expérimentale de la flexion dans les pièces en béton armé," Annales de L'Institute Technique du Bâtiment et des Travaux Publics (Paris), Concrete. Reinforced Concrete No. 4, New Series No. 61, 1949.

E. Hognestad, "A Study of Combined Bending and Axial Load in Reinforced Concrete Members," Univ. of Ill. Eng. Exp. Sta. Bul. 399, 1951.

(g) There is no connection between the slab and the I-beam; therefore slip can take place freely between these two elements.

(h) Perfect interaction exists between the reinforcing bars and the slab.

(i) At first yielding of the steel beam the contribution of the slab is in proportion to the relative stiffnesses of the slab and the beam. At failure this contribution is given by the individual capacities of the beam and the slab. A straight-line interpolation was used for the intermediate conditions.

(j) The stress distribution in the steel beams at failure is rectangular. The compressive stress block in concrete is also assumed to be rectangular.

From assumptions (a)–(d) and (g)–(j) and from the conditions of equilibrium, strain may be computed at any desired point on the beam at any load with the exception of the failure load.

55. Inelastic Deflections of Composite Beams

Theoretical deflections of composite beams may be computed from known angle changes, which may be determined from strains. The angle changes must be determined at several locations along the beam and then integrated twice to obtain deflections. The integration may be done easily either graphically or numerically. For the purposes of this bulletin numerical integration was used.*

For composite beams with complete interaction the angle changes may be expressed simply as

$$a = \frac{d^2y}{dx^2} = \frac{\epsilon_s + \epsilon_b}{h}$$

where

a = angle change
ϵ_s = compressive strain at the extreme upper slab fiber
ϵ_b = tensile strain at the extreme lower beam fiber
h = distance between the extreme upper slab and lower beam fibers

For composite beams with no interaction the expression for the angle change may be simplified because the top and bottom fiber strains in the beams are equal. Then

$$a = \frac{d^2y}{dx^2} = \frac{2\epsilon_b}{h_b}$$

where h_b is the depth of the I-beam.

* N. M. Newmark, "Numerical Procedure for Computing Deflections, Moments and Buckling Loads," Trans. ASCE, 1943, Vol. 108, pp. 1161–1234.

APPENDIX B: ADDENDUM TO ANALYSIS OF COMPOSITE BEAMS WITH INCOMPLETE INTERACTION

The tests have shown that composite beams with incomplete interaction may be analyzed accurately by Newmark's elastic analysis published in the Appendix of Bulletin 396.* This method takes into account the stiffness of the shear connection by the so-called connector modulus k, for which no rational expression was available. The theoretical analysis of channel shear connectors gives the needed semi-empirical formulas for a rational determination of the modulus k.

The connector modulus is defined as the load transmitted by a connector per unit of slip:

$$k = \frac{Q}{y_o}$$

For a channel shear connector slip may be computed from Eq. 26, Section 27, from which

$$k = k_2 \left(\frac{1}{2} t + h\right)$$

where k_2 is an empirical parameter given in Section 27, Eq. 29.

One other factor, which enters Newmark's analysis, requires an additional remark—the spacing of the connectors. That analysis is strictly applicable only when the ratio

$$\frac{k}{s} = \text{constant}$$

Since k is taken as a constant, the analysis should be applicable only for beams with connectors at constant spacings. Comparisons of the test data with the theory show, however, that for small variations of spacing the theory will yield good results if s is taken as the average spacing.

The connector modulus k is needed also for the evaluation of the measure of the degree of interaction $1/C$ defined in Section 42.

* Reference 112, pp. 115–33.

APPENDIX C: SELECTIVE BIBLIOGRAPHY

1929

1. Caughey, R. A., "Composite Beams of Concrete and Structural Steel," Proceedings, 41st Annual Meeting, Iowa Engineering Society, 1929, pp. 96-104.
2. Caughey, R. A., and Scott, W. B., "A Practical Method for the Design of I-Beams Haunched in Concrete," Structural Engineer, Inst. of Struct. Engrs. (London). 1929, Vol. 7, No. 8, pp. 275-93.

1932

3. Stüssi, F., "Profilträger, kombiniert mit Beton oder Eisenbeton, auf Biegung beansprucht," Final Report, First Congress, Int. Assoc. Br. and Struct. Eng., Paris 1932, pp. 579-95.

1934

4. Knight, A. W., "The Design and Construction of Composite Slab and Girder Bridges," Journal, Inst. of Engrs., Australia, 1934, Vol. 6, No. 1, pp. 10-22.
5. Paxson, G. S., "Loading Tests on Steel Deck Plate Girder Bridge with Integral Concrete Floor," Oregon Highway Department Technical Bul. No. 3, 1934.
6. Roš, M. "Les constructions acier-béton, système Alpha," L'Ossature métallique (Bruxelles), 1934, Vol. 3, No. 4, pp. 195-208.
7. Voellmy, A., "Eisen-Beton-Verbundkonstruktionen Alpha," Schweizerische Bauzeitung (Zurich), 1934, Vol. 103, No. 22, pp. 258-61.

1935

8. Blévot, M., "Hourdis de planchers métalliques," L'Enterprise francaise, Paris 1935.
9. Burn, A., "Simplified Calculations for Composite Beam Bridges," Journal, Inst. of Engrs., Australia, 1935, Vol. 7, No. 3, pp. 99-100.

1936

10. Kolm, R. C., "The Compound Action of Concrete Slabs and Rolled Steel Girders for Bridge Decking," Prelim. Publication, Second Congress, Int. Assoc. Br. and Struct. Eng., Berlin-Munich, 1936, pp. 1009-14.

1938

11. Bowden, E. W., "Roadways on Bridges," Eng. News Rec., 1938, Vol. 120, No. 11, pp. 395-99 and No. 12, pp. 442-44.
12. Krebitz, J., "Verbund zwischen vollwandigen Stahlträgern und darüberliegender Fahrbahnplatte aus Eisenbeton durch Bügel," Beton und Eisen (Berlin), 1938, Vol. 37, No. 14, pp. 227-30.

1939

13. Batho, C., Lash, S. D., and Kirkham, R. H. H., "The Properties of Composite Beams, Consisting of Steel Joists Encased in Concrete, under Direct and Sustained Loading," Journal, Inst. of Civ. Eng. (London), 1939, Vol. 11, No. 4, pp. 61-104.
14. Cueni, C. P., "Composite Steel and Reinforced Concrete Construction for Highway Bridges," Roads and Streets, 1939, Vol. 82, No. 12, pp. 48-49.

1941

15. Grover, LaMotte, "Welded Bridge Practice in Europe," Eng. News Rec., 1941, Vol. 127, No. 5, pp. 166-70.
16. Maier-Leibnitz, H., "Versuche über das Zusammenwirken von I-Trägern mit Eisenbetondecken," Die Bautchnik (Berlin), 1941, Vol. 19, No. 25, pp. 265-70.

1942

17. Cohen, A. B., "Major Bridge Replacement under Traffic," Eng. News Rec., 1942, Vol. 128, No. 23, pp. 926-29.

18. Newmark, N. M., and Siess, C. P., "Moments in I-Beam Bridges," Univ. of Ill. Eng. Exp. Sta. Bul. 336, 1942.

19. Pavlo, E. L., "Strengthening Our Highway Bridges," Eng. News Rec., 1942, Vol. 128, No. 9, pp. 339-42.

1943

20. Legrum, R., "Betondecken im Verbund mit Walzprofilträgern," Beton und Stahlbetonbau (Berlin), 1943, Vol. 42, No. 11/12, pp. 92-97.

21. Newmark, N. M., and Siess, C. P., "Design of Slab and Stringer Highway Bridges," Public Roads, 1943, Vol. 23, No. 7, pp. 157-64.

22. Tratman, E. E. R., "Impact Tests on a Railroad Bridge," Eng. News Rec., 1943, Vol. 131, No. 25, pp. 899-901.

23. Willis, J. F., "Welded Plate Girder Bridge Separates Connecticut Highways," Civil Engineering, 1943, Vol. 13, No. 9, pp. 407-8.

1944

24. Cueni, C. P., "Composite Action," Discussion to (22), Eng. News Rec., 1944, Vol. 132, No. 18, pp. 650-51.

25. Enke, G. L., "Welding to Ensure Composite Beam Action," Civil Engineering, 1944, Vol. 14, No. 1, pp. 9-12.

26. Cueni, C. P., "Composite Construction on Highway Bridges," Discussion to (25), Civil Engineering, 1944, Vol. 14, No. 4, p. 166.

27. Knight, A. W., "Construction of Composite T-Beam Bridges in Australia," Discussion to (25), Civil Engineering, 1944, Vol. 14, No. 5, p. 212.

28. Ozanne, W. A., "Composite Action," Discussion to (22), Eng. News Rec., 1944, Vol. 133, No. 14, pp. 400-1.

29. Roš, M., and Albrecht, A., "Träger in Verbund-Bauweise," Swiss Federal Mat. Test. Lab. (EMPA) Report No. 149, Zurich, 1944.

30. Siess, C. P., "Composite Action," Discussion to (22), Eng. News Rec., 1944, Vol. 132, No. 2, p. 23.

31. Stüssi, F., Hübner, Fr., Rychner, G. A., Albrecht, A., Minnig, A., Pestalozzi, E., Halder, M., and Roš, M., Discussion to (29), Swiss Federal Mat. Test. Lab. (EMPA) Report No. 149, Zurich, 1944.

1945

32. Albrecht, A., "Der Verbundträger," Schweizerische Bauzeitung (Zurich), 1945, Vol. 125, No. 2, pp. 11-15, No. 3, pp. 30-33, and No. 4, pp. 37-41.

33. Cueni, C. P., "Composite Action," Discussion to (22), Eng. News Rec., 1945, Vol. 134, No. 8, pp. 246-47.

34. Hindman, W. S., and Vandergrift, L. E., "Load Distribution over Continuous Deck Type Bridge Floor Systems," Ohio State Univ. Eng. Exp. Sta. Bul. 122, 1945.

1946

35. Manning, R. C., "Combined Action of Concrete Slabs and Supporting Structural Steel Beams," Engineering Journal, Eng. Inst. of Canada, 1946, Vol. 29, No. 3, pp. 149-53.

36. Newmark, N. M., Siess, C. P., and Penman, R. R., "Studies of Slab and Beam Highway Bridges—Part I: Tests of Simple-Span Right I-Beam Bridges," Univ. of Ill. Eng. Exp. Sta. Bul. 363, 1946.

37. Wendell, E. W., "Welded Girder Bridge of Composite Design Carries Deck Area of Two Acres," Eng. News Rec., 1946, Vol. 137, No. 26, pp. 856-58.

38. Willis, J. F., "Designs of Wilbur Cross Parkway Bridges," Eng. News Rec., 1946, Vol. 136, No. 20, pp. 792-97.

1947

39. Albrecht, A., "Der Verbundträger als Kombination von Stahlträger mit Eisenbetonplatte," Ingenieur (Uttrecht), 1947, Vol. 59, pp. 81-88.

40. Cohen, A. B., "Repairs to Spruce Street Bridge, Scranton, Pennsylvania," Proceedings, Amer. Concrete Inst., 1947, Vol. 43, pp. 241-48.

41. Ridet, J., "La construction mixte acier-béton armé dans les ouvrages d'art," Publications. Int. Assoc. Br. and Struct. Eng., Zurich, 1947, Vol. 8, pp. 171-94.

42. Stüssi, F., "Zusammengesetzte Vollwandträger," Publications, Int. Assoc. Br. and Struct. Eng., Zurich, 1947, Vol. 8, 249-69.

1948

43. Balog, L., "Composite Girder Bridges," Discussion to (37), Eng. News Rec., 1948, Vol. 140, No. 2, p. 64.

44. Crater, D. H., "Composite Girder Bridges," Discussion to (37), Eng. News Rec., 1948, Vol. 140, No. 10, pp. 372-73.

45. Coff, L., "Composite Girder Bridges," Discussion to (37), Eng. News Rec., 1948, Vol. 140, No. 18, p. 665.

46. Faltus, F., "Détails des poutres soudées à âme pleine," Final Report, Third Congress, Int. Assoc. Br. and Struct. Eng., Liège, 1948, pp. 197-204.

47. Godfrey, E. W. C., "The Causeway Bridges—Swan River, Perth, W. A.," Journal, Inst. of Engrs., Australia, 1948, Vol. 20, No. 12, pp. 185-91.

48. Hadley, H., "Horizontal Shear Connectors," Discussion to (37), Eng. News Rec. 1948, Vol. 140, No. 12, p. 440.

49. Haulena, E., "Brücken in Verbundbauweise," Zeitschrift VDI (Düsseldorf), 1948, Vol. 90, No. 5, pp. 145-50.

50. Newmark, N. M., Siess, C. P., and Peckham, W. M., "Studies of Slab and Beam Highway Bridges—Part II: Tests of Simple-Span Skew I-Beam Bridges," Univ. of Ill. Eng. Exp. Sta. Bul. 375, 1948.

51. Szechy, Ch., and Palotas, L., "The Application of Prestressing at Composite Steel Plate Girder Bridges Cooperating with the Overlying Reinforced Concrete Slab," Final Report, Third Congress, Int. Assoc. Br. and Struct. Engineers, Liège, 1948, pp. 443-52.

52. ——— "A Causeway Built to Withstand Hurricanes," Eng. News Rec., 1948, Vol. 140, No. 16, pp. 568-71.

1949

53. Cornelius, W., Fröhlich, H., and Haulena, E., "Brücken in Verbundbauweise," Discussion to (49), Zeitschrift VDI (Düsseldorf), 1949, Vol. 91, No. 21, pp. 553-55.

54. Dischinger, F., "Stahlbrücken im Verbund mit Stahlbetondruckplatten bei gleichzeitiger Vorspannung durch hochwertige Seile," Der Bauingenieur (Berlin), 1949, Vol. 24, Nos. 11 and 12, pp. 321-32, 364-76.

55. Fröhlich, H., "Einfluss des Kriechens auf Verbundträger," Der Bauingenieur (Berlin), 1949, Vol. 24, No. 10, pp. 300-7.

56. Granholm, H., "Om sammansatta balkar och pelare med särskild hänsyn till spikade träkonstruktionen," Transactions of Chalmers Univ. of Technology, No. 88, Gothenburg, 1949.

57. Jäger, K., "Die Verbundwirkung Zwischen Stahlträger und Stahlbetonplatte," Oesterreichisches Ingenieur-Archiv (Wien), 1949, Vol. 3, No. 4, pp. 295-311.

58. ——— "Alpha Composite Construction Engineering Handbook," Porete Manufacturing Company, North Arlington, N. J., 1949.

The following papers were published in the Symposium on Highway Bridge Floors, Trans. ASCE, 1949, Vol. 114; published also as Univ. of Ill. Eng. Exp. Sta. Reprint 45, 1949.

59. Newmark, N. M., "Design of I-Beam Bridges," pp. 997-1022.

60. Richart, F. E., "Laboratory Research on Concrete Bridge Floors," pp. 980-96.
61. Siess, C. P., "Composite Construction for I-Beam Bridges," pp. 1023-45.
62. Slack, S. B., Wendell, E. W., Tachau, H., Furrer, R., Balog, L., and Newmark, N. M., Richart, F. E., Siess, C. P., Discussions of (59), (60) and (61), pp. 1046-72.

1950

63. Braithwaite, R. G., Davies, D. J., "Welded Highway Bridges," Journal, Inst. Civ. Engrs. (London), 1950, Vol. 34, No. 6, pp. 109-73.
64. Cornelius, W., "Entwicklungsmöglichkeiten des Stahlbaues durch die Verbundbauweise," Zeitschrift VDI (Düsseldorf), 1950, Vol. 92, No. 24, pp. 667-70.
65. Faltus, F., "Svařované konstrukce spřažené s betonovou deskou," Technický Obzor (Prague), 1950, Vol. 58, No. 9, pp. 129-33.
66. Fritz, B., "Vereinfachtes Berechnungsverfahren für Stahlträger mit einer Betondruckplatte bei Berücksichtigung des Kriechens und Schwindens," Die Bautechnik (Berlin), 1950, Vol. 27, No. 2, pp. 37-42.
67. Guérin, T., and Pigeau, H., "La construction mixte fer-béton dans les ouvrages d'art a travées continues," Annales de L'Institut Technique du Batiment et des Traveaux Publics (Paris), Theories and Methods of Design No. 10, New Series No. 157, 1950.
68. Norman, R. G., "Vibrations of a Highway Bridge," New Zealand Engineering, 1950, Vol. 5, No. 3, pp. 239-43.
69. Steinhardt, O., "Ein neues Bau- und Montageverfahren für genietete Stahlträger im Verbund mit Stahlbeton-Druckplatten," Die Bautechnik (Berlin), Vol. 27, No. 3, 1950, pp. 81-83.
70. "Road Practices of Country Roads Board, Victoria," Commonwealth Engineer (Australia), 1950, Vol. 37, No. 12, pp. 497-98.
71. "Vorläufige Richtlinien für die Bemessung von Verbundträgern in Strassenbrückenbau," Der Bauingenieur (Berlin), 1950, Vol. 25, No. 9, pp. 357-64.

The following papers were published in the Special Issue on Composite Construction, Der Bauingenieur (Berlin), 1950, Vol. 25, No. 3.
72. Albers, K., "Vorschlag für Schubsicherungen," p. 91.
73. Fritz, B., Fröhlich, H., Dörnen, Steinhardt, O. H., Hilfer, Kesper, E., Miesel, K., Kohl, E., Schleicher, F., Klingenberg and Zendler, Discussion, pp. 91-95.
74. Fröhlich, H., "Betonfahrbahnen von Strassenbrücken," pp. 106-10.
75. Fröhlich, H., "Theorie der Stahlverbund-Tragwerke," pp. 80-87.
76. Gaede, K., "Die Baustoffe der Stahlverbund-Bauweise," pp. 75-77.
77. Hampe, "Anwendung und Bedeutung der Verbundträgerbauweise," pp. 73-75.
78. Homberg, H., "Bericht über ausgeführte Stahlverbund-Brücken," pp. 98-99.
79. Kesper, E., "Schwindspannungen bei statisch unbestimmten Systemen," p. 100.
80. Klingenberg, W., "Schubsicherungen," pp. 77-80.
81. Lautz, E., "Lahnbrücke Friedensdorf," pp. 97-98.
82. Nickel, "Entwurf einer erdverankerten Hängebrücke in Verbund-Bauweise," p. 100.
83. Paul, Leonhardt, Homberg, Lautz, Discussion, p. 99.
84. Pirlet, "Fragen der Verbundwirkung von Stahl und Beton beim Bau der neuen Rheinbrücke Bonn," pp. 99-100.
85. Schleicher, F., "Schweizer Versuche mit Stahlverbunträgern," pp. 101-5.
86. Thümecke, M., "Wiedbrücke Segendorf," p. 97.
87. Wiechert, U., "Brücke über den Leopoldskanal bei Oberhausen (Breisgau)," pp. 95-96.
88. Zendler, K., "Beitrag zur Entwicklungsgeschichte der Verbund-Trägerdecke," pp. 88-91.

The following papers were published in the Second Special Issue on Composite Construction, Der Bauingenieur (Berlin), 1950, Vol. 25, No. 8.
89. Becker, R., "Eisenbahnbrücke über die Birs bei Bärschwil (Schweiz)," pp. 310-13.

90. Esslinger, M., and Endries, J., "Schwinden und Kriechen bei Verbundträgern in statisch unbestimmten Systemen," pp. 278-79.

91. Fritz, B., "Vorschläge für die Berechnung durchlaufender Träger in Verbund-Bauweise," pp. 271-77.

92. Fuchs, D., "Versuche mit Spannbeton-Verbundträgern," pp. 289-94.

93. Graf, O., "Versuche über den Verschiebewiderstand von Dübeln für Verbundträger," pp. 297-303.

94. Hampe, "Stahlbrücken mit unten liegender vorgespannter Stahlbeton-Fahrbahnplatte," pp. 306-8.

95. Hirschfeld, K., "Der Temperatureinfluss bei der Verbund-Bauweise," pp. 305-6.

96. Homberg, H., "Ältere Messungen an ausgeführten Brücken," pp. 303-4.

97. Jessberger, L., "Der Verbundträger. Ausführungsbeispiele," pp. 313-14.

98. Kesper, E., "Die Gestaltung von Stahlbrücken in Verbund-Bauweise, insbesondere bei statisch unbestimmten Systemen," pp. 286-89.

99. Kleineberg, F., "Die wichtigsten Probleme der Verbund-Bauweise," pp. 269-71.

100. Kramer, A., "Kontinuierlicher Träger in Verbund-Bauweise mit durch Seile vorgespannten Platten," pp. 294-96.

101. Kriesche, H., "Verbund-Bauweise im Hochbau," pp. 316-18.

102. Lauterburg, "Tannwaldbrücke über die Aare bei Olten," pp. 309-10.

103. Lautz, E., Seeger, Steinhardt, Kesper, E., Rüsch, Klingenberg, Dörnen, Discussion, pp. 296-97.

104. Leonhardt, F., "Gedanken zur baulichen Durchbildung von Durchlaufträgern in Verbund-Bauweise," pp. 284-86.

105. Sander, H., "Umbau und Verstärkung eines Gasofengebäudes in Verbund-Bauweise," pp. 314-16.

106. Steinhardt, O., Dimitrov, N., Fritz, Rüsch, Dörnen, Klingenberg, Discussion, pp. 280-83.

107. Steitz, "Stabbogenbrücke in Verbund-Bauweise," p. 283.

108. Zendler, K., "Die konstruktive Gestaltung und Ausführung der Verbundträgerdecke im Industriehochbau," pp. 319-22.

1951

109. Klöppel, K., "Die Theorie der Stahlverbundbauweise in statisch unbestimmten Systemen unter Berücksichtigung des Kriecheinflusses," Der Stahlbau (Berlin), 1951, Vol. 20, No. 2, pp. 17-23.

110. Newmark, N. M., Siess, C. P., and Viest, I. M., "Tests and Analysis of Composite Beams with Incomplete Interaction," Proceedings of the Society for Experimental Stress Analysis, 1951, Vol. 9, No. 1, pp. 75-92.

111. Schürmann, J., "Ein praktisches Verfahren zur Bestimmung der Gurtplattenlängen bei Verbundträgern," Der Stahlbau (Berlin), 1951, Vol. 20, No. 1, pp. 14-15.

1952

112. Siess, C. P., Viest, I. M., and Newmark, N. M., "Studies of Slab and Beam Highway Bridges—Part III: Small-Scale Tests of Shear Connectors and Composite T-Beams," Univ. of Ill. Eng. Exp. Sta. Bul. 396, 1952.

This page is intentionally blank.

The Engineering Experiment Station was established by act of the University of Illinois Board of Trustees on December 8, 1903. Its purpose is to conduct engineering investigations that are important to the industrial interests of the state.

The management of the Station is vested in an Executive Staff composed of the Director, the Associate Director, the heads of the departments in the College of Engineering, the professor in charge of Chemical Engineering, and the director of Engineering Information and Publications. This staff is responsible for establishing the general policies governing the work of the Station. All members of the College of Engineering teaching staff are encouraged to engage in the scientific research of the Station.

To make the results of its investigations available to the public, the Station publishes a series of bulletins. Occasionally it publishes circulars which may contain timely information compiled from various sources not readily accessible to the Station clientele or may contain important information obtained during the investigation of a particular research project but not having a direct bearing on it. A few reprints of articles appearing in the technical press and written by members of the staff are also published.

In ordering copies of these publications reference should be made to the Engineering Experiment Station Bulletin, Circular, or Reprint Series number which is just above the title on the cover. Address

THE ENGINEERING EXPERIMENT STATION
UNIVERSITY OF ILLINOIS
URBANA, ILLINOIS